The Thesis committee for Charles Roberts Upshaw
certifies that this is the approved version of the following thesis:

Thermodynamic and Economic Feasibility Analysis of a 20 MW Ocean Thermal Energy Conversion (OTEC) Power Plant

APPROVED BY

SUPERVISING COMMITTEE:

Michael E. Webber, Supervisor

Alexandre K. da Silva

Thermodynamic and Economic Feasibility Analysis of a 20 MW Ocean Thermal Energy Conversion (OTEC) Power Plant

by

Charles Roberts Upshaw, B.S.M.E.

THESIS

Presented to the Faculty of the Graduate School of

The University of Texas at Austin

in Partial Fulfillment

of the Requirements

for the Degree of

MASTER OF SCIENCE IN ENGINEERING

The University of Texas at Austin

May 2012

Dedicated to my wife Emily, and my parents Caren and Jim Upshaw. I would not be where I am today without their unending love and support.

Acknowledgments

I wish to thank the Mark Swann for his support to make this research possible, as well as Jim Anderson, and the Anderson family, for their contributions to this work.

Thermodynamic and Economic Feasibility Analysis of a 20 MW Ocean Thermal Energy Conversion (OTEC) Power Plant

Charles Roberts Upshaw, M.S.E.
The University of Texas at Austin, 2012

Supervisor: Michael E. Webber

Ocean Thermal Energy Conversion (OTEC) is the process of harnessing the temperature differential that exists in the equatorial oceans between the warm surface water and the cool water thousands of feet below to produce electricity. Due to the massive scale of the ocean thermal resources, OTEC power generation is appealing. The purpose of this thesis was to investigate OTEC and assess its potential viability as an energy source from both engineering and economic perspectives.

This thesis provides an introduction to the research, and outlines the scope of the project in Chapter 1. Chapter 2 proves an overview of OTEC, from the basic operation and viable locations, to information on some of the major components that make up the plant. Chapter 3 describes the thermodynamics, heat transfer, and fluid mechanics that govern the physical operation of the OTEC plant. Chapter 4 provides an analysis of different plant design parameters to examine effects different parameters have on plant operations and equipment sizing. Chapter 5 describes the cost estimation for an OTEC plant, and provides subsequent analysis by comparing the estimated cost with other technologies and electricity prices from four island communities.

The primary research of this thesis was the development of an integrated thermal fluids systems model of a closed-cycle OTEC power plant for the purpose of analyzing the effects of key design parameters on the plant performance. A simple Levelized Cost of Electricity (LCOE) economic model was also developed and integrated with the Thermal Fluid Systems model in order to assess the potential economic viability of a 20 MW OTEC power plant. The analyses from these models suggest that OTEC is definitely viable from an engineering standpoint, but economic viability for a 20 MW plant would likely be limited to small or remote island communities.

Table of Contents

Acknowledgments **v**

Abstract **vi**

Chapter 1. Introduction: Motivation and Scope for this Thesis **1**

1.1 Motivation 1

1.2 Project Scope 3

Chapter 2. OTEC Overview and Literature Review **6**

2.1 Introduction 6

2.2 Basic Overview of Ocean Thermal Energy Conversion (OTEC) 6

2.3 Background History of OTEC Research and Development 10

2.4 Design Considerations of Major OTEC Plant Components and Subsystems 13

2.4.1 Plant Platform 14

2.4.2 Ocean Water Systems and the Cold Water Pipe 16

2.4.3 Boiler and Condenser Heat Exchangers 18

2.4.4 Electrical Power Equipment and Transmission 20

2.4.5 Vapor Turbines and Power Cycle Working Fluid 21

2.5 Potentially Viable Locations for OTEC Power Generation 23

2.6 Environmental Concerns regarding OTEC Plant Deployments 24

Chapter 3. Thermal-Fluid Systems Modeling of a Closed Cycle OTEC Plant **26**

3.1 Introduction 26

3.1.1 Modeling Literature Review 28

3.1.2 Initial Simplifying Assumptions 29

3.2 Thermodynamic Modeling of the Power Cycle Sub-system 31

3.2.1 Power Cycle Staging for Increased Performance 40

3.2.2 Heat Engines and Carnot Efficiency Calculations 44

3.3 Heat Transfer and Temperature Modeling of the Heat Exchanger Subsystems 46

3.3.1 Scaling Overall Heat Transfer Coefficient $\bar{U}$ with Water Velocity 54

3.4 Hot and Cold Water Pressure Drop and Pump Demand Analysis . . . 56
3.5 Implementation of the Thermal-Fluids Systems Model in MATLAB . 60
3.6 Modeling Conclusions . . . 61

Chapter 4. Thermal-Fluids Systems Analysis of 20MW OTEC Plant Model 63
4.1 Introduction . . . 63
4.1.1 Literature Review to Determine Parameter Ranges . . . 64
4.1.2 Design Parameter Ranges for Analysis . . . 65
4.2 The Reference Case . . . 69
4.3 Analysis of Power Cycle Staging . . . 72
4.4 Analysis of the Overall Heat Transfer Coefficients and Heat Exchanger Pressure Drop . . . 75
4.5 Analysis of Water Inlet Temperatures . . . 79
4.6 Analysis of Terminal Temperature Difference and Water Discharge Temperature . . . 84
4.7 Analysis of Cold Water Pipe Diameter and Length . . . 89
4.8 Analysis of Working Fluid Mass Flow Rate . . . 94
4.9 Conclusions from Thermal Fluids Systems Analysis . . . 97

Chapter 5. Economic Feasibility Analysis 103
5.1 Introduction . . . 103
5.2 Economic Literature Review . . . 103
5.3 Economic Modeling Methodology . . . 108
5.4 Calculation and Comparison of LCOE with Current Technologies and Markets . . . 112
5.5 Conclusion . . . 121

Chapter 6. Conclusions and Final Thoughts 123

Appendices 126

Appendix A. Glossary of Abbreviations, Symbols, Subscripts, and Terms 127
A.1 Abbreviations . . . 127
A.2 Equation Symbols . . . 128
A.2.1 Power Cycle Model . . . 128
A.2.2 Heat Exchanger Model . . . 130
A.2.3 Pressure Drop and Pump Demand Model . . . 131

A.2.4 Economic Model 132
A.3 Subscripts 133

Appendix B. Reference Case Model Inputs and Outputs **135**

Appendix C. MATLAB Code **137**
C.1 Thermal-Fluids Systems Model Code, Thesis_baseline.m 137
C.2 Thermal-Fluids and Economic Model: subsystem functions, and other files 141
C.2.1 Temperature Calculations for Staging: pcstaging.m 141
C.2.2 Power Cycle Subsystem: powercycle.m 141
C.2.2.1 powercycle.m sub-functions 142
C.2.3 Heat Exchanger Subsystem: heatexchangers.m 147
C.2.4 Hot and Cold Water Pump Subsystem: coldwaterpump.m, warmwaterpump.m 148
C.2.5 Economic Modeling Subsystem: economics_thesis.m 150

Bibliography **152**

Chapter 1

Introduction: Motivation and Scope for this Thesis

1.1 Motivation

Fears of climate change, declining fossil fuel resources, and increasing demand for electricity has pushed renewable energy technology development and commercialization back into the global spotlight. These issues are driving scientists and policy makers to create and develop technologies that can provide commercial-scale replacement of our current power generation infrastructure. There are already several renewable energy technologies that have been developed and commercially tested. Large-scale wind farms currently produce approximately 6.4% of the electricity in Texas [1]; solar photovoltaics are not yet at grid parity in terms of cost to produce electricity, but the industry is growing and prices are falling fast; biomass and hydropower are two of the oldest forms of energy generation known to man .

However, there are shortcomings with all of these technologies that prevent them from completely displacing fossil fuels. One problem with wind and solar generation technologies is that they are inherently variable, and therefore require back-up to cover any sudden drop-offs. Therefore, renewable energy from wind and solar will ultimately be limited by the amount of variability the grid can absorb [37]. Hydropower and biomass are not dependent on such limitations, and can provide the dispatchability to balance wind and solar. The problems with hydropower and biomass is that there is simply not enough of their respective resources to power significantly more than they already produce; the US has already built out the majority

of its hydropower capacity, and scaling biomass to be a significant portion of power production would lead to deforestation or loss of arable cropland to fuel production. Consequently, there is a desire for dispatchable utility-scale renewable power, for which there are a few options: existing systems coupled with large-scale energy storage, geothermal, and Ocean Thermal Energy Conversion (OTEC). OTEC might be an appealing option, and is the topic of this thesis.

OTEC utilizes the vast amount of energy stored in the ocean's natural thermal gradient to generate electrical power. Due to the volume of the ocean, the thermal gradient is nearly constant from day-to-day, and only sees real variation on a seasonal level [40–42]. Therefore, OTEC can be considered a base load power source. If proponents of OTEC are correct in their assertions, then OTEC power plants could potentially provide cost-competitive base load electricity for many coastal and island communities including Hawaii, Puerto Rico, the southern Pacific coast of Mexico, coastal India, and many other areas where there are favorable ocean thermal gradients nearby and where prevailing electricity prices are high or unreliable [4, 8, 68]. Advocates also claim that added benefits of OTEC could include desalinated water and re-distribution of ocean nutrients back to the surface, increasing marine life and fish stocks [4, 68].

Despite these potential upsides, comparatively little research and development has been performed during the current boom of renewable energy build-out. This dearth in OTEC development is due to a variety of factors, in particular the high capital cost due to large generating equipment, heat exchangers, and other components [62]. This paper covers the development of an integrated systems model to help optimize plant design and component sizing for OTEC plants.

1.2 Project Scope

The original scope of this project was to assess the feasibility and viability of an power generation facility from different engineering and economic perspectives. First a simplified thermal-fluid systems analysis was performed to assess the feasibility of OTEC based on fundamental principles; then cost variables were included for assessment from an economic perspective; and lastly OTEC power generation was evaluated within the context of other power generation technologies, primarily for island and coastal communities.

The analysis presented here is focused on a 20MW OTEC power plant because the original modeling work was based on a 20MW plant proposal by Sea Solar Power Inc. The reason for proposing to build a smaller plant (rather than a 100MW plant) is that a utility-scale OTEC plant has yet to be built, and there are still many uncertainties about the costs for manufacturing, installation, and operation. A 20 MW plant would be large enough to generate significant power for a small community, while still being small enough to limit financial risks. Another reason for modeling a smaller plant is that a large (50 to 100+ MW) plant would likely use modules of 10-20MW power systems in parallel, so the physical performance model would be essentially the same, and the model could be easily adapted in the future. Finally, a 20MW plant size was also selected to allow for comparison with feasibility studies of similarly sized plants. Further discussion on the OTEC economies of scale will be discussed in Chapter 5.

The engineering assessment was performed by developing a mathematical model of the performance of an OTEC power plant based on a simplified systems-level analysis using the fundamentals of thermodynamics, heat transfer, and fluid flow. Economic analysis consisted of assigning cost variables to plant components and out-

puts to estimate an estimated range for the Levelized Cost of Electricity (LCOE). Finally, OTEC was compared with other power generation technologies, both conventional and alternative, as well as the prices for electricity in Hawaii, Puerto Rico, Fiji and the Cayman Islands in order to assess the potential financial viability of a first generation OTEC plant. The breakdown of this paper by chapter is as follows:

- Chapter 1 provides the introductory motivation and scope of the project.
- Chapter 2 contains general background information on OTEC power plants in order to provide the reader with context for the modeling and analysis. First, a basic overview of OTEC power generation is given in Section 2.2, along with discussion on the global location and theoretical potential of OTEC resources. Next, Section 2.3 discusses the history of OTEC research and development. Section 2.4 describes the major subsystems and components that make up an OTEC power plant. A short discussion on potentially viable locations for OTEC power generation is provided in Section 2.5. Lastly, Section 2.6 briefly describes some of the potential environmental concerns associated with OTEC.
- Chapter 3 describes the underlying thermodynamics, heat transfer, and fluid flow relationships that make up the thermal fluid systems model. Section 3.1 introduces the model sub-systems and the initial assumptions. The power cycle sub-system, and its thermodynamic relationships and assumptions are described in Section 3.2. Section 3.3 describes the heat transfer governing equations for the boiler and condenser heat exchangers. Section 3.4 provides the fluid flow-pressure drop relationships needed to calculate the hot and cold water pump power demands. The description of how these three models were tied together and programed is provided in Section 3.5. The chapter concludes with a few closing remarks reflecting on the modeling process.

- Chapter 4 implements the thermal fluids system model for the purposes of modeling a 20 MW OTEC power plant. An introduction to the analysis and description of the reference case can be found in Sections 4.1 and 4.2. Sections 4.3 through 4.8 analyze the effects of varying different model parameters.

- Chapter 5 models the potential economic viability of OTEC power generation by coupling cost variables to the thermal fluid systems model. Section 5.2 describes the previous plant feasibility studies that were used to help establish potential cost ranges for major plant components and other expenses. The equations used for calculating the Levelized Cost of Electricity (LCOE) are described in Section 5.3 and 5.4, respectively.

- Lastly, Chapter 6 concludes the paper with an overview of the major takeaways from this research, and describes potential next steps for future research.

Chapter 2

OTEC Overview and Literature Review

2.1 Introduction

Fundamentally, OTEC power generation is the same as power generation in any coal, natural gas boiler, or nuclear power plant; namely, a heat source is used to boil a working fluid into vapor, which is then expanded through a turbine, and then re-condensed to begin the cycle again. The difference lies in the magnitude of the temperature differential between the hot and cold sources. Where fossil fuel and nuclear boilers create super heated steam at hundreds of degrees Celsius, an OTEC plant operates on a thermal temperature difference less than that between the hot and cold water in a typical household sink. This low-grade thermal source is what makes OTEC unique. This chapter will discuss the resource that drives OTEC and the types of plants in Section 2.2; Section 2.3 describes the history of OTEC R&D; Section 2.4 provides an overview of the major sub-systems and components in a typical OTEC plant; potentially viable locations for OTEC power generation are discussed in Section 2.5; lastly, Section 2.6 discusses potential environmental concerns regarding large-scale OTEC operation.

2.2 Basic Overview of Ocean Thermal Energy Conversion (OTEC)

Ocean Thermal Energy Conversion relies on the temperature differential between the warm surface water and the cold deep water [17, 23]. OTEC is an alluring

solution to our energy problem because of factors of scale. The tropics alone contain approximately 60 million km^2 of ocean surface, and this surface is subject to the most direct radiation by the sun [40]. The millions of gigawatts of power absorbed into the tropics help maintain a near-surface temperature of 25 - 30 °C (77 - 86 °F). Since warm water is less dense than cold water, this warm water stays at the surface layer. The surface absorbs and reemits nearly all of the solar energy back out of the surface keeping the deep ocean water at a cold, constant temperature. In tropical locations with depths of 1000m or more, the water temperature is usually only 4 - 5 °C (39- 41 °F). Thus, certain areas of the tropics contain waters with temperature differentials of approximately 20 - 25 °C, as shown in Figure 2.1 by the green to red areas [42].

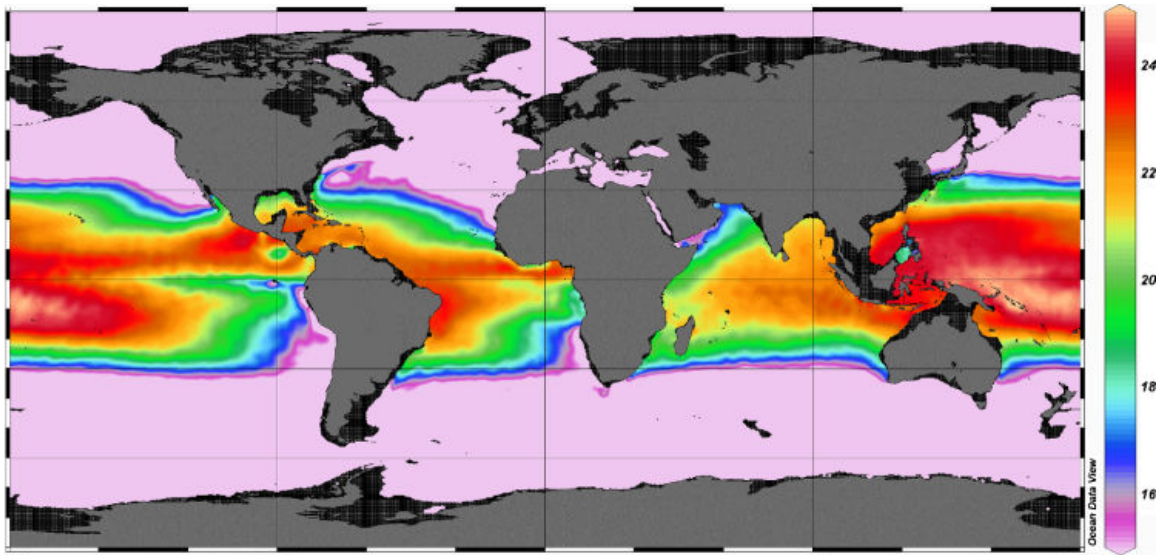

Figure 2.1: A world map of Oceanic Temperature Difference between the surface and a depth of 1000 meters shows an extensive band of ocean surface in the tropics with 15-25 C temperature difference [42].

The estimates for world-wide, sustainable OTEC power generation varies widely, from 10-1000 TW (Terra Watts); recent calculations by Nihous in 2005 and 2007 estimate the number to be more on the order of 3 TW [40, 41]. While 3 TW cannot

meet the total world's energy consumption, it could still easily cover the demand for any island and coastal communities who have favorable OTEC resources nearby.

Utilizing the hot and cold waters as a heat source and sink respectively, a low temperature Rankine cycle can be utilized to produce electrical power [23]. While there have been dozens of OTEC plant designs proposed, nearly all fall into three basic categories: Open Cycle (OC), Closed Cycle (CC), and Hybrid Cycle (HC) [8, 33, 62]. OC-OTEC plants utilize ocean water itself as the working fluid. For this configuration, warm surface water is depressurized until it vaporizes, runs through a low-pressure steam turbine to produce power, and condenses on heat exchangers cooled by ocean water from below [8,33,62]. While OC-OTEC plants have been built, they suffer from the poor thermodynamic and chemical properties of ocean water as a low-temperature working fluid. The benefit of OC plants is that the condensed ocean water is pure water, and can be collected as drinking water [8, 62].

CC-OTEC plants utilize heat exchangers to vaporize and condense a working fluid contained inside a separate low temperature Rankine power cycle [8, 62]. Proposed working fluids have generally been ammonia and various refrigerants, due to their high vapor densities and thermodynamic properties that are optimal for the temperature range [6, 18, 62]. CC-OTEC plants have extra costs and added logistics associated with the massive heat exchangers. However, the power cycle equipment is simpler and more efficient than those used in OC plants. Since the closed power cycle is not directly utilizing the ocean water, the plant does not need to shut down the entire water pumping operation to take a single power unit out of service [4]. A HC-OTEC plant utilizes a closed cycle for power, but has heat exchangers similar to OC plants. Depressurized water is evaporated and then condensed on the outside of the boiler to heat the working fluid; this configuration provides both power and fresh

water. While most of the pilot scale plants have been open cycle, many consider CC-OTEC to be more feasible for first generation utility-scale plants because most of the major components are off-the-shelf, or are modified designs based on already understood technology [4,62]. Further discussions of the technical operation and feasibility will focus on CC-OTEC for this reason.

The thermodynamic operating principles of an OTEC power plant are relatively simple. However, since the operating temperature differences are so low (compared with traditional thermal plants), the Carnot efficiency is approximately 7-9%, and the actual efficiency of a commercial-scale plant is expected to be closer to 2-4% [4, 8, 62]. Further explanation of Carnot efficiency can be found in Section 3.2. The extremely low thermodynamic efficiency is a design constraint, but it is not as critical as it would be in a fuel-burning power plant because there is no fuel cost for the OTEC system.

Because the thermodynamic efficiency is so low, a very large water flow-rate is required for the vaporization and condensation of the working fluid. The power to move this water through the heat exchangers is provided by the power cycle, which in turn derives its power from the water. The expected power consumption for the hot and cold water pumps is on the order of 20-30% of the gross power output [4, 8, 62], which is due to the huge volume of water that must be moved through the heat exchangers. If the heat exchangers could more effectively transfer heat to and from the working fluid, then less water would be needed to provide power output, which in turn would mean a higher power output for a given plant size. The heat exchangers in a CC-OTEC plant are the prime example of the confluence of factors that have driven, and prevented, OTEC development: performance, optimization, and cost. The heat exchangers must be designed to transfer the maximum amount of energy

to the working fluid at minimal pumping power and heat exchanger size, so that the net power output compared to cost will decrease. However, since the cost of building a full-scale OTEC plant is very capital intensive, proving new designs and components has been the major hurdle for OTEC developers. Because of the self-reinforcing advantage, improved heat exchanger modeling can be found in Section 3.3, and analysis of this effect can be found in Chapter 4. The heat exchanger performance is just one of many different parameters looked at as part of the analysis performed for this thesis.

2.3 Background History of OTEC Research and Development

French physicist Jacques d'Arsonval first proposed OTEC in the 1880s, and in 1930 his former student Georges Claude built, and successfully operated, the first OTEC plant in Cuba [17,23]. Claude's plant barely broke even on net power produced, but the plant did prove, with 1930s technology, a plant could be built that could at least power its own equipment required for operation. Unfortunately, the land-based plant in Cuba was destroyed by a storm soon after it was built [62].

OTEC research fell off after the World War II as the world developed cheaper, easier sources for power. However, the technology reemerged in the 1970s when the first oil embargo raised concerns about the cost and security of energy sources based on fossil fuels. In 1979, the first floating OTEC plant, dubbed Mini-OTEC, operated at Keyhole Point in Hawaii. The converted Navy barge was retrofitted with mostly off-the-shelf components to produce a gross power of 50kW, with a net power between 10 to 17kW [62].

In the 1970s to early 1980s, OTEC research was being performed by not only

academia and National Labs, but by large industrial and defense companies. One good example of the breadth and depth of research performed during that time can be found in the conference proceedings of the Ocean Thermal Energy Conversion Conference, which was held annually from 1973 to 1981. The topics covered within the conference proceedings range from high-level assessments of marketability and legal issues, to very focused experimental research on various components. There were feasibility and optimal design studies by Lockheed, TRW, GE, Westinghouse, and many others which will specifically be discussed later in Chapters 4 and 5 . Similarly, heat exchanger testing was a prime focus by many of those same companies, as well as Sea Solar Power, Argonne National Labs, and major refrigeration and cooling companies such as Trane, Alfa-Laval, and Linde [3, 5, 13, 14, 19, 22, 26, 44, 45, 48, 49, 56, 60, 61]. Although these conference reports hint at the excitement surrounding OTEC in the 1970s, the excitement never materialized into utility-scale projects. Once the price of oil and energy came back down in the early 1980s, the enthusiasm surrounding renewable energy technologies subsided. Government budgets for R&D of renewables decreased drastically, and with OTEC being such a large-scale and capital intensive technology, it was quickly abandoned by most of the major companies who were driving the research.

Since Mini-OTEC, two other small-scale OTEC plants have been successfully built and operated. A Japanese consortium built and ran a closed cycle 100kW gross power land-based plant on the island nation of Nauru in 1982, producing a better than expected 31.5kW net power [62]. The last large-scale demonstration was a land-based open cycle power and desalination plant that operated from 1992-1998 in Hawaii. That system set the records for power and water production by OTEC, with 255kW gross power, 103kW of net power, and approximately 6 gallons per minute of fresh water produced [62].

These successes have basically been the extent of full-scale OTEC power plant testing. There have been dozens of feasibility studies, site evaluations, and plant designs commissioned and developed over the last 30 years, but none of them have come to fruition due to a combination of high capital costs and cheap fossil fuels. With rising fuel costs and concerns over fuel supply and environmental damage, governments and industries are looking at OTEC again.

The past few years have seen a boom in OTEC activity. In 2009 Lockheed-Martin won a $12.5 million contract from the US Naval Facilities Engineering Command for a 10 MW pilot plant off the coast of Hawaii. Currently, work is still progressing on this project, with full-scale testing of the heat exchanger elements as well as tests on manufacturing and installing the cold water pipe [27,38]. In November 2011, the Natural Energy Laboratory of Hawaii Authority (NELHA) selected OTEC International LLC to build a 1 MW demonstration plant in Keahole, Hawaii [16]. NELHA is the Hawaiian state agency that funded and housed the Open Cycle OTEC plant that operated from 1992 to 1998, and is hoping to remain a global leader in OTEC by actively pursing demonstration and commercialization projects. There have also been various levels of discussions between OTEC companies and island communities for OTEC power generation, although whether or not any actual generation contracts have been signed remains unclear [15].

The potential for OTEC commercialization is greater now than it was 30 years ago because of the extensive growth and maturation of the offshore oil and gas industry. Oil and Gas platforms now operate a hundred miles off the coast, and in water that is thousands of feet deep, whereas most platforms in the 1970s were still limited to submerged towers located on the continental shelf. Building compressors, motors, and other large equipment for use in the offshore environment is also better

understood now than 30 years ago. These cross-over skills and technologies, along with the global focus on renewable energy by governments around the world, all bodes well for future OTEC technology development. OTEC proponents are cautiously optimistic about the future of OTEC, but time will tell if this is just another boom-and-bust like the 1970s.

2.4 Design Considerations of Major OTEC Plant Components and Subsystems

The size and capacity of OTEC power plants is usually described by the amount of net electricity they produce, i.e. a 100MW plant produces 100MW of electricity while it may actually produce 120 to 130MW of gross power. While there are many different proposed OTEC plant designs, they are all fundamentally the same in terms of operation and basic design. All closed cycle plants pump warm and cold water through heat exchangers to boil and condense a working fluid, which is flowing in a Rankine power cycle loop. Nearly all proposed plants pump the cold water to the surface through a large cold water pipe, though some have proposed locating the condenser portion of the power cycle at great depth. Figure 2.2 depicts a conceptual design by Sea Solar Power for a 100MWe OTEC power plant [2]. The basic components are indicative of OTEC plants in general, but the configuration and design varies greatly.

As seen in Figure 2.2, closed-cycle OTEC plants consist of a base platform, equipment for thermodynamic power generation, heat exchangers that transfer heat between the power cycle and ocean water, water pumps and piping to move the ocean water, and electric power transmission equipment to turn the thermodynamic power into electricity and transfer that power to the shore. This section will provide an overview of the major components and sub-systems within an OTEC power plant, as

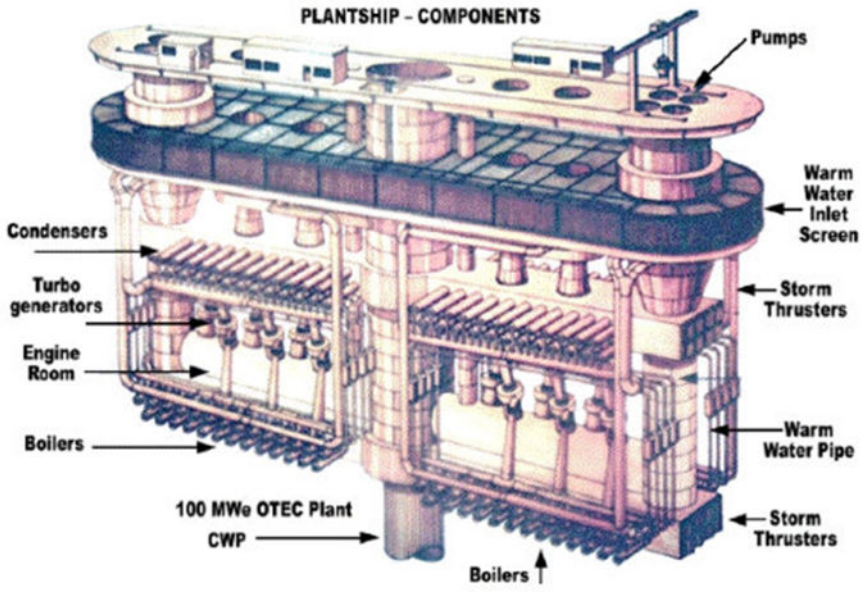

Figure 2.2: An OTEC power plant design, proposed by Sea Solar Power Inc. with major components labeled.

well as discuss the various nuances between different designs and component choices.

2.4.1 Plant Platform

There are two basic categories for OTEC plants: land-based and offshore. There are several benefits of a land-based plant. Capital, installation, and operational costs are kept lower for the power cycle portions of the plant because it is located on land, and the added complications of operating miles offshore are avoided. Aside from Mini-OTEC, all of the OTEC pilot plant projects have been land-based due to the added costs and uncertainty of operating a power plant on a floating platform.

While not being located directly in the water is a benefit in terms of ease of installation and maintenance, it is often a non-ideal solution from an efficiency standpoint because the cold water pipe must be miles long. The benefit of an offshore OTEC plant is can be located directly over the cold water source so that cold water

pumping distance is minimized, which in turn leads to a higher net power output for a given sized plant.

Thermal pollution is another potential issue for land-based plants; the cold discharge water must be pumped back out to sea, far away from the warm water intake. By operating out in the open water, the natural currents, combined with limited mobility, could allow floating plants to more easily avoid thermal degradation of the warm water source. These factors have prompted most large-scale OTEC plant designers to focus on floating platform designs.

Proposed designs for floating platforms range from retrofitted super-tankers, to fully submerged designs where all of the major components are located under water [52, 64]. Ship or barge type platforms are typically proposed because of the potential to retrofit an older vessel, as well as the knowledge base and fabrication capabilities at shipyards around the world. There are benefits and drawbacks to locating most or all of the plant's equipment inside of a hull or on a ship's deck. The power cycle and water systems are all easily reached for repair and maintenance, but the drawback is the added weight that must be displaced by the hull. There is a similar trade-off for locating equipment on top of a floating platform. Semi-submerged platform designs avoid much of the need to displace a large volume by locating equipment in equilibrium with the seawater. Exposed equipment adds complications from possible water leaks, corrosion, and servicing equipment. However, it could potentially reduce the overall size, and cost, significantly, and there could be added benefits in that the hydrostatic pressure of the water could help limit stresses on the heat exchangers from internal pressure [3].

Cold water resources for OTEC operation typically exist at depths greater than 3,000 ft, which is too deep for a sea-floor mounted tower structure, and so all

offshore OTEC platforms are floating designs. Because the platform is floating in the water, mooring or active station keeping with thrusters is required for an OTEC plant because it is tethered to the shore via an expensive and vital power transmission cable. The design must be flexible enough to allow the OTEC plant to move enough to avoid localized thermal degradation, but at the same time, it is important to minimize stresses on the power cable. There have been numerous studies on mooring systems and station keeping controls for OTEC systems, not to mention those already heavily used in the offshore energy industry already [9, 24, 47].

2.4.2 Ocean Water Systems and the Cold Water Pipe

Since an OTEC plant is driven by the low temperature differential of the ocean thermocline (thermal gradient), there are significant design considerations for all components involved in moving water and transferring heat in order to maximize performance while keeping costs minimal. The cold water pipe and water systems pumps are significant components of an OTEC plant, and both exemplify the kind of engineering challenges involved with designing an optimal plant.

The cold water pipe draws up thousands of gallons per second of cold water from depths of 1000 to 1200 meters (approximately 3,400 to 4,000 ft), depending on the local water temperature conditions. The amount of cold water needed on a per-MW of net power produced is typically approximated as 2 cubic meters per second (approx. 530 gal/second) [62]. Therefore, for a 20 MW plant, the cold water flow rate could be on the order of 10,600 gallons per second, and a 100 MW plant would have a cold water flow rate on the order of 53,000 gal/s. To move this amount of water, without significant pressure drop losses, a large pipe diameter must be used. Pipe diameters typically range from 4 meters for a 20 MW plant, up to over 10 meters for a 100 MW plant [4, 8, 62]. In order to move the massive volumes of water required,

equally massive pumps must be used. The design criteria for the OTEC water pumps dictate a very high flow rate, at very high efficiencies, but at a fairly low pressure. Therefore, OTEC water pumps are typically massive axial flow impeller pumps, which are well understood technology, with good efficiencies at large scales.

Different materials have been proposed for the cold water pipe, including steel, aluminum, rubber, concrete, plastic, and fiber-reinforced composites. The most important factors are weight, cost, durability, effects on pumping power, and ease of installation [32, 39]. Each material has varying benefits and drawbacks in these categories. For the later analysis, a smooth-sided material, as would be expected with a plastic or fiber composite, is assumed as the cold water pipe material. Most modern designs include fiber-reinforced composites due to its potential for extrusion of pieces on-site, allowing for easier and quicker installation. Another reason why the fiber-reinforced composites are being pursued is because they can be formed with internal cavities, which could allow for different sections of the pipe to be flooded to help keep the pipe and platform stable in the water [21].

Suspending a kilometer-long, meters-wide pipe from a floating platform presents a multitude of engineering problems, from complicated loading of the platform-pipe coupling, to challenges with installation logistics. These are significant design and installation challenges, and were one of the many factors holding back OTEC development in the 1980s. Dynamic loading of the cold water pipe from ocean currents could potentially lead to pipe or connection joint failure. There have been many studies of the potential problems from vortex-shedding-induced dynamic loads, which has led to many flexible plant-to-pipe joint designs [12, 54, 59]. Since the last OTEC boom, design and manufacturing technology has developed significantly, especially in the area of computer simulation and modeling, which have given designers much

better insight into how pipe and platforms perform without needing to build any physical models. There has also been significant development of similar large sub-sea piping technologies by the offshore oil industry over the same period, which could carry over to OTEC cold water pipe and platform connection design. While these issues are not the focus of this project, it is important to understand factors like these will ultimately affect the design.

2.4.3 Boiler and Condenser Heat Exchangers

Since the temperature gradient utilized by an OTEC plant is so small, the water flow rates have to be very large, and the heat exchangers must be as efficient as possible at transferring heat from one fluid to the other. There is a trade-off however, as the design must weigh added heat transfer capability with added pressure losses due to added viscous losses. Therefore, in designing the heat exchangers it is important to optimize performance and cost of the heat transfer area along with heat transfer coefficient and water flow rate.

The heat exchangers in an OTEC plant are massive due to the low operating temperature differential, with effective surface area requirements on the order of 7 m^2 per net kW of electricity produced. For a 20MW plant, the required area comes out to approximately 140,000 m^2, which is nearly 1.5 million ft^2; this calculation will be shown later with the thermal fluid systems analysis reference case in Section 4.2. Such a high area is needed because the goal is to minimize pressure and temperature changes in the water and working fluid so that maximum efficiency can be achieved. These high heat-duty, high flow rate heat exchangers have the same basic designs and operating principles of normal heat exchangers, but they are uniquely large, which means that custom heat exchangers are often required for reasonable performance.

There are three main types of heat exchangers that have been investigated

for OTEC heat transfer applications: Shell and Tube, Plate-Fin, and Plate Heat Exchangers (PHE). Shell and tube heat exchangers consist of large bundles of tubes housed inside of an outer shell. In the case of OTEC shell and tube heat exchangers, water is pumped through the small tubes, of which there are hundreds or thousands in parallel in each heat exchanger; the working fluid flows through the outer shell over the tube bundles, where the fluid is either boiled or condensed. Plate-fin heat exchangers are layered plates with bridging fins between them. The plates and fins are arranged and assembled to create alternating flow paths, which allows for high heat transfer surface area densities. Lastly, plate heat exchangers are individually grooved plates that when bolted or brazed together form small flow paths with very large surface area densities [53].

These heat exchanger types each have their strengths and weaknesses, and the analysis of which type is better really comes down to comparing individual designs due to all of the performance and cost variables. Upon further investigation, it was determined that such heat exchangers are nearly always custom built to order. General cost and performance data are typically not quoted unless a formal request is made, because of all of the dependencies on exact flow geometry, material types chosen, labor rates at the time, and a whole host of other variables. As such, the modeling and analysis for this thesis consider only the effective overall heat transfer coefficient and total pressure drop on the water side of the heat exchanger, and do not take into account the exact flow geometry or other variables into the heat transfer and pressure drop calculations. The modeling and the associated assumptions will be discussed in much more detail in the following chapter.

When compared with traditional power plants, these heat exchangers are an order of magnitude larger per net kW of electricity output because of the low cycle

efficiency. Most power plant cooling heat exchangers are operating with temperature differences of hundreds of degrees, so high heat flux can be obtained with a smaller area because the temperature difference is high. In this case the temperature difference is low, and so the overall heat transfer coefficient needs to be as high as it can be without adversely affecting pressure too much in order to help minimize the area. Ultimately, heat exchanger design for OTEC applications comes down to the cost of the heat exchanger compared to the heat transfer it can provide compared to the pressure drop it causes in the water. All of these factors have a large effect on the final cost of the plant, and by extension the cost of electricity.

2.4.4 Electrical Power Equipment and Transmission

The electric generators and transformers on the plant itself are not fundamentally any different from those in other power generation applications. There are added complications that come from the waterproofing and weatherization of the equipment for service in a sub-sea environment due to the corrosive nature of salt water and sea air. However, there could be a potential up-side if the equipment could be designed to use the sea water for increased thermal management ability, which could increase efficiency.

Getting the power from the platform to the shore is a daunting task, but the technology of making and laying such cables is much more mature now than when OTEC was first being developed. High voltage undersea cables crisscross the English Channel and North Sea, connecting Islands to the European mainland. There are also thousands of miles of undersea oil and gas pipelines that connect underwater production terminals to collection terminals, as well as the shore. While installing undersea power transmission cabling would be a non-trivial cost, it would not be unprecedented, and is technologically feasible.

2.4.5 Vapor Turbines and Power Cycle Working Fluid

The turbines used in an OTEC power plant are not typical multi-stage, large steam turbines used in steam power plants. The molecular weight and low cycle pressure difference make the design of an OTEC turbine similar to designs that are closer in performance and operation to that of a hydraulic turbine, like those found in hydroelectric dams [4]. The turbines are typically single stage, either axially or radially designed. Because the tip velocity of the turbine blades is relatively low and the operating temperatures are on the order of room temperature, the turbine material and fins do not have to be high performance super-alloys like those found in combustion gas or superheated steam turbines [6]. Sea Solar Power Inc has designed an OTEC-specific radial-flow turbine that should have an efficiency above 90%. A rendered model of the Sea Solar Power turbine is provided in Figure 2.3 [36].

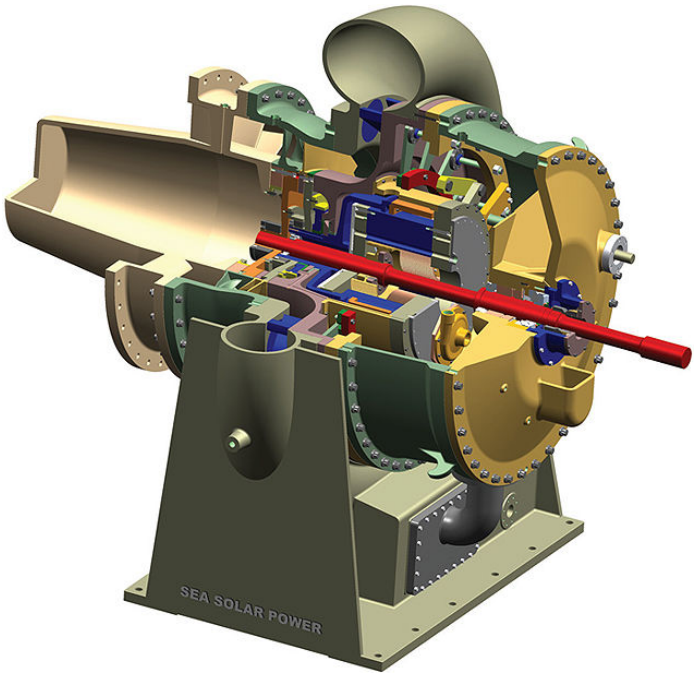

Figure 2.3: Sea Solar Power has designed a radial flow turbine specifically for use in OTEC applications.

Different power cycle working fluids have been proposed for closed cycle OTEC plants, but most designs use ammonia as the working fluid due to its superior thermal properties. Other working fluids have been analyzed and proposed for use, including propane, propylene, R-134a, and other refrigerants and hydrocarbon fluids. James Anderson performed an analysis of potential working fluids, taking into account factors such as fouling potential, and determined that ammonia is a sub-optimal choice, and that R-134a was a better compromise between thermal performance and fouling potential [6]. The issue at hand is that grease and other oils from bearings might leak into the working fluid; these are dissolvable into R-134a, but not into ammonia, and therefore the ammonia might end up depositing the undissolved material into those areas with small passages and large surface areas–the heat exchangers [6]. The effect of the fouling could potentially negate the thermal performance gains in the long run, and therefore it would be better to design a system from the beginning around a better working fluid. Based on this argument, this thesis uses R-134a as the working fluid.

These fluids, including ammonia, are used for the working fluid instead of water because they boil and condense at the provided water temperatures under moderate pressure. Water must be de-pressurized to a few kPa to boil and condense in these temperature ranges, whereas the hydrocarbons operate at several hundred kPa. The higher pressure is only a few atmospheres, and if placed at the correct depth, the power cycle and related components could be effectively at neutral pressure with the surroundings; with a very low pressure water vapor, the system would be buoyant, and there would be a great potential for external ocean water leaking into the power cycle.

2.5 Potentially Viable Locations for OTEC Power Generation

Hawaii has been the primary focus of OTEC research and development for the US, but it is not the only location with viable OTEC resources, even in the US. Hawaii has the benefit of being a volcanic island in the middle of the ocean. The water becomes deep relatively close to shore, compared to a continental shelf. Puerto Rico has the benefit of being near oceanic trenches, and so it also has cold water resources close to the shore. There have been studies on other potential North American locations such as the coasts of Florida, or other coastal Southeastern states, where the OTEC resource is a hundred miles or more from shore. The cost of the electric cabling would obviously be much higher, but access to the coast, and hence the US electric grid, could mean that a larger plant could be built to meet a larger demand.

Generally, for OTEC to be a viable power generation option for a location, there are a few basic constraints. The first and most important is the temperature differential of the ocean water nearby; even if the surface temperature is very warm, OTEC might not be viable if there is a lack of a cold water heat sink. The lack of cold-water resources is the limiting factor for areas such as the Middle East, where water temperatures can approach 90 °F on occasion, but the seas are shallow and so the water near the bottom is still quite warm. Another constraint is the cost of electricity for the area. For an island community like Hawaii, which is in a very remote location, the cost of generating power is much higher than the cost on the main land because fuel and equipment must be shipped halfway across the Pacific ocean. The high cost of power for island communities offers a potential opportunity for OTEC developers to build a smaller-scale pilot plant that would still be financially viable for electricity generation.

The west coast of Africa has access to good thermal resources, as does the southern pacific coast of Mexico. India has been pursuing OTEC because of its rapidly growing electricity needs and relative lack of pre-existing infrastructure. Various Indian institutions have performed feasibility studies, and a 1MW plant was actually pursued in the early 2000's but was never successfully put into operation [46]. Many hopeful proponents see OTEC as a potentially long-term solution for the developing countries near the equator who have coastal access to the thermal resources. However, OTEC projects are capitally intensive and unproven in the real world over years of operation, which are huge hurdles OTEC plant builders would first need to overcome.

2.6 Environmental Concerns regarding OTEC Plant Deployments

The primary environmental concerns relate to the unintended consequences of pumping such massive amounts of cold water to the surface. One such concern is about what will happen because of all the nutrients pumped up with the cold water. There are concerns of large algal blooms forming around the plant, which could lead to a dead-zone if the water becomes deoxygenated [35, 57]. However, some think that the redistribution of nutrients to the surface could also help promote regrowth of fish stocks by increasing food at the bottom of the food chain [4]. To help negate the problem, many designs intend to mix the warm and cold waters, and re-inject them back at a depth well below the surface.

The other primary concern is the long-term potential effect on local water temperature and salinity. It the surface temperature is decreased, or salinity increased, over time due to the massive cold water draws, then local wildlife could be affected. There are also concerns about large-scale OTEC operations affecting weather patterns or ocean currents [35, 57].

In the end, most of these large-scale effects involve Gigawatts of OTEC power production operating for decades. At this point, trying to determine the effects OTEC will have on the environment will ultimately be speculation. Until a full-size plant is built and operated for years, the environmental impacts will be unknown.

Chapter 3

Thermal-Fluid Systems Modeling of a Closed Cycle OTEC Plant

3.1 Introduction

In order to analyze the operation of a closed cycle OTEC plant, a simplified integrated systems model was developed from basic principles of thermodynamics [50], fluid mechanics [30], and heat transfer [34]. For this project, the operation of an OTEC power plant was reduced to three main sub-systems: the power cycle, the hot and cold water systems, and the heat exchangers. Each sub-system has its own governing equations, which were simplified to provide a reasonable approximation of how the sub-system would operate. Figure 3.2 shows a simple single stage OTEC plant schematic, with all the major power producing components labeled, as well as the major sub-systems identified. The power cycle is made up of the turbine, the condenser, the working fluid pump, and the boiler. The hot and cold water systems are represented in this diagram by the red and blue lines, as well as their respective pumps. These two systems interface in the boiler and condenser heat exchanger–the third sub-system. For simplicity, auxiliary equipment and control systems are left out of the model, and are not shown Figure 3.2. This schematic also introduces some of the terminology and variables that will be referenced throughout the rest of the analysis.

This diagram helps to capture how the flow of heat energy driving the plant, from the water systems, is dependent on the electrical output of the plant, from the

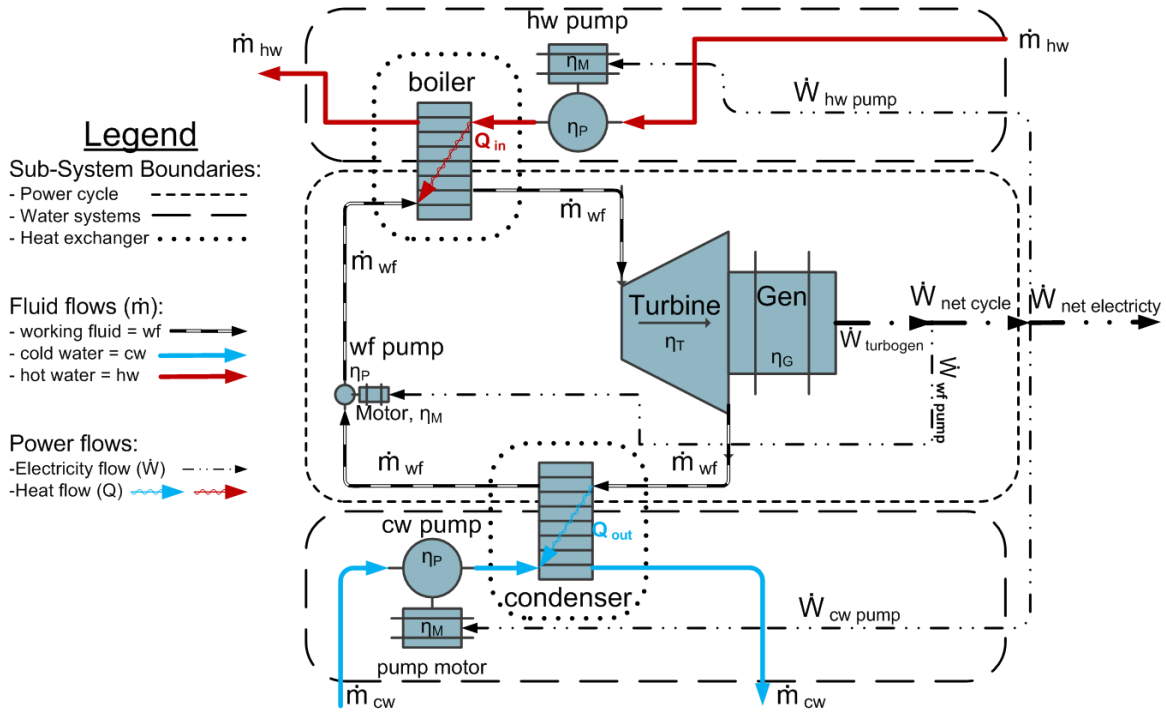

Figure 3.1: A Single Stage OTEC plant diagram highlighting the major components important to power generation.

power cycle, and passes from one sub-system to the other through the heat exchangers. This chapter will explore the modeling of this interaction by looking at the governing equations for each sub-system. First, this chapter will discuss how the operation of the plant was modeled using simplified thermodynamic, fluid flow, and heat transfer equations, as well as discuss the assumptions made in order to simplify the system modeling. Included in the description of the plant modeling will be discussion of some of the underlying physical phenomena that affect system performance, particularly in the heat exchanger sub-system. After discussing the development of the system equations, this chapter discusses the approach taken in programing the model in MATLAB. This section includes a discussion of the MATLAB programs hierarchy and operation, as well as a description of how the thermodynamic properties are calculated.

3.1.1 Modeling Literature Review

While this model was an original creation, modeling of OTEC systems has been a major topic of OTEC research, and there exists numerous papers that focus on various systems and components. The model developed for this paper is similar to many done previously, but differs in a few key ways discussed below [55, 58, 66, 67].

In 1987, a 5kW OTEC model and corresponding experimental module were developed by Hiroyuki Takazawa and Kajikawa Takenobu and documented in the paper entitled "Sensitivity Analysis of Ocean-Based Closed Cycle OTEC Power System" [58]. The model and test loop were primarily developed to better understand the effects of inlet water temperatures and water flow rate. The model was not an entirely first principles model, with correlations and curve fits developed from the testing to help bring the model into agreement with the test results. The power cycle was a single-stage system running ammonia as the working fluid, with artificially chilled and heated water used to represent the cold and hot ocean water [58].

A modeling effort more along the lines of the modeling work performed in this thesis was done by Wu and Burke in the 1997 journal paper "Intelligent Computer Aided Optimization on Specific Power of an OTEC Rankine Power Plant" [66]. This paper focused on optimizing the pressure in the condenser and boiler in order to maximize the gross power output per unit of heat exchanger area. The performance analysis in Chapter 4 uses a similar metric (net power output per unit heat exchanger) as one measure of performance, however other performance metrics are also employed. Additionally, unlike the modeling performed in this thesis, their model was of the power cycle only, and did not include the impacts of heat exchanger area or water pump power demands [66].

One of the more recent and in-depth modeling efforts was performed by Rong-

Hau Yeh, et. al. in the 2005 journal paper "Maximum Output of an OTEC Power Plant" [67]. Like the modeling performed in this thesis, the plant model in the Yeh paper is a full systems model of a plant, including water system and detailed modeling of the heat exchangers. The model is specifically for a single stage Rankine cycle, with shell and tube heat exchangers, and an ammonia working fluid. The heat transfer and water systems models use convection equations developed for shell and tube heat exchangers based on their diameters, wall thickness, etc. and also uses the specifics on the heat exchanger tubes to perform the water system pressure drop calculations. While the detailed model is more representative of an actual system than the modeling in this thesis, the more generalized thesis model allows for flexibility is comparing systems with different heat exchangers by just using heat transfer coefficient scaled with water velocity [67].

The performance model developed in the subsequent sections is unique from these models because it has the capability to model cascaded power cycle stages. Additionally, unlike several of the models mentioned above, it does account for the heat exchanger and water systems in an attempt to gain an overall systems perspective. This work is not meant to be an exact model of the actual performance, but rather it is meant to help understand the underlying impacts of the interactions of the different sub-systems. As part of the original research scope, and independent model was developed from fundamental thermodynamics, heat transfer, and fluid mechanics relationships, and therefore none of the modeling from the above papers was used in the modeling process.

3.1.2 Initial Simplifying Assumptions

This model is meant to provide a first-cut analysis of an OTEC plant based on a limited number of design variables. The model is by no means a true operational

simulation or design analysis, but rather an investigation into the general relationships between certain major design and operational variables and the performance of the plant.

There are several simplifying assumptions inherent in this model:

- The plant operates under steady-state conditions; there are no dynamic changes in temperature, velocity, or mass flow rates,
- Heat losses (and gains on the condenser side and in the cold water pipe) to the surroundings are negligible,
- Phase change occurs at a constant temperature and pressure for a single-component fluid; the effective specific heat of the fluid is infinite because the saturated fluid will not increase in temperature with added heat (only change phase),
- The heat transfer coefficients are assumed to be the average of the heat exchanger, and constant throughout,
- All fluid temperatures are the average, or bulk temperature at that location,
- All fluid velocities are assumed to be uniform and constant throughout the plant, and
- All water properties (density, viscosity, specific heat) are considered constant, and at their respective inlet temperature,
- All liquids are assumed to be incompressible.

These assumptions allow for the simplification of what would otherwise be overwhelmingly complex equations into more manageable ones that are more easily calculable. While understanding the transient operation of the plant would ultimately

be important, studying such effects are not the purpose of this model. Rather, this model is meant to provide a first-cut look as to whether or not a set of design and operating parameters are viable.

The heat transfer with the surroundings are assumed to be negligible because the thermal gradient between the inside and outside of the plant is small, and more importantly, calculating the heat loss would be highly design- and materials-specific. The phase change is assumed to be at a constant temperature and pressure in order to simplify calculations, and because the pressure drop is very small in comparison to the overall pressure drop across the turbine. The heat transfer coefficient is assumed to be the average, and constant throughout, because it greatly simplifies the heat exchanger area calculation. Further analysis of required the heat exchanger area would be needed to determine more accurate heat exchanger requirements, but assuming an average is accurate enough for preliminary modeling.

Assuming bulk temperatures and average flow rates avoid integrations that would be dependent on specific geometries and flow conditions, which help broaden the model while still keeping it grounded in the fundamentals. Assuming constant properties for the hot and cold water is reasonable for this model because the temperature change between the inlet and exit is small, and the resultant change in properties is on the order of fractions of a percent.

3.2 Thermodynamic Modeling of the Power Cycle Sub-system

This section describes the governing thermodynamics of the power cycle, and develops a system of simplified equations based on certain assumptions. For a glossary of thermodynamic terms and symbols please see Appendix A; more information on the fundamentals of thermodynamics can be found in the cited textbook, or any other

introductory thermodynamics textbook [50]. There are several important simplifying assumptions made in this model, in order to keep the calculations simple and the general.

The boiling and condensing temperatures are assumed to indirectly specified variables. This will be discussed in much greater detail in Section 3.3.

The working fluid flow rate is assumed to be constant throughout the entire plant. This assumption is not exactly true in an actual plant because typically there is a fluid recirculation loop that pumps un-boiled fluid out of the boiler back into the incoming fluid stream. This operation would typically occur if the heat exchanger was not providing the expected heat transfer, due to either lower than expected temperature differentials, or lower than expected heat transfer coefficient. fluid flow rate is also a function of heat exchanger design. Poor fluid flow inside the shell could leave stagnant areas where the working fluid is not receiving much heat flux.

This model also makes uses the incompressible fluid assumption. The feed pump pressurization is assumed to equal to the change in pressure multiplied by the specific volume of the working fluid at the initial pressure. This assumption is reasonable because the working fluid is only pressurized by a few hundred kPa (the change in density is very small).

The temperature at state 2 is assumed to be the condensing temperature (i.e. the same as state 1). This assumption is not completely accurate, especially since the pump is not modeled as isentropic. However, any heating that occurs from the pump offsets heating that must be done in the boiler. The working fluid pump power might be underestimated, and the working fluid temperature might be low, but this underestimation is balanced out by the slight increase in required heating in the boiler, which means more hot water needs to be pumped, and so these essentially

cancel out each other.

The working fluid flowing into the boiler is assumed to be completely phase changed to vapor (i.e. the quality is 1). This assumption is optimistic , and many actual plant designs have vapor separators because the quality, x, of the saturated vapor is typically taken at .9 to .97, and separated out to .99 quality.

There is also assumed to be no pressure drop in the working fluid inside any of the piping or the heat exchangers. Literature typically cites pressure drops on the order of approximately 10 kPa (1-2 psi), but the overall change in pressure is on the order of 150kPa, so the drop is something relatively non-trivial. However, since the pressure drop occurs in the phase-changing portion of the cycle, where Saturation temperature and pressure are non-independent variables, it can be assumed the pressure drop manifests as a lower boiling temperature or higher condensing temperature. For simplification purposes, we will assume the pressure drop is accounted for in the assumed terminal temperature difference specified for the heat exchanger.

It is assumed there is not any super-heating of the working fluid in the boiler, and expansion through the turbine is assumed to be all the way to the saturated pressure of the condenser. This assumption is relatively reasonable because the temperature differences are so low in the heat exchanger, it would require a significant amount of added surface area to appreciably increase the vapor temperature. Expansion into the saturated vapor phase is a safe assumption for an organic working fluid because the saturated vapors low temperature, low turbine tip speed, and non-corrosive nature do not endanger the turbine, as it does in a typical steam turbine.

Based on these assumptions, a simplified model of the power cycle was developed. The cycle was modeled as a low temperature Rankine cycle using an organic chemical working fluid. The design parameters that are used for calculations in this

section include: the working fluid mass flow rate, the inlet and outlet temperatures of the hot and cold water, the number of power cycle stages, and the terminal temperature difference between the water and the working fluid in the heat exchangers. The water temperatures and terminal temperature differences indirectly set the boiling and condensing temperatures. The relationships between all of these variables are discussed in much greater detail in Section 3.3, the section focused on the heat exchangers sub-systems. The number of stages only affects the boiling and condensing temperature, and does not change the operation of the power cycle; each stage is it's own complete power cycle. Figure 3.2 shows the power cycle State relations for the idealized Rankine cycle. The simple ideal Rankine cycle model calculates the work output from the power cycle and cycle efficiency based on the specified design parameters.

There are four principal states in a Rankine cycle, and four principal processes. the first process, from state 1 to state 2, pressurizes the saturated liquid working fluid from the condenser temperature and pressure to the saturation pressure of the boiler. Next, from state 2 to state 3, the working fluid is boiled to change phase from a liquid to a saturated vapor. The vapor is then expanded through a turbine to generate work from state 3 to state 4. Finally, from state 4 to state 1, the saturated liquid-vapor mix is condensed back down to saturated liquid. The thermodynamic equations governing this process will now be explained.

The 'Zeroth' Law of Thermodynamics begins the thermodynamic modeling; during steady state operation, all of the mass is conserved on both the water and working fluid sides. The mass flow rate of the working fluid, $\dot{m}_{wf}$, flowing into pumps, turbines, and heat exchangers is equal to the $\dot{m}_{wf}$ flowing out. Hence $\dot{m}_{wf}$ is constant, and assumed to be constant across all stages of the power cycle. This mass

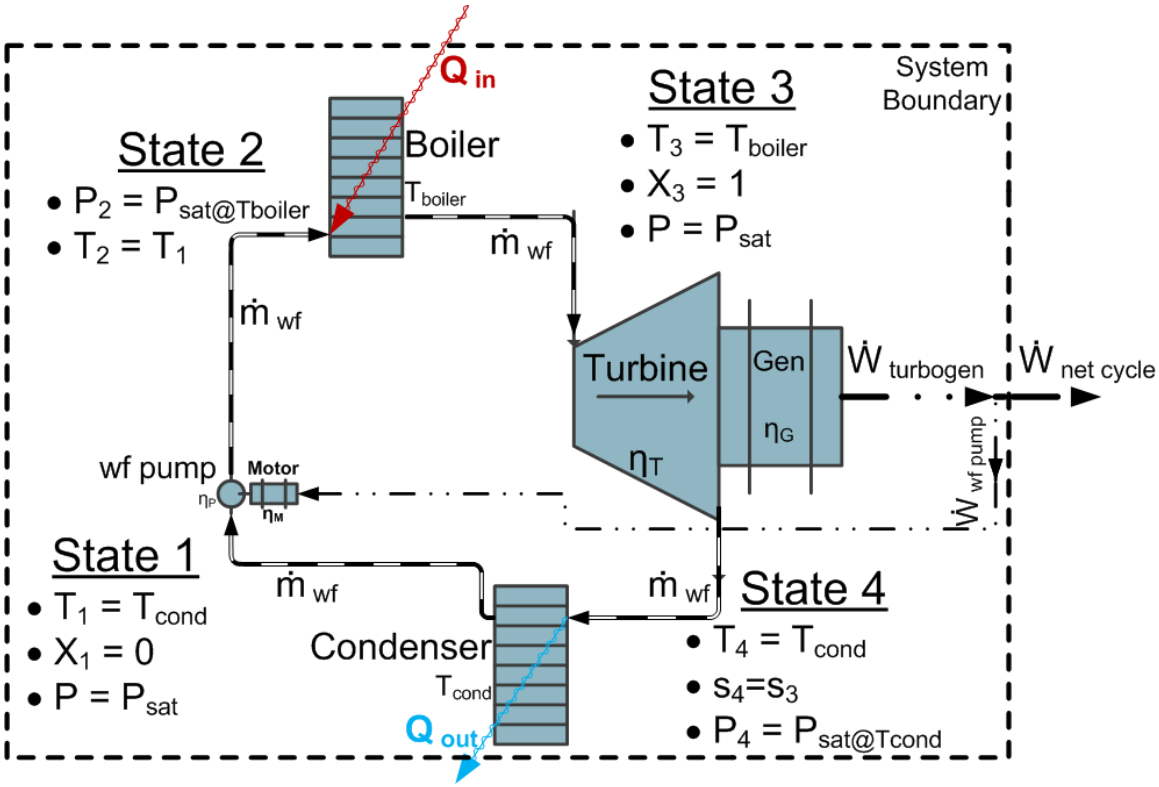

Figure 3.2: The OTEC power cycle State relations are modeled as an idealized Organic Rankine Cycle.

conservation balance is represented in Equation .

$$\dot{m}_{wf,in}\left[\frac{kg}{s}\right] = \dot{m}_{wf,out} = \dot{m}_{wf} = const. \tag{3.1}$$

The water mass flows through the heat exchangers are outside of the power cycle system boundary, but the heat exchange between water and working fluid passes through the boundary. These flows of heat into and out of the system are $\dot{Q}_{in}$ and $\dot{Q}_{out}$ respectively, and are shown in Figure 3.2 as the red and blue arrows. The difference between the heat transferred into and out of the system ultimately leads to the net power produced, $\dot{W}_{net,cycle}$, plus losses from inefficiencies in the turbine, generator, pump, and motor. This relationship is the conservation of energy, the First Law of

Thermodynamics, and is presented in Equation 3.2.

$$\dot{Q}_{in}\,[kW] - \dot{Q}_{out}\,[kW] = \dot{W}_{net,cycle}\,[kW] + \sum losses\,[kW] \tag{3.2}$$

The formulation of $\dot{W}_{net,cycle}$ from $\dot{W}_{turbogen}$ and $\dot{W}_{wf,pump}$ is given in Equation 3.3, and the calculation for the losses term is given in Equation 3.4. The *losses* are specifically mechanical-to-electrical conversion losses from converting shaft work to electrical power through the generator with an efficiency of $\eta_G(\leq 1)$. Similarly, the pump motor converts electrical power back to shaft power for the working fluid pump with an efficiency of $\eta_M(\leq 1)$. The purpose for such accounting is due to the assumption that the power cycle would not directly drive the feed pump or the water pumps, but rather generate electricity to power the pumps' motors.

$$\dot{W}_{net,cycle}\,[kW] = \dot{W}_{turbogen}\,[kW] - \dot{W}_{wf\ pump}\,[kW] \tag{3.3}$$

$$\sum losses[kW] = (1-\eta_G) \times \dot{W}_{turbogen}\,[kW] + (1-\eta_M) \times \dot{W}_{wf,pump}\,[kW] \tag{3.4}$$

These equations account for the overall flow of energy into and out of the plant, but they do not capture the processes within the power cycle that convert the thermal energy to mechanical. $\dot{Q}_{in}$, $\dot{Q}_{out}$, $\dot{W}_{turbogen}$, and $\dot{W}_{wf,pump}$ are all calculated outputs of the model, and solved for with the specified temperatures and working fluid mass flow rates. The four individual processes and the respective governing thermodynamics relations that make up the Rankine power cycle will now be examined. For a more complete explanation of the thermodynamic terms and symbols used in these equations, please see Appendix A, or consult an introductory Thermodynamics textbook.

Traditionally analysis of the power cycle starts at the lowest energy state, where the low pressure condensate has just exited the condenser; this is State 1.

Both Equations 3.5 and 3.6 represent the power required by the pump to change the working fluid properties from State 1 to State 2. In Equation 3.5 , the pump power input, $\dot{W}_{wf,pump}$, compresses the working fluid, which increases the enthalpy, h, from h_1 to h_2, with a working fluid mass flowrate of $\dot{m}_{wf}$.

$$\dot{W}_{wf\ pump} = \frac{\dot{m}_{wf} \times (h_{2s} - h_1)}{\eta_P} \tag{3.5}$$

For simplification purposes, and because of the relatively low magnitude change in pressure, the working fluid is assumed to be incompressible. Based on this assumption, the change in enthalpy can be approximated as Equation 3.6. The variable v_1 is the specific volume at stage 1, and is equivalent to $\frac{1}{\rho}$.

$$\dot{W}_{wf\ pump} = \frac{\dot{m}_{wf} \times v_1 \times (p_2 - p_1)}{\eta_P} \tag{3.6}$$

The denominator is the pump efficiency, $\eta_P (\leq 1)$, and it adjusts the isentropically calculated pump power requirement to the actual power requirement. Since the beginning and ending states are specified, the inefficiencies do not decrease the actual pressure at Sate 2, but rather more power is required to reach State 2.

From State 2 to State 3, the working fluid is heated to the saturated temperature, and then boiled into a vapor. Equation 3.7 balances the incoming heat ($\dot{(Q)}_{in}$) from the hot water with the enthalpy change in the working fluid ($h_3 - h_2$) from the compressed liquid at State 2 to the saturated vapor at State 3. The pressure drop in the working fluid across the boiler is assumed to be zero. Equation 3.8 breaks apart the enthalpy change into the heating of the working fluid from liquid at T_2 to saturated liquid at T_3 ($T_{3,sl} - T_2$), and then the constant temperature phase change from saturated liquid to saturated vapor ($T_{3,sv}$). The energy required to vaporize a saturated liquid, which is the same as the difference between h_{sl} and h_{sv} is referred

to as the latent heat of vaporization, and is often given as a single value, h_{lv}, which is shown in Equation 3.8.

$$\dot{Q}_{in} = \dot{m}_{wf} \times (h_3 - h_2) \tag{3.7}$$

$$\dot{Q}_{in} = \dot{m}_{wf} \times [h_{3,lv} + (h_{3,sl} - h_2)] \tag{3.8}$$

From State 3 to State 4, the working fluid vapor is expanded through the turbine, which produces the power output that drives the plant. As shown in Equation 3.9, the turbogenerator's mechanical power output, $\dot{W}_{turbogen}$ is equal to the difference between the enthalpy at State 3 minus the isentropic enthalpy of the expanded vapor mixture at State 4, multiplied by the working fluid mass flow rate and the turbine efficiency, η_T. The 'isentropic enthalpy' refers to the enthalpy that the vapor mixture would reach at State 4 if the turbine were 100% efficient.

$$\dot{W}_{turbogen} = \eta_T \times \dot{m}_{wf} \times (h_3 - h_{4_s}) \tag{3.9}$$

A 100% efficient turbine means that all of the thermal energy is expended reversibly, and that as a consequence, the entropy, s of the vapor is constant from State 3 to State 4, as shown in Equation 3.10. This relationship is required to calculate h_{4_s}, and by extension h_4.

$$s_3 = s_4 = const. \tag{3.10}$$

In order to calculate the h_{4_s}, the quality of the vapor mixture at State 4, x_{4_s} must be calculated. Quality refers to the mass fraction of vapor to liquid in the saturated mixture, and by extension, can be calculated with any of the thermodynamic properties. Equation 3.11 uses the insentropic assumption's entropy, which is a thermodynamic property known at State 4, to calculate x_{4_s}. To learn more about the calculation of quality, please see Appendix A. With the isentropic quality, Equation 3.11 calculates

h_{4_s} by taking the calculated fractions of the saturated liquid and saturated vapor enthalpies. Equation 3.12 shows how to similarly calculate the actual enthalpy of State 4, h_{4_a}, with use of h_{4_s} and η_T.

$$h_{4_s} = x_{4_s} \times h_{sv} + (1 - x_{4_s}) \times h_{sl} \tag{3.11}$$

$$h_{4_a} = h_{4_s} + (1 - \eta_T) \times h_3 \tag{3.12}$$

In the last step, the excess heat energy, which is the energy latent in the working fluid that is still vapor, must be expelled from the plant to get from State 4 back to State 1. The working fluid is fully phase changed from a saturated vapor mixture back into a liquid inside the condenser. Equation 3.13 relates the heat that must be rejected from the plant and absorbed by the cold water, $\dot{Q}_{out}$, to the change in enthalpies from State 4 to State 1.

$$\dot{Q}_{out} = \dot{m}_{wf} \times (h_{4_a} - h_1) \tag{3.13}$$

Once back at State 1, the cycle begins anew. Figure 3.3 illustrates this cycle with a 'Temperature-entropy', or T-s diagram. A T-s diagram is a useful method for visualizing the states and processes that occur to create a thermodynamic cycle, and they are useful for visualizing the energy flows in and out of the system. The area inside the cycle represents the power output of the cycle, while all of the area below the red line represents the heat flow required to generate that output.

The area under the red lines is proportional to the amount of heat flow in, $\dot{Q}_{in}$, required for the cycle; the area under the blue line on the bottom is proportional to the amount of heat that must be carried away by the cold water, $\dot{Q}_{out}$. The working fluid pump power, here $\dot{W}_{pump}$, required to pressurize the working fluid is negligible, and appears as a point on this graph. Finally, the turbogenerator's power

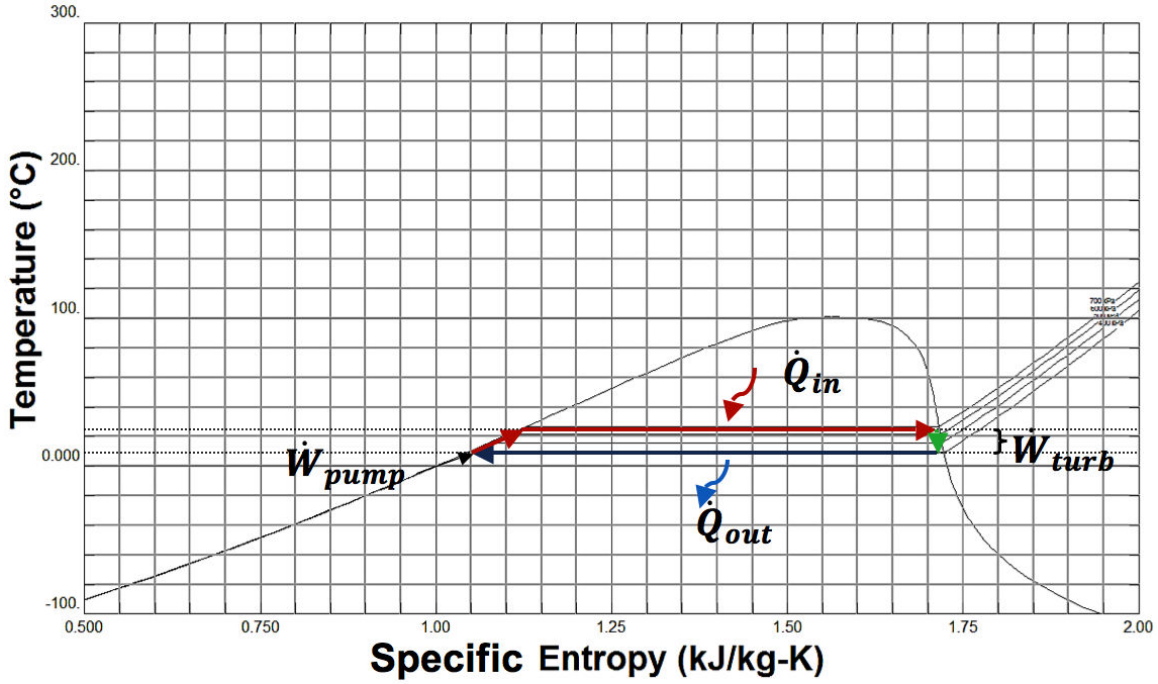

Figure 3.3: T-s diagram of the Rankine Cycle used in the power cycle sub-system model.

output is proportional to the modest green arrow to the right of the cycle, as pointed out by $\dot{W}_{turb}$ with the bracket. The T-s diagram demonstrates very succinctly how almost all of the heat coming into the plant is ultimately passed through to the cold water. This startling inefficiency is an unavoidable consequence of the Second Law of Thermodynamics and the low temperature differential.

3.2.1 Power Cycle Staging for Increased Performance

The single stage ideal cycle provides an idea of the scale of the operating conditions of an OTEC plant. However, to maximize the thermal resource available it might be advantageous to stage power cycles, which effectively increases the operating temperature differential and improves the thermodynamic efficiency. A second iteration of the power cycle model incorporates the ability to model multiple stages

operating at cascaded boiling and condensing temperatures in order to maximize the use of the water temperature differential. The schematic of this operation is provided in Figure 3.4. The water flows out of one heat exchanger into the next, and the hot and cold water are fed in from opposite directions.

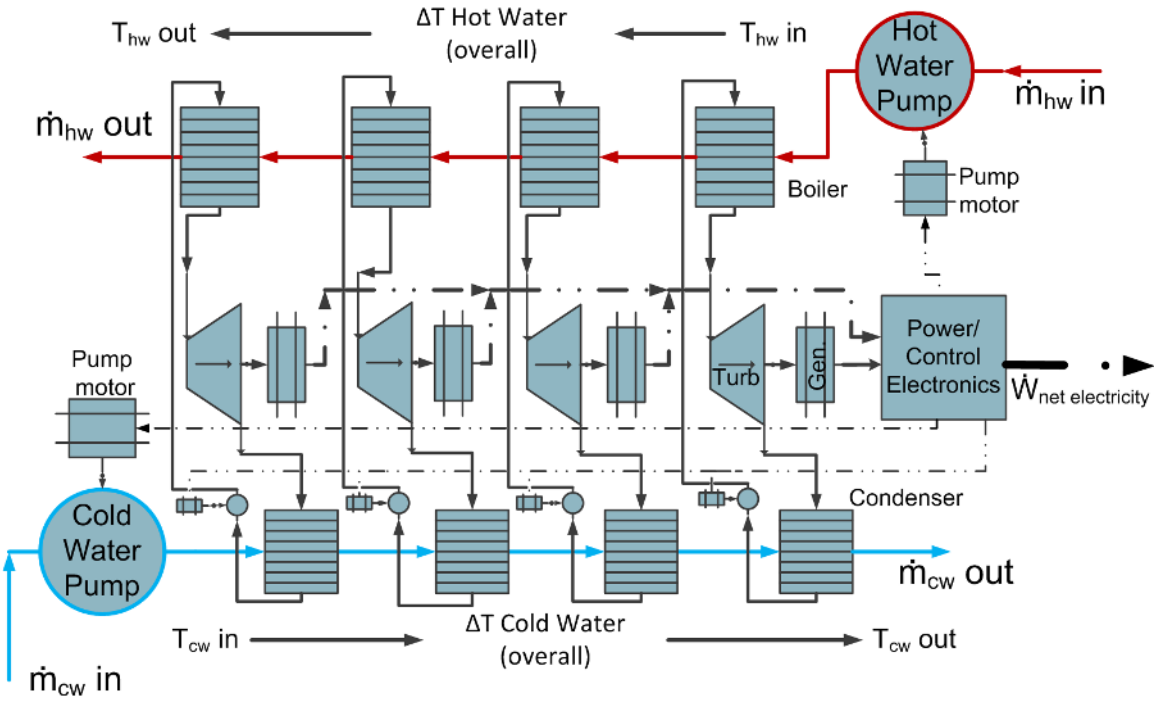

Figure 3.4: Multiple power cycles can be utilized in order to make use of more of the temperature differential.

The mass flow rate and temperature difference across each stage are functions of the number of stages, n, such that the individual mass flow rate and temperature changes all add up to the same amount overall, regardless of the number of stages. Fixing the overall working fluid mass flow rate, $\dot{m}_{wf,total}$, and overall water temperature changes, $(T_{cw\ out} - T_{cw\ in}) = \Delta T_{cw,overall}$ (similarly for $\Delta T_{hw,overall}$), allows for a comparison between plant configurations with different numbers of stages, while keeping the overall temperature differential across the plant constant. Equations 3.14 and 3.15 show the calculations for working fluid mass flow rate per stage, $\dot{m}_{wf,stage}$,

and the water temperature changes per stage, $\Delta T_{cw,stage}$ and $\Delta T_{hw,stage}$.

$$\dot{w}_{wf,stage} = \frac{\dot{m}_{wf,total}}{n_{stages}} \tag{3.14}$$

$$\Delta T_{cw,stage} = \frac{\Delta T_{cw,overall}}{n_{stages}}, \Delta T_{hw,stage} = \frac{\Delta T_{hw,overall}}{n_{stages}} \tag{3.15}$$

Since the inlet temperature is known, and the outlet temperature is specified, the temperature change in the water sets the necessary water mass flow rate to provide the proper amount of heating or cooling. The specifics of these calculations are discussed in greater detail in Section 3.3 on the heat transfer between the power cycle and the ocean water via the heat exchangers. More important for the power cycle calculations are the boiling and condensing temperatures in each of the stages. This model specifies a Terminal Temperature Difference, TTD_{cond} and TTD_{boiler}, which is the temperature difference reached between the exiting water and the exiting working fluid. In order to find the condenser and boiler temperatures ($T_{cond,i}, T_{boiler,i}$) for a stage i, the TTD temperature difference is either added (in the case of the condenser) or subtracted (in the case of the boiler) from the water temperature exiting from that stage. Equations 3.18 and 3.19 demonstrate how to calculate these values. Equations 3.16 and 3.17 show how to calculate the exiting water temperatures for a stage i ($1 \leq i \leq n$), which are needed to find $T_{cond,i}$ and $T_{boiler,i}$.

$$T_{cw,out,i} = \sum_{1}^{i} \Delta T_{cw,stage} + T_{cw,in} \tag{3.16}$$

$$T_{hw,out,i} = T_{hw,in} - \sum_{1}^{i} \Delta T_{hw,stage} \tag{3.17}$$

$$\Delta T_{cond,i} = T_{cw,out,i} + TTD_{cond} \tag{3.18}$$

$$\Delta T_{boiler,i} = T_{hw,out,i} - TTD_{boiler} \tag{3.19}$$

The condensing and boiling temperatures are based on the specified terminal temperature difference and the exiting water temperature for that stage, which

additionally means that the plant no is no longer limited to a single boiling and condensing temperature difference. The exiting water temperature for each stage is no longer the ultimate exiting water from the plant, which in turn increases the boiling temperature, or decreases the condensing temperature. This effect can be seen in Figure 3.5 which is a hypothetical T-s diagram for an ideal Carnot cycle. The shaded area is proportional to power; staging increases the amount of energy that can be captured from the given water temperature difference. Increasing the temperature differential improves the thermodynamic efficiency of each cycle, and hence the overall thermodynamic efficiency of the overall power generation system.

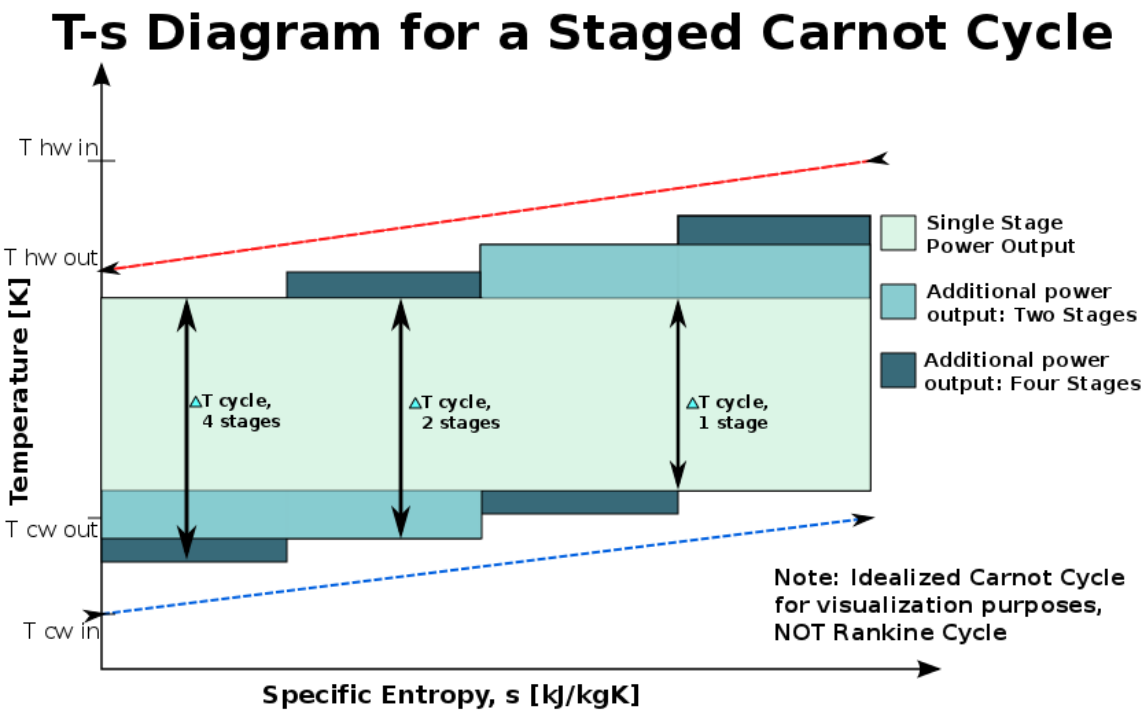

Figure 3.5: The highlighted area represents energy; staging increases energy generation capabilities, with the same water temperature differentials.

If the water temperature changes in the hot and cold water are approximately the same, then the net effect is an increase in the average ΔT across the entire

plant ($T_{boiler} - T_{cond}$), as compared to a single cycle with the same set temperature parameters. In an OTEC plant, the overall cold water temperature change is often higher than that of the hot water. Therefore the cycle temperature differential is different cycle-to-cycle, but staging still have the same beneficial effect.

Staging leads to the effect of several miniature power cycles operating in parallel, utilizing a greater amount of the temperature differential than would be available to a single-stage plant operating with the same overall conditions. In addition to staging, a more detailed model beyond the power cycle is needed to provide a more comprehensive look at the plant's operation, which will in turn provide a more complete picture of the overall plant efficiency.

3.2.2 Heat Engines and Carnot Efficiency Calculations

Calculating the ideal thermodynamic efficiency is beneficial because it provides a means of assessing the operation of the power cycle, and its utilization of the available resources. Heat engines are often described in terms of their thermodynamic efficiency, and compared with their corresponding theoretical maximum efficiency. Equation 3.20 defines the Heat Engine Efficiency as the net work from the cycle, $\dot{w}_{net\ cycle}$, divided by the heat input into the cycle, $\dot{Q}_{in}$, required to produce that work. The net work is also equal to the difference between the incoming and outgoing heat, which is also expressed in Equation 3.20.

$$\eta_{HE} = \frac{\dot{W}_{net,cycle}}{\dot{Q}_{in}} = \frac{\dot{Q}_{in} - \dot{Q}_{out}}{\dot{Q}_{in}} = 1 - \frac{\dot{Q}_{out}}{\dot{Q}_{in}} \tag{3.20}$$

Therefore, to maximize thermodynamic efficiency, $\dot{Q}_{out}$ must be minimized in relation to $\dot{Q}_{out}$. The relationship between the two is governed by the Second Law of Thermodynamics, which places an upper bound of the amount of heat that can be utilized by the system. For a closed system, the change in entropy from one state to

another is greater than or equal to the sum of the heat transfer into the system divided by their respective absolute reservoir temperatures, which is shown in Equation 3.21. For a closed cycle, the net change in entropy is zero, since it begins and ends at the same thermodynamic state. Therefore, summation of heat transfers divided by their absolute reservoir temperatures must be less than or equal to zero, as expressed in Equation 3.22.

$$\delta s_{1-2} \geq \sum \frac{\dot{Q}_{in,i}}{T_i} \tag{3.21}$$

$$\sum \frac{\dot{Q}_{in,i}}{T_i} \leq 0 \tag{3.22}$$

The Carnot Efficiency is a theoretical maximum efficiency obtained by an ideal heat engine cycle. The Carnot cycle assumes there is isentropic compression, followed by reversible heating, then isentropic expansion, and lastly reversible cooling. A Carnot cycle is not perfectly representative of a Rankine cycle since the working fluid must be pre-heated before it can be phase changed, but it does provide the uppermost bound on efficiency that can be attained from the available thermal resource. The Carnot efficiency of a power cycle is given in Equation 3.23, which is derived from the relationship for reversible heat transfer, and the fact that the change in entropy from states 2 to 3 is equal to the difference from states 4 to 1

$$\eta_{Carnot} = 1 - \frac{\dot{Q}_{out,rev}}{\dot{Q}_{in,rev}} = 1 - \frac{T_{lo}(\Delta s_{1-2})}{T_{hi}(\Delta s_{4-3})} = 1 - \frac{T_{lo}}{T_{hi}} \tag{3.23}$$

These measures of efficiency are useful for assessing the performance of a power plant compared to its theoretical maximum performance. Equation 3.24 provides an calculation of η_{Carnot} for a hypothetical OTEC plant. Equation 3.24 assumes the surface water temperature is 25 °C, while the cold water temperature is 5 °C, and shows the maximum possible utilization of that thermal resource are as follows:

$$\eta_{Carnot} = 1 - \frac{T_{lo}}{T_{hi}} = 1 - \frac{(5\,^{\circ}\mathrm{C} + 273)K}{(25\,^{\circ}\mathrm{C} + 273)K} = 0.067 \tag{3.24}$$

The absolute upper-most bound on thermodynamic efficiency of an OTEC power plant operating at these temperatures is 6.7%. This efficiency does not account for the inevitable temperature losses in the heat exchanger. There must be a temperature drop in the water, since there is not an infinite flow rate. Similarly, there must be a temperature gradient between the water and the working fluid, since there is not an infinite amount of surface area. These issues will be discussed further in the section on heat exchanger modeling.

Comparing Carnot efficiencies is not the best way to assess different thermodynamic power generation technologies, because it does not factor in the actual costs to build and operate the plant. A more complete comparison between OTEC and other power generation technologies will be made in Chapter 6. The Carnot efficiency does not tell the entire story for any power plant, because it is the absolute theoretical maximum, which is unattainable by any real-world power plant. More useful analysis can be performed using the general heat engine efficiency, Equation 3.20, to assess real-world performance of a power cycle. This measure will be used in later analysis to help demonstrate which design and operating configurations help provide optimal performance.

3.3 Heat Transfer and Temperature Modeling of the Heat Exchanger Sub-systems

The power cycle requires both a heat source and a heat sink to provide the necessary heating and cooling. The hot and cold water pumped through the boiler and condenser provide the requite $\dot{Q}_{in}$ and $\dot{Q}_{out}$ for the power cycle. In order to calculate the amount of water required to provide these heat fluxes, information about the boiler and condenser heat exchangers must be known or calculated. This section will provide the heat transfer relations used to model the exchange of heat between the ocean

waters and the power cycle. Just as in the thermodynamic modeling of the power cycle, several assumptions were made to simplify the equations. Many assumptions made in the heat exchanger modeling have already been discussed above, as they pertain to specific assumptions. Below is a list of the simplifications and assumptions inherent in the heat exchanger model:

- All calculations assume steady state, i.e. there are no transient effects considered in this analysis.
- All of the inlet and exit temperatures are assumed to be known and specified design variables., as discussed in Section 3.2.1 on power cycle staging.
  - The water temperature in a stage is defined based on the overall inlet and exit temperatures, and the number of stages.
  - The boiling and condensing temperatures are a function of the water exit temperature for that stage, and the specified terminal temperature difference.
  - The terminal temperature difference is assumed to be the same and constant in each stage, regardless of the number of stages.
- The water-side flow is assumed to be approximated by the Dittus Bolter equation for turbulent flow in a smooth-walled pipe. The flow is definitely turbulent, and since there is not an assumed knowledge of the heat exchangers surface roughness, assuming a smooth pipe provides a minimum bound. This approximation will be discussed further on in the section.
- The Overall heat transfer coefficient is assumed to be known, along with a reference water velocity. The value is scaled as $\bar{U}_{ref}\frac{\bar{v}^{(4/5)}}{\bar{v}_{ref}^{(4/5)}}$ based on the scaling analysis performed later in this section.

- The log mean temperature differential ($LMTD$) assumes a counter-flow arrangement for the boiler and condenser. Since the water temperature drop is small, and phase change dominates the working fluid side, the $LMTD$ correction factor is assumed to be 1. This assumption also means the working fluid entering the boiler is heated to the boiling temperature by the exiting boiler water. This arrangement leads to a slightly lower boiling temperature, but a slightly better $LMTD$ for the boiling portion. Depending on the $\bar{U}$ value for heating the working fluid compared to the boiling $\bar{U}$ value, it may be beneficial to reverse the flow arraignment.

- Volumetric flow rate is taken as the mass flow rate divided by the density of the water.

- Average water velocity is calculated by dividing the volumetric flow rate by the cross-sectional area of the inlet pipe. Flow is assumed to be uniform at this velocity.

Water flow through the heat exchangers is also a primary part of the water systems analysis, so scaling and assumptions similar to those used for the heat transfer are also used for the pressure drop. The water pressure drop calculations will be discussed in Section 3.4.

Based on these simplifying assumptions, the calculations for the water mass flow rate can be performed. The calculations of the hot and cold water mass flow rates, $\dot{m}_{hw}$ and $\dot{m}_{cw}$, and the heat exchanger surface area, A_{boiler} and A_{cond}, are the ultimate purpose of the heat exchanger sub-system model. The requisite heat fluxes in and out were calculated in the power cycle sub-system model based on the input working fluid mass flow rate and temperature parameters. The mass flow rates are dependent

on these heat flux requirements and the specified water temperature changes (ΔT_{stage} from Equation 3.15). The calculation of the required heat exchanger surface area is a function of working fluid temperature, water temperature, the TTD, and the Overall Heat Transfer Coefficient $\bar{U}$. The details of these calculations will now be discussed.

The required harm water mass flow rate, $\dot{m}_{hw}$, can be calculated from combined energy balances across the boiler between the working fluid and the water; the heat energy passes out of one fluid, and into the other, assuming no losses to the surroundings. Equation 3.25 shows this relationship between the change in working fluid enthalpy, $\dot{m}_{wf}(h_3 - h_2)$, to change in hot water enthalpy. The hot water enthalpy is simplified to $\dot{m}_{cw}(C_{water} \times (\Delta T_{hw,stage}))$ by assuming the hot water is an incompressible fluid with a constant thermal heat capacity. This assumption is common for calculations involving small temperature changes in liquids.

$$\dot{m}_{wf}(h_3 - h_2) = \dot{Q}_{in} = \dot{m}_{hw}(C_{hw} \times (\Delta T_{hw,stage})) \tag{3.25}$$

Since $\dot{Q}_{in}$ is already known from the power cycle calculations, Equation 3.25 can now be rearranged to find $\dot{m}_{hw}$, as shown in Equation 3.26

$$\dot{m}_{hw} = \frac{\dot{Q}_{in}}{C_{hw} \times (\Delta T_{hw,stage})} \tag{3.26}$$

Similarly, the cold water mass flow rate, $\dot{m}_{cw}$, can be calculated from an energy balance across the condenser, as seen in Equation 3.27.

$$\dot{m}_{cw} = \frac{\dot{Q}_{out}}{C_{cw} \times (\Delta T_{cw,stage})} \tag{3.27}$$

The heat transfer portion of the model can also be used to calculate the required heat exchanger area for an overall heat transfer coefficient from the required heat transfer rate. The area will later be used as part of the pressure loss equations

for the hot and cold water systems. Since the heat exchangers are so large, heat exchanger area is also an important factor in the cost of the plant, and so it will be used later in the economic modeling as well. Equation 3.28 shows the calculation of the heat transfer through the a heat exchanger with the log-mean temperature differential (cross-flow orientation) between the working fluid and the water, $LMTD$, as well as the heat exchanger surface area, A, and the average overall heat transfer coefficient, $\bar{U}$. Equation 3.29 provides the calculation of $LMTD$ for a cross-flow oriented heat exchanger. For more information on the derivation of these heat transfer calculations, please consult any undergraduate Heat Transfer textbook [34].

$$\dot{Q} = \bar{U} \times A_{heat\ exchanger} \times LMTD \tag{3.28}$$

$$LMTD = \frac{(T_{hi,in} - T_{lo,out}) - (T_{hi,out} - T_{lo,in})}{\ln \frac{T_{hi,in} - T_{lo,out}}{T_{hi,out} - T_{lo,in}}} \tag{3.29}$$

Equation 3.30 rearranges the terms in Equation 3.28 in order to solve for the heat exchanger area.

$$A = \frac{\dot{Q}}{\bar{U} \times LMTD} \tag{3.30}$$

The average overall heat transfer coefficient must be known in order to perform the area calculations. The average overall heat transfer coefficient, $\bar{U}$, is the composite average of the convection heat transfer resistances on the water and working fluid sides, fouling resistances, and wall conduction resistance, as shown in Equation 3.31. The specific resistances are further broken down into their respective constituents in Equation 3.32. Please see the Glossary of variables in Appendix A for a more detailed description of the variables in the equation. The value of $\bar{U}$ is dependent on which area is used as the reference side; this report assumes the working fluid-side for the reference area. Fouling resistance factor, $R"_{w,foul}$, is typically considered a constant when calculating the overall heat transfer coefficient, and will be treated as

such during scaling analysis. The convection heat transfer coefficient is a function of flow rate, fluid properties, flow geometry, and surface properties. These equations will be used to develop a scaling relationship between $\bar{U}$ and average water velocity through relating the convection coefficient, $\bar{h}_{water}$, though the Nusselt Number. The value of $\bar{U}$ is dependent on which area is used as the reference side; this report will always use the working fluid-side for the reference area.

$$\bar{U}A = (R_{water} + R_{water,foul} + R_{wall} + R_{wf,foul} + R_{wf})^{-1} \tag{3.31}$$

$$\bar{U}A = \left(\frac{1}{(\eta_0 \bar{h} A)_{water}} + \frac{R''_{w,foul}}{A_{water-side}} + \frac{t_{wall}}{(kA)_{wall}} + \frac{R''_{wf,foul}}{A_{wf-side}} + \frac{1}{(\eta_0 \bar{h} A)_{wf}} \right)^{-1} \tag{3.32}$$

R_{wall} assumes flat plate conduction through a slab of thickness t with conductivity k_{wall}. An alternative wall heat transfer resistance, $R_{wall,rad}$, is that of a cylindrical pipe in Equation 3.33. Radial conduction causes a non-linear relationship between conduction distance and temperature gradient because of the non-constant area through which the heat conducts.

$$R_{wall,rad} = \frac{ln(r_o/r_i)}{2\pi(kL)_{pipe\ wall}} \tag{3.33}$$

As the ratio of wall thickness to diameter decreases, the value of $R_{wall,rad}$ approaches the R_{wall} value of a flat plate. Since the wall thicknesses in the heat exchangers are typically less than 0.1 inches for tubes of hydraulic diameter 1 inch or more [19,44,48]. the error for using a flat plate assumption is approximately 10% below that of the actual value. This approximation is acceptable for the purposes of this analysis because the goal is to capture general trends and orders of magnitude; it is also beneficial because it allows for more flexibility when comparing different types of heat exchangers.

A simplified calculation for the water- side convection heat transfer coefficient, $\bar{h}_{water}$, arises from approximating the internal flow in the heat exchanger as turbulent duct flow. The Nusselt number is related to $\bar{h}_{water}$ by the formulation provided in Equation 3.35. There are many Nusselt Number correlations for different flow geometries and heat exchangers, but Colburn Equation, Equation 3.34, captures the general variables that effect heat transfer. This equation, while not extremely accurate, is valid to a good approximation over the range of temperatures and flow rates expected in an OTEC heat exchanger.

$$Nu_{D_h} = 0.023(Re_{D_h})^{4/5}(Pr)^{1/3} \tag{3.34}$$

$$Nu_{D_h} = \frac{\bar{h}D_h}{k}, \bar{h} = \frac{Nu_{D_h}k}{D_h} \tag{3.35}$$

Equation 3.34 assumes a smooth walled pipe, and factors in the friction factor dependence on Reynolds Number, Re. While assuming a smooth pipe is not necessarily representative of a heat exchanger that might have surface enhancements, it does provide a reasonable representation of the overall dependencies. By combining Equations 3.35 and 3.34, average water velocity, $\bar{v}_{water}$, and the water-side hydraulic diameter of the heat exchanger, D_h, scaling factors for $\bar{h}_{water}$ were determined. Since $Re_{D_h} = \frac{\bar{v}_{water}D_h}{\nu}$, solving for $\bar{h}_{water}$ shows that it scales as $\bar{v}_{water}^{4/5}$, and $D_h^{-1/5}$. Therefore, heat transfer increases/decreases with increasing/decreasing water velocity, and increases with decreasing diameter (and visa versa), although the diameter scaling is weaker than that of velocity. Further scaling development in Sub-section 3.3.1 show that the overall heat transfer coefficient ($\bar{U}$) also scales similarly.

The hydraulic diameter, D_h, is an approximation of a non-circular-cross-section duct as a circular pipe, and it is useful as it allows for rough comparison between circular and non-circular ducts. Equation 3.36 shows the calculation of the

hydraulic diameter from the cross-sectional duct area, A_{cs} and the wetted perimeter, P.

$$D_h = \frac{4A_{cs}}{P} \tag{3.36}$$

Using D_h in equations provides a reasonable approximation of the heat ransfer or pressure drop coefficients, but ideally the correlation for the actual duct shape or heat exchanger should be determined and used. For the purposes of this analysis, the D_h approximation offers an easier means of comparison for heat exchangers with different geometries, such as comparing shell-and-tube and plate-fin, on a common basis.

Boiling and condensing heat transfer are different from the typical forced convection calculations because there is a phase change occurring at the surface. On the working fluid size of the boiler, the phase change is usually assumed to be pool boiling. Equation 3.37 demonstrates the added complications of calculating the heat transfer coefficient for film boiling on the surface of a horizontal tube [34].

$$\bar{Nu}_D = 0.62 \left[\frac{g(\rho_l - \rho_v)h'_{lv}D^3}{\nu_v k_v (T_{wall} - T_{sat\ vapor})} \right] \tag{3.37}$$

Equation 3.37 is not used directly in the model, but this equation does demonstrate the typical important variables involved in boiling phase change. Condensation is similar to boiling, except that instead of a vapor film rising through the saturated liquid, a saturated vapor is condensing into the surface, and flows down under the force of gravity. Neither of these phenomena were calculated within the model because doing so would require more in depth knowledge of heat exchanger geometry, working fluid flow velocities, and local surface temperature information. Instead, experimental values for the boiling and condensing heat transfer coefficients were compiled from literature in order to establish an overall range of expected values

3.3.1 Scaling Overall Heat Transfer Coefficient $\bar{U}$ with Water Velocity

The overall heat transfer coefficient was scaled as a function of velocity in order to capture some of the effects velocity has on heat transfer. It was assumed that the average water inlet velocity was constant throughout the plant, and this value was used to scale $\bar{U}$. It was assumed that only the water-side heat transfer coefficient was changing; all other thermal resistances were considered constant. It was also assumed that the tube area inside and outside are roughly the same, allowing area to be factored out. Based on these assumptions, Equation 3.31 simplifies to Equation 3.38. Note that the equation has been divided through by an assumed constant area, and so the resistances are now per unit area.

$$\bar{U} \approx \left(\frac{1}{\bar{h}_{water}} + \sum R_i'' \right)^{-1} \approx \left(\frac{1 + \bar{h}_{water} \sum R_i''}{\bar{h}_{water}} \right)^{-1} \tag{3.38}$$

Equation3.38 can the be scaled such that $\bar{U}$ scales as $\bar{h}_{water}$, as shown in Equations 3.39, assuming that the sum of the other thermal resistances is smaller than $\bar{h}_{water}$.

$$\bar{U} \approx \left(\frac{1 + \bar{h}_{water} \sum R_i''}{\bar{h}_{water}} \right)^{-1} \approx \left(\frac{1+1}{\bar{h}_{water}} \right)^{-1} \approx \bar{h}_{water} \tag{3.39}$$

So, for the cases where $\bar{h}_{water}$ dominates the thermal resistance, $\bar{U}$ can be scaled as $\bar{h}_{water}$. Using Equations 3.35 and 3.34, the two can be combined to solve $\bar{h}_{water}$ in terms of Reynolds Number, Re_{D_h}. Equation 3.40 shows how $\bar{U}$ scales to $\bar{h}_{water}$, and how they both in turn scale to Re_{D_h} and average water velocity $\bar{v}_{water}$.

$$\bar{U} \approx \bar{h}_{water} \approx Re_{D_h}^{4/5} \approx \bar{v}_{water}^{4/5} \tag{3.40}$$

Now that a scaling relationship between $\bar{U}$ and $\bar{v}_{water}$ has been found, $\bar{U}$ can be approximated from a reference overall heat transfer coefficient, $\bar{U}_{ref}$, and a reference velocity, $\bar{v}_{water,ref}$ by using a simple direct proportional relationship as shown in

Equation 3.41.

$$\bar{U} \approx \bar{U}_{ref} \frac{\bar{v}_{water}^{4/5}}{\bar{v}_{water,ref}^{4/5}} \tag{3.41}$$

In order to test this scaling theory, $\bar{U}$ was calculated using Equation 3.31 with typical wall, fouling, and phase-change thermal resistance constants over a range of flow rates expected in OTEC operations, and compared with a scaled calculation of $\bar{U}$, as shown in Figure 3.6. The sum of the wall resistance and fouling factor was taken as

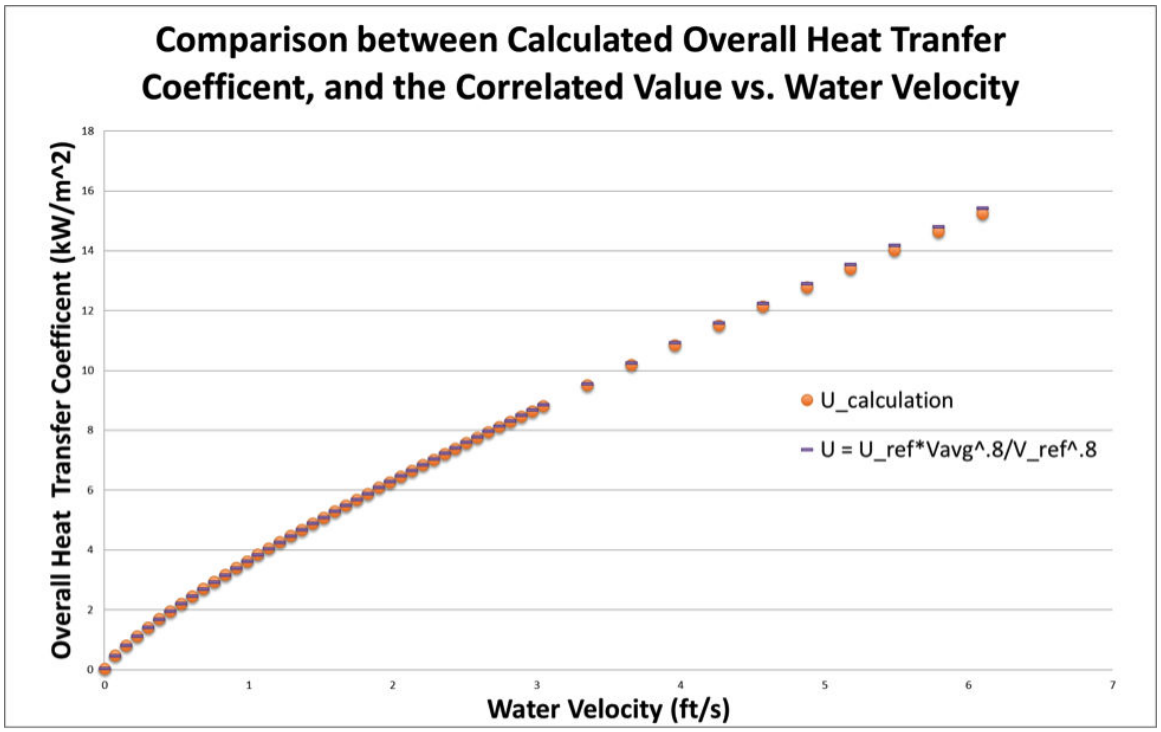

Figure 3.6: The overall heat transfer coefficient scales as water velocity when wall, fouling, and phase-change convection resistances are small.

.0001 $\frac{m^2K}{kW}$, and the phase-change resistance was assumed to be constant at 1/4000 $\frac{m^2K}{kW}$. The reference velocity was taken as 6 $\frac{ft}{s}$, and $\bar{U}_{ref}$ was the calculated value at the point. Figure 3.6 demonstrates that this scaling method does an accurate job of capturing the variation $\bar{U}$ based on change in the water-side heat transfer coefficient from a change in average velocity. Based on this scaling technique, the model adjusts

the heat transfer coefficient if the water velocity is higher than the reference water velocity. The coefficient is not adjusted lower for water velocities slower than the reference because it is assumed the flow would be constricted to speed the water up to the reference value, so as to reach the reference heat transfer coefficient.

3.4 Hot and Cold Water Pressure Drop and Pump Demand Analysis

In general, both hot and cold water pump calculations are the same in that they calculate the required pump power based on the pressure drop in the fluid system, as represented by the generalized Equation 3.42. Equation set 3.43 show the simplification of the 'delta' terms in Equation 3.42. Water velocity is assumed to be approximately constant through the length of the pipe, and the pressure at the inlet is assumed to be that at the outlet, because both ends ultimately connect to the open ocean. The cold water pump energy balance also accounts for the effective added pressure head due to the difference in density inside and outside the pipe, $g\Delta z_{cw\ pump}$, as well as the pressure drop due to the viscous losses in the cold water pipe. Both hot and cold water pumps must overcome the pressure drop caused by the heat exchangers and to a lesser extent, the piping and fittings ($\sum h_{losses}$).

$$\dot{W}_{cw/hw\ pump} = \dot{m}_{water}\left[\Delta(\frac{p}{\rho} + \frac{\bar{v}^2}{2} + gz) + \sum h_{losses}\right] \tag{3.42}$$

$$\Delta p \approx 0, \quad \Delta\bar{v}^2 \approx 0, \quad \Delta z_{cw\ pump} \approx L_{cwp}\left(\frac{\rho_{cw} - \rho_{ocean,avg}}{\rho_{cw}}\right) \tag{3.43}$$

To account for losses in components, additional terms are added to the pump power requirement. Specifically, the heat exchanger pressure loss is an important variable to properly capture. Equation 3.44 expands the $\sum h_{losses}$ term so that the various sources of pressure loss are individually represented. The head losses have units of

power per unit of mass flow rate, or pressure change per unit of fluid density, shown in Equation 3.45.

$$\sum h_{losses} = h_{l,hx} + h_{l,piping} + h_{l,inlet} + \sum h_{l,fittings} \tag{3.44}$$

$$h_{losses} = \left[\frac{\dot{W}}{\dot{m}}\right] = \left[\frac{\Delta p}{\rho}\right] \tag{3.45}$$

Heat exchanger pressure drop, $h_{l,hx}$, is dependent on the geometry of the heat exchanger, the size of the heat exchanger, and the flow rate. To limit uncertainty and capture the general relationship with the area and flow rate, Equation 3.46 was developed from pressure drop relationships to scale the head loss term to velocity and surface geometry [53]. The calculation for pressure drop in the heat exchanger was taken as the scaling of a reference head loss coefficient value, $h_{l,hx\ ref}$, with functions for velocity and geometry relationships. Equations 3.46, 3.47, and 3.48 show the scaling relationships for flow geometry and the velocity.

$$h_{l,hx} = \left(\frac{\left(\frac{L}{D_h^3}\right)}{\left(\frac{L}{D_h^3}\right)_{ref}}\right) \times h_{l,hx\ ref} \times \left(\frac{\bar{v}^{1.8}}{\bar{v}_{ref}^{1.8}}\right) \tag{3.46}$$

$$\Delta p \approx \frac{L}{D_h^3} \approx \frac{A}{D_h^4} \tag{3.47}$$

$$\Delta p \approx \bar{v}^{1.8} \tag{3.48}$$

The heat exchanger pressure head scaling allow for the correction of reference pressure drop values with changes in flow rate or geometry. This scaling relationship is particularly useful when trying to assess the value of added heat exchanger surface area. Increasing area could be done by increasing tube diameter, by increasing the length, or by putting more tubes in parallel with the flow. Increasing tube length, while maintaining a constant average flow velocity, would linearly increase pressure drop. Adding more tubes of the same length and diameter in parallel would cause

more mal-distribution of the water, but if the overall mass flow rate were held constant, then the water velocity in each tube would decrease, along with the pressure drop. Increasing tube diameter, while maintaining a constant overall mass flow rate, would decrease pressure drop by reducing pressure drop both directly through the geometrical dependence, along with lower average water velocity, but would also decrease the heat transfer coefficient. The effect of decreasing water velocity does have a negative impact on the heat transfer coefficient, as seen in the scaling previously discussed in the heat transfer section.

Increasing the number of stages requires increasing the overall flow length of the water through the heat exchangers because the temperature drop per section gets smaller, and the total amount of area increases. To keep the model simple, it was assumed that the pressure drop was scaled linearly with added area, since it was assumed that a fixed tube diameter only leaves added overall flow length as a means of increasing heat exchanger area. Therefore, it is assumed that pressure is scaled linearly with area, and the reference area is assumed to be the area calculated for a single stage, as shown in Equation 3.49.

$$\Delta p \approx \Delta p_{ref} \frac{A_{hx}}{A_{hx,ref}} \tag{3.49}$$

In order to determine $A_{hx,ref}$, the model was run for a single-stage cycle, and the calculated condenser and boiler areas were taken as the reference areas.

Velocity in the heat exchanger was scaled as shown in Equation 3.50, which was developed directly from Equation 3.48.

$$\Delta p \approx \Delta p_{ref} \frac{\bar{v}^{1.8}}{\bar{v}_{ref}^{1.8}} \tag{3.50}$$

Velocity in the system is also needed to calculate losses in pipes and fittings. For the cold water, an average velocity is calculated based on cold water pipe diameter

and cold water volumetric flow rate; the hot water velocity is calculated similarly. Equations 3.51 through 3.54 represent flow losses from wall friction, pipe inlet, and pipe fittings respectively [30]. The reason why these equations scale as $\bar{v}^2$ instead of $\bar{v}^{1.8}$ is because there is an approximate $\bar{v}^{-.2}$ imbedded within the friction factor, f, which is not explicitly factored out of the heat exchanger pressure drop.

$$h_{l,pipe} = f\frac{L}{D_h}\frac{\bar{v}^2}{2} \tag{3.51}$$

$$h_{l,inlet} = K_{inlet}\frac{\bar{v}^2}{2} \tag{3.52}$$

$$h_{l,inlet} = f\frac{\bar{v}^2}{2}\sum K_{fittings} \tag{3.53}$$

Cumulatively, these equations indicate that pressure drop is highly dependent on the heat exchanger pressure drop, as well as the number and type of fittings, elbows, and valves in the fluid network. The number and types of fittings present is highly design specific, and for modeling simplicity the sum of the piping pressure drop is estimated as a single lumped coefficient. As the design and layout of a plant became better developed, these equations could be expanded to accurately capture the effects of each elbow and valve. Without these values, the analysis is still valid as long as the order of magnitude is close, along with its relative relation to the heat exchanger pressure drop. Since the pumping power acts a parasitic loss within the system, it is advantageous to design the water flow paths to be as low-loss as possible with wide-arcing elbows, low profile valves and fittings, and minimization of redirection. In order to account for some fittings losses, as well as increased number of vales, connections, and flow meters, the fittings coefficient is assumed to be approximated by Equation 3.54.

$$\sum K_{fittings} = 200 + 20n \tag{3.54}$$

The $K_{fittings}$ coefficient represents an added equivalent dimensionless length that would cause a pressure drop equal to that caused by the fitting. These values are typically on the order of 10 or less for low profile fittings, fully open valves, and any other fixture that might be in the flow path. This lumped $K_{fitting}$ coefficient assumes an approximate base value that represents the elbows, values and flanges in order to get the water into and out of the heat exchangers; the added '$20n$' value represents an approximation for an added flanges, sensors or valves that might exist between heat exchanger stages. The total pressure drop caused by the fittings is minor in comparison to the pressure drop in the heat exchangers, so even a large error has a minimal effect on the estimation of the total system pressure drop.

3.5 Implementation of the Thermal-Fluids Systems Model in MATLAB

Once the governing equations and relationships were determined for the power cycle, heat exchangers, and water systems, each was programmed in MATLAB as its own standalone function, and then all three were integrated together in one program that allowed for total solution of the three systems all at once. Appendix C contains all of the code for the MATLAB model, as well as a list of all the input and output variables. MATLAB was chosen as the modeling program of choice because of familiarity with the programming language and interface.

The program follows the same progression as the sections in this chapter. First the power cycle function, *powercycle.m*, takes the temperature information and plant flow rates and calculates the heat duties ($\dot{Q}_{in/out}$) and the sum of the net power output of the power cycles ($\sum \dot{W}_{net,cycle}$). The heat exchanger function, *heatexchangers.m*, then calculates the hot and cold water mass flow rates ($\dot{m}_{hw/cw}$), as well as the required area based on the given temperature and heat exchanger properties. Lastly, the water

pump fluids models, *coldwaterpump.m* and *warmwaterpump.m*, calculate the pressure drop and corresponding pumping power demands for the hot and cold water pumps ($\dot{W}_{hwpump/cwpump}$) based on heat exchanger area, water mass flow rates, and flow path variables (i.e. loss coefficients, diameter, etc.). The pump power demands are subtracted from the sum of all the net cycle power outputs to get the net electricity power output for the plant ($\dot{W}_{net,electricity}$).

In order to calculate the thermodynamic properties at each stage, a function called *propcalc.m* takes the available state information and performs a table look-up on a pre-generated table. Equations for determining thermodynamic properties of saturated fluids are complex and difficult to manipulate to find different thermodynamic values. *Refprop* is a thermodynamic property calculator developed by NIST, and it was used to generate a comprehensive saturation table for the working fluids with temperature increments of 0.025°C, over a range of 0 to 30°C. Determination of properties is simplified because the boiling and condensing temperatures of the cycles are pre-specified. If water mass flow rate were pre-specified, and one of the temperatures was a dependent variable, there would have to be several layers of loops within the overall model, in order to correctly iterate to the correct value. The iterative modeling method was avoided since the purpose of this model is theoretical evaluation of plant design parameters on performance, and not attempting to model the performance of a pre-designed system.

3.6 Modeling Conclusions

The Thermal-Fluids Systems Model is an idealized and steady-state representation of the thermodynamics, heat transfer, and fluid mechanics that govern the energy flows into and out of an OTEC plant. The plant was divided into three pri-

mary sub-system models: the power cycle model, the heat exchangers model, and the water pressure drop/pumping power model. The power cycle sub-system model utilizes thermodynamic relationships to determine the heat flows in and out, as well as the net power out from the power cycle. The heat exchanger sub-system model determines the necessary water flow rates and heat exchanger areas based on specified temperature and heat exchanger properties. Lastly, the water pressure drop sub-system model determines the corresponding pump power demands for the warm and cold water flows. The assumptions made for each sub-system were deemed reasonable for the modeling, since the ultimate goal was to use the model for first-cut analysis rather than operational simulation.

The model solves for heat exchanger area, pumping power demands, water mass flow rates, and net electrical power produced. An actual plant in operation would be designed from the start with a set heat exchanger area as well as pump and turbine capacity ranges, and would not likely be able to completely control all temperature variables. As such, this model solves for variables that would typically be specified in an operational simulation. This model is meant to help assess heat exchanger, pump, and turbine sizing. If an operational type of model were desired, the model could be integrated into an optimization routine that could iteratively solve for the necessary variables based on a specified power output, heat exchanger size, or some other variable that is currently an output of the model.

The next chapter uses the thermal fluids systems model to assess the effects of certain design parameters on plant performance. The analysis will look at the effects of individual inputs by first establishing a base-case set of reference plant parameters, and then vary individual variables to assess the individual impacts.

Chapter 4

Thermal-Fluids Systems Analysis of 20MW OTEC Plant Model

4.1 Introduction

This model is meant to act as a quick means of determining which design parameters could have the largest relative effects on energy production and plant component sizing, both of which ultimately affects the final financial viability of the plant. A reference set of parameters was established, and then parameters were varied from the reference value in order to analyze the effects that parameter has on plant performance. This was done by adjusting design parameters until the outputs roughly matched that of a 20 MWe OTEC plant proposed by Sea Solar Power for the Cayman Islands [1]. With a reference set of operating parameters in place, the basic analysis process was as follows:

I Enter plant design variables, using a range of values for the variable to be tested, and keeping all others constant

II Calculate gross power output of the plant, and water flow rates for each value of the tested variable

III Calculate net power output and pumping power demands with given variables

[1] This proposal was not published, but was provided by Sea Solar Power for research purposes

IV Use net power output calculation to calculate performance metrics for sensitivity analysis with base case

This process was repeated for each design parameter chosen for analysis.

4.1.1 Literature Review to Determine Parameter Ranges

In order to evaluate the effects of different design and operational parameters, acceptable ranges needed to be determined for each variable. For the analysis, operational design parameters, such as the TTD, inlet and exit temperatures, and working fluid mass flow rate were chosen based on knowledge of the general system, and not taken from any specific source. Additionally, the cold water pipe length and width ranges were chosen in order to examine the effects of sizing at each end of the spectrum; in the literature, the pipe diameter was either not discussed or was typically 3-4 meters in diameter. However, many different sources were drawn upon for information on specific heat exchanger performance values in order to determine a robust representative range of heat transfer coefficients and pressure drops.

Two major testing efforts for OTEC heat exchangers were performed by Oak Ridge National Labs and Argonne National Labs in the late 1970s [19,49]. These tests analyzed different surface treatments and design effects on heat transfer coefficient, and served as a benchmark for other heat exchanger tests performed by others at the time. The Oak Ridge tests were focused specifically on the heat transfer coefficients for condensing vapor on vertical fluted tubes [19]. The Argonne National Labs tests were more broad, and involved the testing of five different heat exchangers provided by Linde (a division of Union Carbide) and Carnegie Mellon University. The five types of heat exchangers tested were: a horizontal shell and tube pool boiler supplied by Linde; vertical falling film evaporator, and a vertical falling film condenser, both

designed by Carnegie-Mellon; a horizontal spray-tube evaporator supplied by Linde; and a thin-film condenser provided by Linde [22, 48, 49]. There were several rounds of tests over between 1978 and 1981 at both Oak Ridge and Argonne National Labs, with other types of heat exchangers tested [26, 45, 60].

There were many more tests performed outside of these by various companies. Lockheed, Westinghouse, TRW, Alfa-Laval, Sea Solar Power, and many others tested their own versions of heat exchangers, not just including shell and tube, but also various plate heat exchangers as well as plate-fin heat exchangers [3, 13, 14, 44, 56, 61]. Based on the measured heat transfer coefficients and pressure discussed in these reports, the approximate test ranges for the overall heat transfer coefficient and water-side pressure drop were chosen. The specifics of the ranges chosen for each varaible will be discussed further in the following subsection.

4.1.2 Design Parameter Ranges for Analysis

Table 4.1 has the parameters that were analyzed, as well as the range over which they were varied about the reference design. These Parameters were chosen for analysis because they affect one, or more, of the three sub-systems on a fundamental level. Parameters like pump or turbine efficiency are more obvious in their effect, since they are simply a ratio of power converted to the total available power; variables like temperature can affect multiple systems, as well as affect the systems on more fundamental levels, where the relationship might not be simply linear, as it is with efficiency.

The first design parameter analyzed was number of power cycle stages, over a range of 1 to 10 stages. Since the reference case was ultimately based on a 4-stage system, the analysis of staging is used as an introduction and benchmarking of the analysis methodology used for the other parameters. Power cycle staging affects plant

Table 4.1: Plant design and operating variables analyzed, and their respective analysis range

Plant Parameter	*Symbol*	*Range of Variation*
Number of stages,	n	1 to 10 stages (ref. of 4 stages)
Overall heat transfer coeffs.,	$\bar{U}_{cw}$, $\bar{U}_{hw}$	1 to 12 $\frac{kW}{m^2K}$ (varying both at the same time)
Heat exchanger pressure drop,	Δp_{hx}	1 to 6.5 psi (varying both at the same time)
Cold water inlet temperature,	$T_{cw,in}$	1.5 to 10.5°C (varying the inlet and outlet to maintain a constant water temperature change in the heat exchangers)
Hot water inlet temperature,	$T_{hw,in}$	17 to 31°C (varying the inlet and outlet to maintain a constant water temperature change in the heat exchangers)
Cold water discharge temperature,	$T_{cw,out}$	9 to 7°C (holding the inlet temperature constant)
Hot water discharge temperature,	$T_{hw,out}$	16.5 to 24.5°C (holding inlet const.)
Terminal Temperature Difference,	TTD	.25 to 4°C (varying both TTD_{boiler} & $TTD_{cond.}$ at same time)
Cold water pipe diameter,	$D_{cw\ pipe}$	2 to 10 meters (-50% to +250% of ref. value)
Cold water pipe length,	L	0 to 20,000 meters (ref. of 1,000m)
Working fluid mass flow rate,	$\dot{m}_{wf}$	2,000 to 10,000 $\frac{kg}{s}$ (ref. of 5,000 $\frac{kg}{s}$

performance greatly at first but faces diminishing returns, as discussed in Chapter 3; because of this phenomenon it was important to first establish a reasonable number of stages as a reference value for the rest of the analysis.

Ranges for the heat transfer coefficients seen in literature are typically 500 to 900 $\frac{\frac{BTU}{hr}}{ft^2 \circ F}$, or approximately 2.5 to 5 $\frac{kW}{m^2 \circ C}$, however there are some that fall above and below this range [3,5,10,13,14,19,22,26,44,45,48,49,56,60,61]. Some companies, like Sea Solar Power, contend that heat transfer coefficients could potentially be achievable beyond the typical values, perhaps as high as 2200 $\frac{\frac{BTU}{hr}}{ft^2 \circ F}$, by means of heat exchangers specially designed for OTEC power generation purposes [5]. The reference case assumes a value at the higher end of the typical range, 4 $\frac{kW}{m^2 \circ C}$, and the sensitivity analysis will use a range of 1 to 12 $\frac{kW}{m^2 \circ C}$ to estimate the limiting effects of heat transfer coefficient on performance. In actuality, the heat transfer coefficient is not a design variable like the diameter, in that it is not independent of the fluid and flow properties. Often, most heat transfer coefficient values are reported for a given fluid velocity and heat duty. The model takes the input value and scales it based on fluid velocity, in order to capture some of the real-world variation. Similarly, the pressure drop range of 1.5 to 6.5 psi; the reference of 4 psi was chosen because it was within the typical range reported in literature [5, 26, 45, 48, 49, 56, 60]. Pressure drop is not simply an independent design value either, but rather it is dependent on flow velocity, fluid properties, and geometry. However, for the sake of this sensitivity analysis, it was treated as an independent parameter. By assuming it to be an independent design parameter, it was possible to directly evaluate performance effects caused by different levels of pressure drop in the heat exchangers.

The cold water temperature range has a practical lower bound, as it would almost certainly not be zero degrees Celsius, as that is only reached in Arctic waters;

the hot water temperature is limited in this analysis by the upper limit of the working fluid table used in the model, which is limited to 30 $^{\circ}C$; therefore the hot water upper limit is 30$^{\circ}C$ plus the specified TTD in the boiler heat exchanger. The actual ranges of 1.5 to 10.5$^{\circ}C$ for the cold water and 17 to 31$^{\circ}C$ for the hot water do not include the practical limits as a bound for their ranges, as those temperature extremes do not occur at the typically proposed OTEC sites. For both hot and cold water, the exit temperature will be varied by the same corresponding amount, in order to maintain a consistent temperature change across the overall hot and cold water systems.

A subsequent analysis looks at the effect of changing the exit temperature by increasing and decreasing the exit temperatures of both hot and cold water. The effect of doing so is equivalent to changing the water temperature inlet/exit difference. The range of analysis is -3$^{\circ}C$ to +3$^{\circ}C$ of the reference value for the condenser water exit temperature, and the corresponding hot water exit temperature range is +3 $^{\circ}C$ to -3$^{\circ}C$ of the reference value. Therefore the analysis goes from smaller-than-reference to larger-than-reference water temperature changes in the heat exchangers.

The terminal temperature difference (TTD) is the approach temperature difference between the exiting working fluid and the exiting water. This parameter relates the water temperature to the working fluid in each stage. The analysis covers a range of 1$^{\circ}C$ to 5$^{\circ}C$, with all other temperature parameters fixed at the reference case. Again, in actuality TTD is not an independent variable, but rather the result of sizing a heat exchanger to a given flow and heat duty. This model works backward, solving for heat duty and the corresponding size based on specified heat exchanger parameters and terminal temperature difference.

Cold water pipe length and diameter are included in the analysis since the cold water pipe is a uniquely large and primary component in all OTEC power plants.

The general size and length varies between designs, but overall they are generally the same in design and function. Since design specifics vary widely for the rest of the water flow path, the pressure loss effects are represented by a lumped minor loss coefficient that only scales minimally with the number of stages (see Equation 3.44). The intention was to minimize unknowns, and let the sensitivity analysis of the cold water pipe be representative of the types of effects caused by the water piping design parameters. The range on the diameter will be set to -50% of the reference case to +250%, in order to determine if a large pipe, and hence a lower flow velocity for a given volumetric flow rate, will increase performance. The analysis of length range will not be entirely representative of the actual performance effects of pipe length, since it will be assuming the same water cold inlet temperature for every length. The reasoning for the analysis will be more to determine, all else being equal, how much effect the length has on performance. In actuality the cold water temperature is a function of depth (pipe length), and as a result the power output from the power cycle will be affected as well as the change in pumping power. Analyzing the trade-off of these two parameters is critical for designing an optimal OTEC plant. However a first-cut analysis of temperature and pipe length separately will first determine whether or not they affect performance with the same order of magnitude.

4.2 The Reference Case

In order to set a benchmark for the sensitivity analysis, a reference case was established to represent a normal OTEC plant. The reference case outputs are used as those expected from a normal OTEC plant, and the sensitivity analysis focuses on the relative difference between the outputs of a given configuration to the reference benchmark values. The absolute magnitudes of the calculated values, from both the reference case as well as the sensitivity analysis, are not claimed to be the actual

expected value; rather, they are expected to be an approximate representation of the values that might be expected for a plant with a given set of design characteristics. In order to utilize an outside source for additional comparison, some of the plant design parameters were calibrated to provide gross and net power outputs and water flow rates close to those specified in Sea Solar Power's Cayman Island proposal for building a 20 MWe plant (see Table 4.2 for known values). The model used the values specified in the report, and then varied some of the other design parameters until the gross power output, water mass flow rates, and net power output were close enough to be considered acceptably representative of the 20MW plant. The input parameters for the reference case are available in Appendix B. The output values of the reference case as well as the corresponding Sea Solar Power plant values are provided below in Table 4.2.

Table 4.2: The output values of the thermal-fluids model for the reference case compared with Sea Solar Power plant.

Output	*Reference Case*	*Sea Solar Power*	*% Error*
Gross electrical power [kWe]	28,100	26,700	5.3
Cold water pump [kWe]	3,480	-	-
Hot water pump [kWe]	2,000	-	-
Net electrical power [kWe]	22,500	20,000	12.5
Cold water vol. flow rate $[\frac{m^3}{s}]$	27.4	27.2	0.7
Hot water vol. flow rate $[\frac{m^3}{s}]$	49.4	49.6	-0.4
Condenser surface area $[m^2]$	68,930	-	-
Boiler surface area $[\frac{m^3}{s}]$	89,600	-	-

Comparing the reference case with Sea Solar Power's values, the gross power and net power are 5% and 12.5% higher respectively. These errors are reasonable for such a broad model because it does not include added losses from auxiliary systems,

the line losses transforming and sending the electricity to shore, or a detailed account of all minor flow losses. Based on discussions with Sea Solar Power, it is reasonable to assume they included these losses in their calculation. The water flow rate values, at less than 1% difference, are in good agreement. The other output values were not provided for comparison. This amount of error is well within the expected ranges of uncertainty, as it is only meant to provide a starting reference point. It is also important to note that the base case also uses the assumption of 4 power cycle stages. The reasoning for using 4 stages will be validated through the analysis in Section 4.3. Other measures of performance are used for the analysis in addition to the direct output values from the plant model. These performance metrics, as shown in Table 4.3, are pump power fraction, heat exchanger area per net kW of power, and water mass flow per kW of net power.

Table 4.3: The output values of the thermal-fluids model for the reference case compared with Sea Solar Power plant.

Performance Metric	*Reference Case*	*Sea Solar Power*	*% Error*
Cold pump fraction	0.124	-	-
Hot pump fraction	0.076	-	-
Condenser area per net kWe	3.05	-	-
Boiler area per net kWe	4.23	-	-
Cold water vol. flow rate per net kWe	0.00122	0.00136	-11
Hot water vol. flow rate per net kWe	0.00220	0.00247	-12

Pump power fraction is the fraction of the pump power demand and the gross power output from the power cycle. This measure embodies the amount of the plant dedicated to powering itself, and is a means of evaluating plant utilization and efficiency. The area per kW of heat exchanger metric is essentially a ratio of plant size and cost to plant performance, because the heat exchangers are large and typically

a large portion of the capital expense. A lower area per kW value means that the plant is producing more power, or using less heat exchanger area, than the reference case. Lastly, water flow rate per kW of net power is a measure of the utilization of the thermal resource of the water. A higher-than-reference value means that more water is required to generate a given new power output, or that less power is being generated for a given water flow rate. The sensitivity analysis uses the operational outputs from the model, combined with the performance metrics, to determine the impact each design parameter has on plant operation.

4.3 Analysis of Power Cycle Staging

The first analysis looked at the effects power cycle staging has on plant performance. This first analysis also serves as an introduction to the visualization methods used in subsequent analysis sections. The number of stages was varied from 1 to 10, while maintaining the same overall mass flow rate through the power cycle (or cycles), as well as maintaining all other operating parameters at their reference values; the reference values are found in Appendix B. While it was known in advance that the reference design would have four stages, the analysis helps to visualize the reasoning for doing so and affirms the designs conclusion.

As can be seen from Figure 4.1, the net power output initially increases greatly, but as the number of stages increases, the increase in net power output becomes negligible. Diminishing returns in gross power production coupled with increased pumping losses caused by more heat exchanger pressure drop lead to the incremental gains being outweighed by the added parasitic losses. The diminishing returns effect was expected, and it demonstrates that while expanding from one stage to two stages can drastic, the payoff becomes less each time, so it is important to strike a balance.

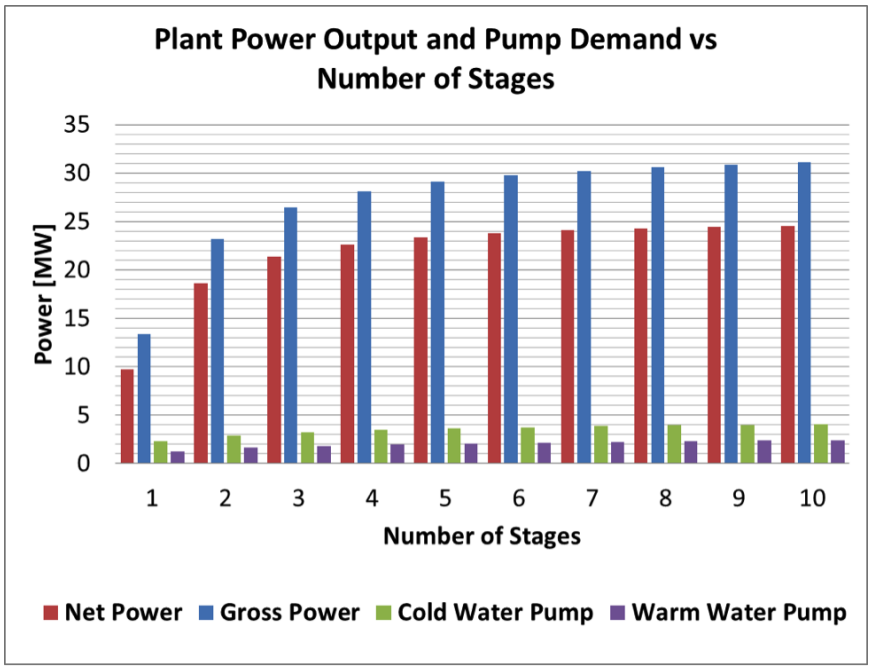

Figure 4.1: Power output increases with number of stages, but faces diminishing returns.

Looking at the graph of fractional amount of power consumed by the water pumps explains this effect of diminishing returns. The pumping power demand as a fraction of the gross power output is shown in Figure 4.2. Even though the pumping power fraction decreases dramatically due to the large gain in additional power output, it later rises again due to the additional losses in the system that come with an increase in the number of stages. After 3 stages, it appears that the incremental gains begin to be outweighed by the added losses incurred in each subsequent stage.

From analyzing Figures 4.1 and 4.2 together, it is concluded that staging the power cycle offers significant benefits when using 2 to 5 stages. The graph of heat exchanger area per kW of net power, as seen on the left in Figure 4.3, also suggests this same conclusion. However, the metric of gallons per second of water pumped per kW of net power produced, shown on the right in Figure 4.3, suggests that 10 or

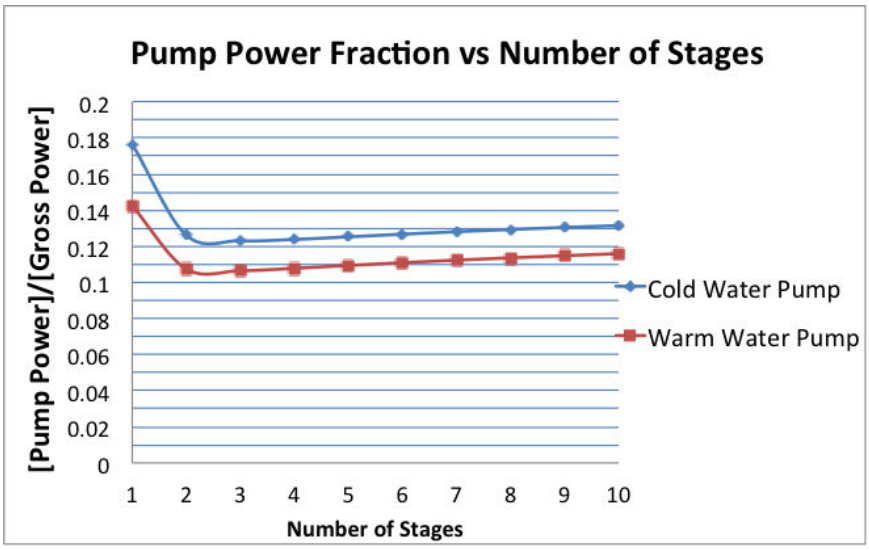

Figure 4.2: Water pump power demands, normalized by gross power output, as a function of the number of stages in the power cycle.

more stages offers the highest utilization of water pumped.

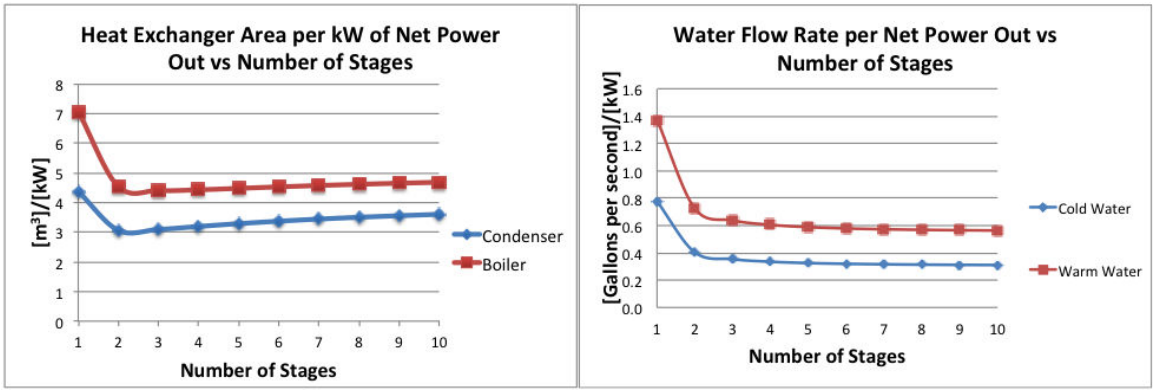

Figure 4.3: The Heat Exchanger area per net kW demonstrates that 2-4 stages is optimal, while the water flow rate per net kW suggests that there are still performance benefits at higher number of stages.

The reasoning for the disagreement between the water flow rate metric and the other metrics from the other figures is that it only takes into account net power and water flow rate. The model output shows slight increases in net power output out past 20 stages, and the water mass flow rate is nearly constant, since all of the temperature

and other parameters are constant. In actuality, having such a high number of stages would require significantly smaller turbines, which in turn are typically less efficient, and so the estimations of this model are overly-optimistic on conversion efficiencies for power output at higher number of stages.

Based on the diminishing returns in net power output, as well as the local minimum seen in the pumper power fraction of Figure 4.2 and the heat exchanger area per net kW of Figure 4.3, this analysis leads to conclusion that 2-4 stages is likely the optimal number for an OTEC plant. The optimal number of stages for an actual OTEC plant will depend on other constraints besides performance, such as capital cost, minimal power delivery requirements, and desired system redundancy. Regardless, this analysis proves that staging power cycles within an OTEC plant can offer benefits, but with diminishing returns.

4.4 Analysis of the Overall Heat Transfer Coefficients and Heat Exchanger Pressure Drop

Overall heat transfer coefficient and pressure drop are two primary measures of heat exchanger performance. In the case of the model, and this analysis, it is assumed that the pressure drop on the working fluid side is negligible compared to that of the water-side pressure drop. This analysis looks at how heat transfer coefficient and pressure drop impact plant performance. The range of analysis of $1\frac{kW}{m^2K}$ to 12 $\frac{kW}{m^2K}$ was chosen to represent the range as covering from an sub-optimized off-the-shelf heat exchanger, up to that of what might be attainable with a highly-specialized custom design [3, 5, 10, 13, 14, 19, 22, 26, 44, 45, 48, 49, 56, 60, 61].

It is important to note that while these other studies have different values for the boiling and condensing heat exchanger coefficients, this analysis will use the

same value and vary both at the same time in order to assess the overall impact of highly optimized heat exchanger versus un-optimized heat exchangers. Since the heat exchanger models cited were designed for different heat duties and working fluids, the goal is not to replicate their performance, but rather use the overall range for assessing the impact of heat exchanger performance on plant operation.

Figure 4.4 shows the gross and net power produced, as well as pump power demand, over the range of heat transfer coefficients tested. The heat transfer coefficient does not have an impact on the gross power produced by the plant, if the water temperature and TTD values used as independent variables. With the temperatures assumed to be fixed, and the heating load determined by the power cycle, the dependent variable is heat exchanger area. The result is that gross power remains the same, while net power output increases with increasing heat transfer coefficients.

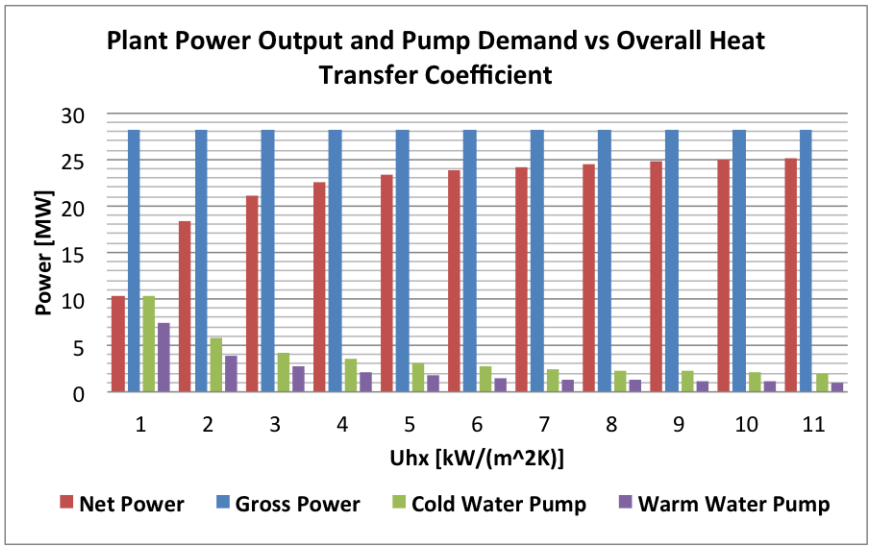

Figure 4.4: The plant net power output increases as a function of the overall heat transfer coefficient of the boilers and condensers.

Figure 4.4 shows that while a low heat transfer coefficient can drastically reduce net power output, a highly-specialized design will not produce drastically more

power than the reference case, when using the same temperature input variables. However, this trend does not mean that heat exchangers with high heat transfer coefficients are not useful; with higher heat transfer coefficients, a smaller TTD or a lower water temperature change may be used, which could increase the gross power output, and thus further improve plant operation. The other benefit not captured in Figure 4.4 is the drastic reduction in heat exchanger surface area, which can bee seen in the decrease of the total and per kW area, shown in Figure 4.5.

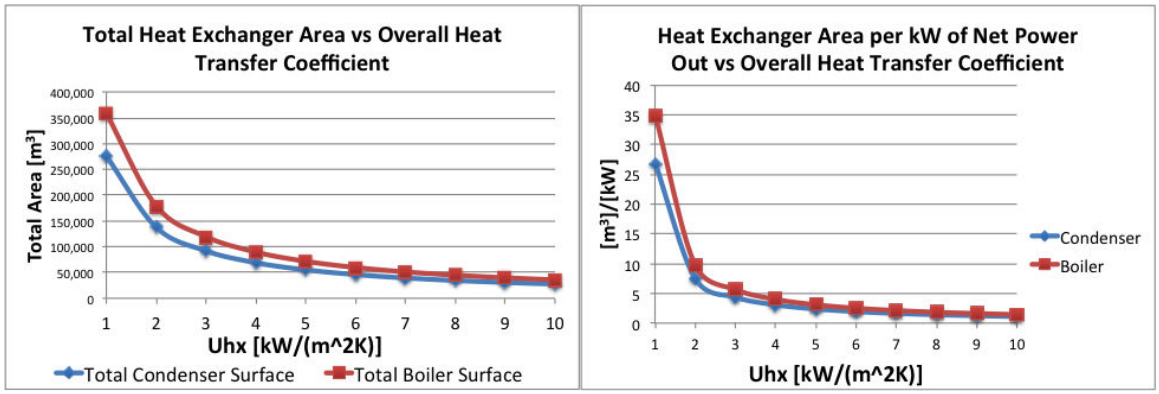

Figure 4.5: Heat exchanger area is inversely affected by the overall heat transfer coefficient, and as a result so is heat exchanger area per kW of net power generated.

From analyzing Figures 4.4 and 4.5 together, it is concluded that the primary effect of heat transfer coefficient is the reduction of heat exchanger area. Reduced area, in turn, impacts net power generated by way of the pump power demand being a function of heat exchanger area. Minimizing heat exchanger area is obviously important, and so it is primarily from that aspect that high heat transfer coefficient heat exchangers are desirable, and less from a higher net power generation standpoint.

The above analysis uses the reference heat exchanger pressure drop and water velocities across all heat transfer coefficient values tested. While this simplification is not entirely representative of real-world heat exchangers, the analysis remains appropriate because in an actual plant, where the heat exchanger area is the chosen design

variable, the water pressure drop could be monitored and the heat transfer coefficient could be backed out from the real-world thermal output.

It is also important to understand the impact of the water pressure drop on the performance of the system, and so an analysis was run for heat exchanger pressure drop values ranging from 1 psi to 6.5 psi, which is a somewhat larger range than the values typically seen in the literature [3, 5, 10, 13, 14, 19, 22, 26, 44, 45, 48, 49, 56, 60, 61]. For this analysis, the pressure drop was assumed to be the same in both the boiler and condenser, and both were varied at the same time. Figure 4.6 plots the net and gross power output, as well as the pump power demands, for heat exchanger pressure drop values ranging from 1 to 6.5 psi.

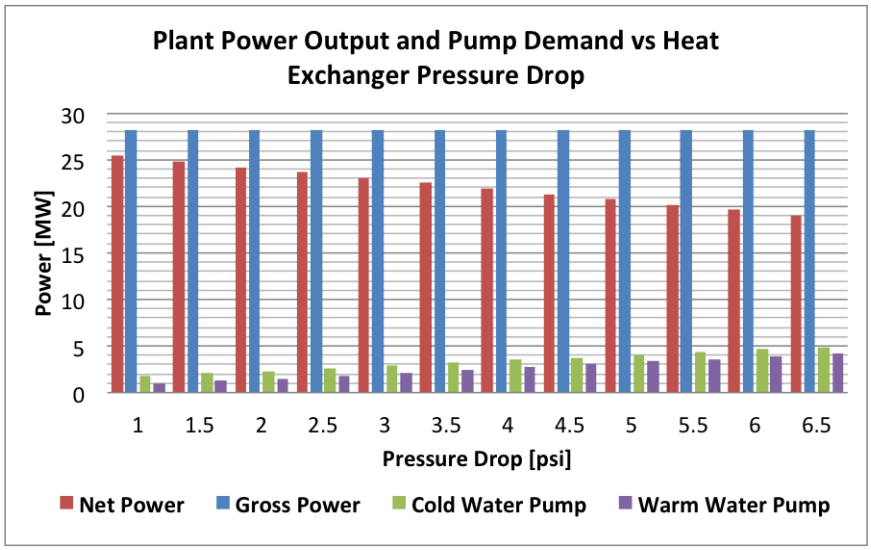

Figure 4.6: The net power output is a linear function of the pressure drop in the heat exchanger water passages.

The linear decrease in net power output was expected, since the heat exchanger pressure drop is treated as a loss coefficient value, as discussed in Section 3.4. Curve fitting a line to the net power output yields a slope of approximately 1.16 MW of total added pumping power demand per psi of heat exchanger pressure drop. Therefore, if

a heat exchanger could be redesigned to maintain the same heat transfer coefficient while reducing pressure drop by 1 psi, it could equate to roughly an added megawatt of net power generation.

Looking at both the overall heat transfer coefficient and pressure drop together, the graphs suggest that when picking a heat exchanger, the pressure drop and heat transfer coefficient need to be optimized together. Often heat transfer coefficient and pressure drop are positively related, since improving heat transfer from surfaces is often done by adding fins, ridges, or other elements that would lead to added pressure losses. A balance must therefore be struck between the heat transfer benefits of surface enhancements, and the added pressure drop incurred as a result. The ultimate factor for any heat exchanger design will be price, which is not reflected in this model. If the added performance gains come at a very high price, then the design could be sub-optimal, and the same could be said of the opposite case of marginal performance and low per-area cost. Therefore, the heat exchangers offer a prime example of a component that must be optimally chosen based on several competing performance and financial criteria.

4.5 Analysis of Water Inlet Temperatures

The purpose of looking at the effects of different water inlet temperatures is to get an idea of the potential performance of an OTEC plant in different ocean temperature conditions. The $80°F$ hot water and $40°F$ cold water inlet temperatures are often cited, but not really representative of all potential OTEC cites; they are simply a good approximate average, and demonstrate a good performance. However, the ocean's temperature distribution is not so uniform, and there are many places interested in deploying OTEC power generation that do not have either such a high

hot water temperature, or such a low cold water temperature. The number of stages and the TTD are held constant, and the exit temperature is adjusted to maintain the same temperature change between inlet and exit. By effectively reducing the temperature differential, this analysis simulates the performance of running a plant designed for one set of temperatures with different thermal resources, as might be experienced with seasonal changes or relocation of the plant.

Figure 4.7 shows the gross power produced, net power produced, and pumping power requirements as functions of varying cold and hot water inlet temperatures respectively. While they were each calculated individually, the model predicts the same type of linear relationship between temperature and gross power generation for both cold and hot water inlet temperatures.

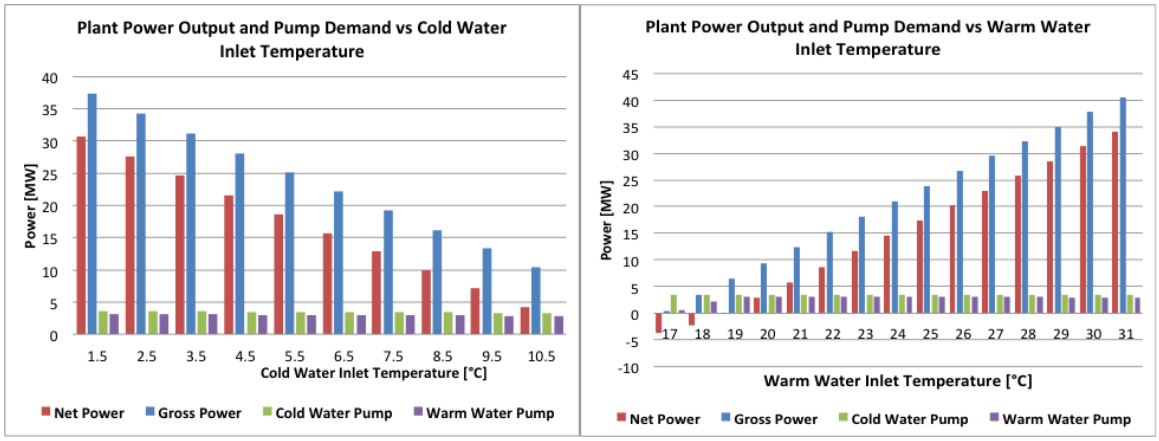

Figure 4.7: The net power output is a linear function of the inlet water temperature when a constant overall temperature change is maintained between inlet and exit.

Figure 4.7 suggests that self-sustaining operation would be impossible at an overall ocean temperature differential of less than about 14.5 to 15°C, as calculated by subtracting the inlet hot water temperature from the inlet cold water temperature. The reference cold water inlet temperature is 4.5°C, and the reference hot water inlet temperature is 26.5°C.

Figure 4.8 is the line-plot version of Figure 4.7. The fitted equations show the changes in power output are nearly linear. The effect of cold water temperature on gross power generation is slightly more pronounced, at 2.99 MW per $°C$, but the effect of hot water inlet temperature is still close at 2.86 MW per $°C$. Hence, operating at even one degree below the designed temperature differential could lead to significant power reductions on the order of 15%. Conversely, operating at a slightly higher than designed temperature could yield 15% per degree above the reference power output.

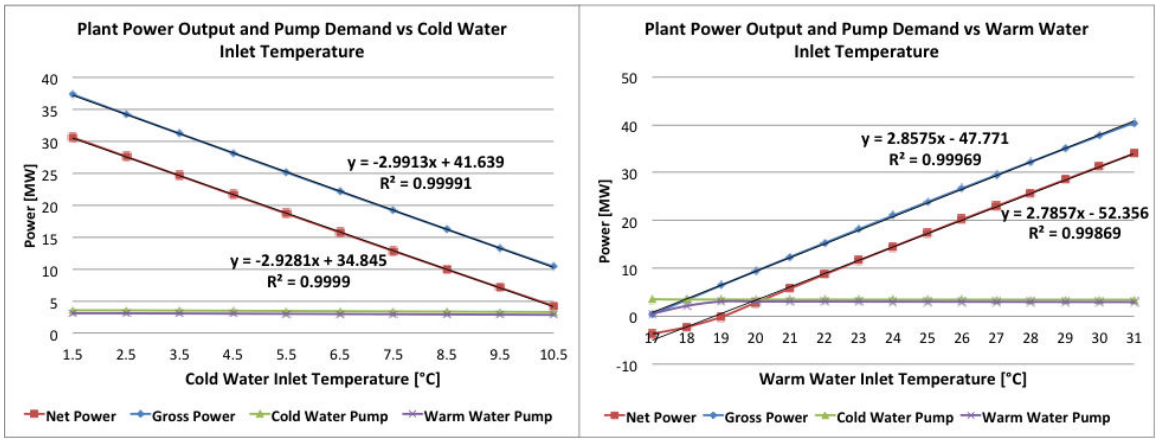

Figure 4.8: Changing cold and hot water inlet temperatures has a nearly linear effect on the gross power generation.

This linear relationship is due to the linear change in available thermal potential entered into the model, and directly equates to a linear increase or decrease in the difference between boiling and condensing temperatures. The model calculates boiling and condensing temperatures based on the inlet temperature, the overall temperature change between inlet and outlet, number of stages, and TTD in the heat exchanger; this calculation is described Section 3.2.1. The power cycle takes the boiling and condensing temperatures and uses them to find enthalpy values which in turn are used to calculate power output. A lower temperature differential leads to a lower enthalpy difference, and less power out. The converse is true for a higher temperature

differential, regardless of whether it is caused by colder condensing temperature, or a higher boiling temperature.

It is also interesting to note that the pumping power is hardly affected by this change, only decreasing slightly with increasing temperature. The pump is mostly unaffected because the enthalpy of vaporization and condensation is not nearly as dependent on temperature as the regular enthalpy value. Roughly the same amount of water must be pumped to vaporize and condense the working fluid; referring to section 3.2, the change in the enthalpy difference from state 2 to state 3 varies much less than the change in the enthalpy difference from state 3 to state 4. Hence, roughly the same amount of water must be used to boil and condense regardless of boiling or condensing temperatures, but the gross power output is highly dependent on the temperature difference between the two. This relationship does not extend over an infinite temperature range, but on this scale of temperature differential, the enthalpy of vaporization is nearly constant.

Since pumping power is nearly unaffected, the pump power fraction has an inverse relationship to the temperature differential due to the linear relationship between temperature and gross power, as discussed above. Figure 4.9 is the pump power fraction for varying cold water inlet temperatures, and its trend is indicative of the trend for varying the hot water inlet temperature as well.

Figure 4.9 offers another visualization of how inlet temperature, and overall temperature differential between hot and cold water, affects plant operation. The figure demonstrates how much harder the plant must work to produce net energy as the ocean temperature differential decreases; conversely, it also suggests pumping power losses asymptotically go to zero, albeit at temperature differences much higher than are found in the ocean.

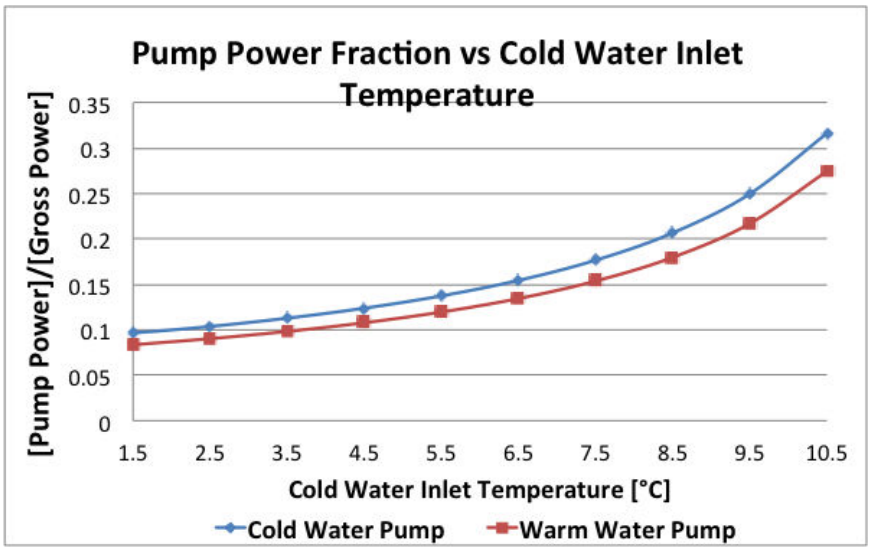

Figure 4.9: Pumping power remains the same while gross power varies, which leads to an inverse relationship with temperature.

Heat exchanger area has a similar relationship to inlet temperature as pumping power. The left side of Figure 4.10 shows the heat exchanger area per kW of net power output varying with cold water inlet temperature; the right side of Figure 4.10 has the overall heat exchanger area required for a particular cold water inlet temperature.

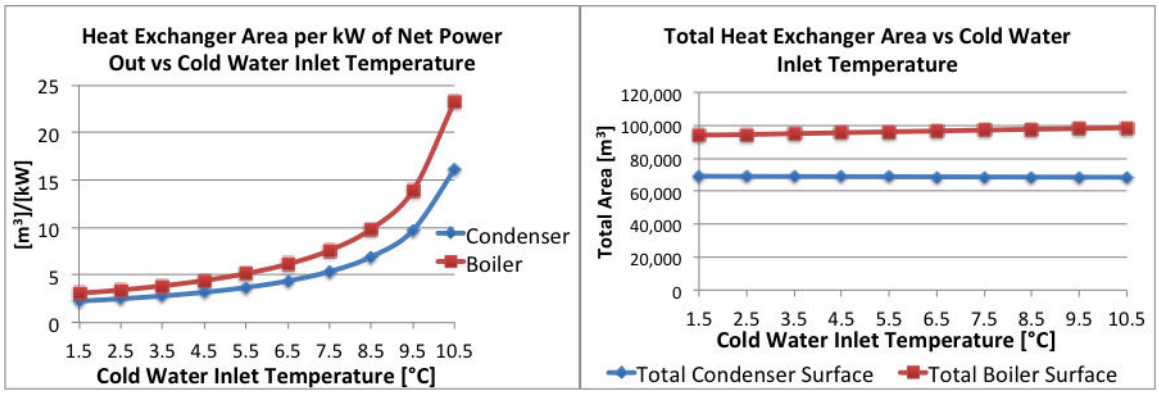

Figure 4.10: Heat exchanger area has a similar relationship to power output as pumping power.

As seen from Figure 4.10, the overall heat exchanger area does not increase substantially with increasing cold water inlet temperature, but the heat exchanger

area per net power generated does because of the comparatively lower power generated. All of the different measures of plant performance point to the conclusion that a higher hot water inlet temperature, and a lower cold water inlet temperature, lead to higher power output. The gross and net power output are both linearly related to water inlet temperature, and by extension overall water temperature differential, by a factor of approximately 2.9 MW per degree Celsius. Both pumping power and heat exchanger area requirements were nearly constant compared to the large variation of the power output. The end result of this analysis was an obvious conclusion, but the constant pumping power and heat exchanger area were two unobvious secondary relationships that might have otherwise gone unnoticed.

4.6 Analysis of Terminal Temperature Difference and Water Discharge Temperature

Terminal temperature difference (TTD) and water discharge temperature are similar variables in this model in that they are both setting a temperature difference between the water and the working fluid in the plant. This section will first look at TTD, and then water discharge temperature. The TTD, also sometimes referred to as the pinch point temperature, is the minimum temperature difference between the water and the working fluid in a heat exchanger. The plant uses a single-component phase-change material, along with a cross-flow heat exchanger design, and so the TTD will always occur at the exit point of both streams.

The TTD was varied in both the condenser and boiler from 0.25 to 4.0°C in an effort to determine the effects of TTD on system performance; for comparison, the reference case TTD is 2°C. OTEC power generation is unique because it operates on such a small temperature differential. In that regard, minimizing the TTD provides more thermal potential to the power cycle, and thus produces more power. However,

based on the heat exchanger relationships discussed in section 3.3, it is seen that when the $LMTD$, which is a function of TTD, decreases, the heat exchanger surface area must increase to take up the slack. Figure 4.11 shows this competition between increased gross power output and increased pump power demands due to increased heat exchanger surface area.

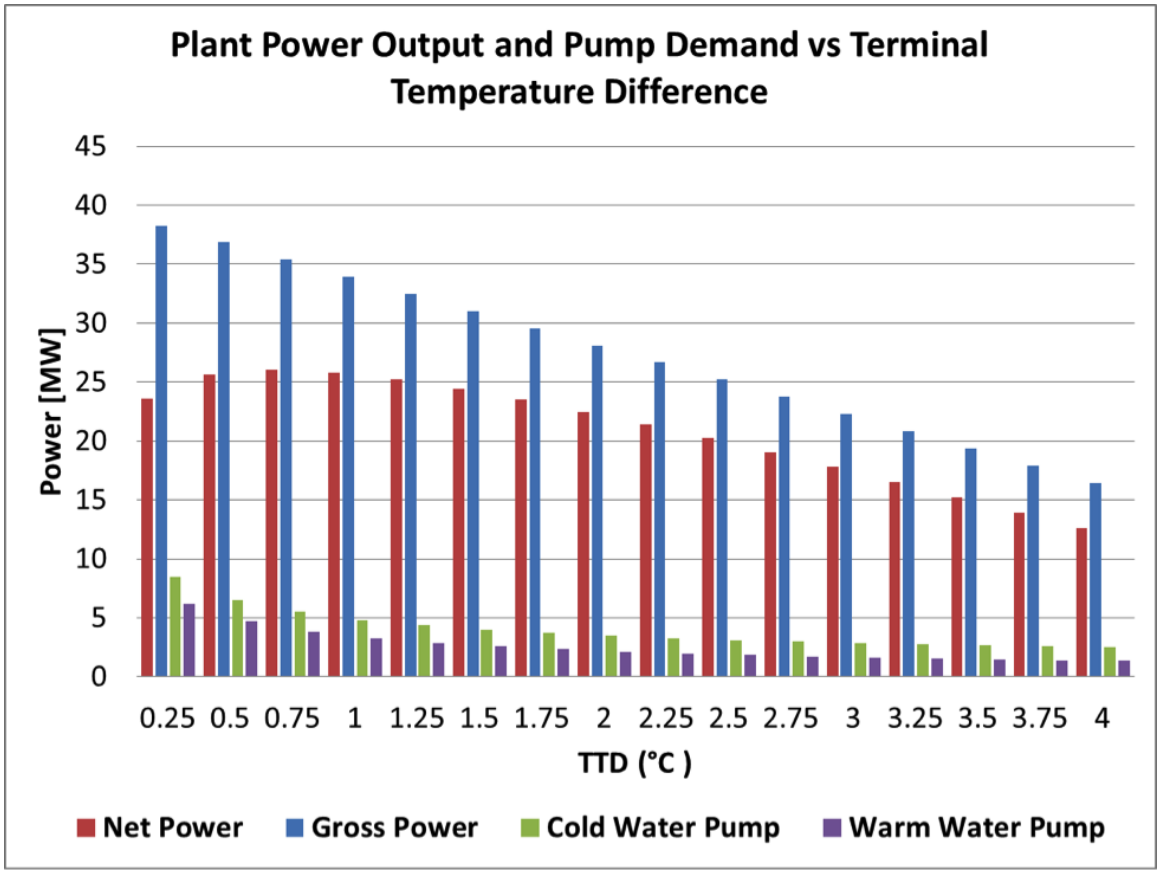

Figure 4.11: Terminal temperature difference affects both the gross power output and the pump power demands, leading to a local maximum.

While net power output peaks in the area of $0.75°C$, other performance metrics suggest $0.75°C$ is not the optimal operating point. Figure 4.12, shown below, contains plots of heat exchanger area per net kW and the pump power fraction. Both of these performance metrics suggest that operating at a low TTD, as suggested by Figure

4.11, would be require a higher amount of pumping power and heat exchanger area.

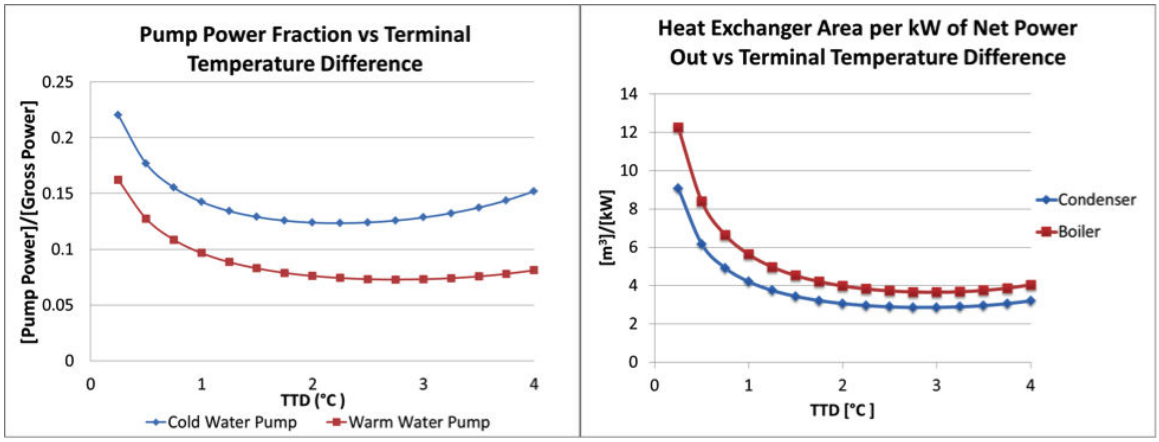

Figure 4.12: Pump power fraction and heat exchanger area per net kW are not optimal in the 0.75 to 1°C TTD range suggested by the net power output.

The cause of both of the trends in these graphs is due to the heat exchanger area. Both trend down to a minimum, and then trend up again at higher TTD because even though the heat exchanger area is much lower, so too is the gross power output from the plant. Heat exchanger area has a complicated nonlinear relationship to TTD because it is inside the logarithmic denominator of the $LMTD$, as seen in Equation 4.1.

$$\dot{Q}_{in/out} = U_{hx} \times A_{hx} \times LMTD = U_{hx} \times A_{hx} \times \frac{\Delta T_{hw/cw,\ stage}}{\ln \frac{\Delta T_{hw/cw,\ stage} + TTD}{\Delta T_{hw/cw,\ stage}}} \tag{4.1}$$

Regardless of the exact relationship, the heat exchanger area drastically increases as TTD approaches zero. Increased heat exchanger area in turn drives up the pumping power demands, and decreases the net power output. These analyses present an interesting case in that the analysis metrics are not in agreement, and demonstrates that TTD is an important design variable with high impact on sys-

tem performance. The next analysis, looking at the water discharge temperatures, exhibits some of the same relationships.

The relationship between plant power output, working fluid temperature, and water discharge temperature is less obvious than it is for TTD. The model specifies water inlet temperature, which is ultimately the uncontrolled ocean water temperature, as well as the temperature of the water discharged back into the ocean. In the inlet water analysis from the previous section, the discharge temperature was varied with the inlet temperature in order to maintain a constant overall water temperature change across the boilers and condensers. This section analyzed the effects of temperature change between the inlet and discharge, by way of adjusting the discharge temperature while maintaining a constant inlet temperature. The cold water discharge temperature was varied from 9 to 17$°C$, and separately the hot water was varied from 16.5 to 24.5$°C$. Figure 4.13 shows the power output and pump power for these temperature ranges; the reference discharge temperatures are 13$°C$ for the cold water and 21.6$°C$ for the hot water.

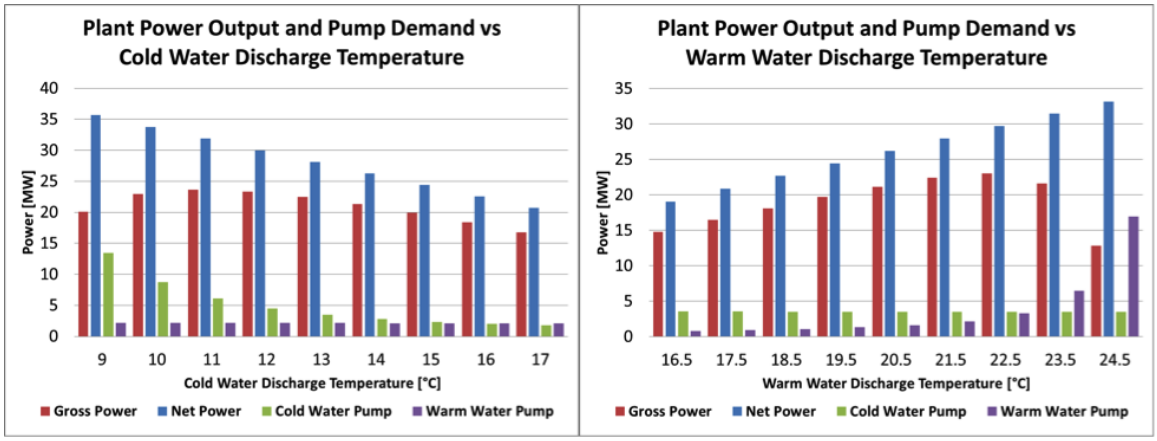

Figure 4.13: Adjusting the cold and hot water exit temperatures, while holding the inlet temperatures constant, could lead to improved plant performance.

As shown in Figure 4.13, varying the exit water temperature has a linear

effect on gross power generation, and non-linear effect on pumping power. This is similar to the mass flow rate analysis because changing the amount of allowable temperature drop via changing water discharge temperature has a direct impact on boiling or condensing temperature. Also similarly, the pump power demand increases non-linearly because the velocity is increasing, and the scaling relationship of pump power to velocity is $v^{1.8}$, as discussed in Section 3.4. These competing functions combine to create a maximum in the net power output curve. These figures suggest that the system could produce a higher net power output than the reference case if the temperature delta between the inlet and discharge was decreased, or rather if the exit temperature were closer to the inlet temperature. For this model, it appears that the optimal temperatures for highest net power output occur at $11°C$ and $22.5°C$, for the cold and hot water discharge temperatures. In reality, making this adjustment would likely require dialing the pump power up or down, since there is no way to directly, physically set the exit temperature. This type of operational control would require some sort of feedback loop to iteratively find the optimal pump power.

If the desire is to operate the plant in the most efficient manner, rather than maximum power output, then the pump power fractions, show in Figure 4.14, suggest that the combined pumping power is minimal when using a larger temperature delta than the reference case. The minima appear at approximately $15°C$ for the cold water discharge, and $20.5°C$ for the hot water discharge. These values are $2°C$ higher for the cold water and approximately $1°C$ lower for the hot water than the values in the reference case.

While all of this analysis has focused only on one exit temperature being varied or the other, in this case the effects are essentially independent. Using the optimal discharge temperature at both the inlet and exit would lead to the combined effects

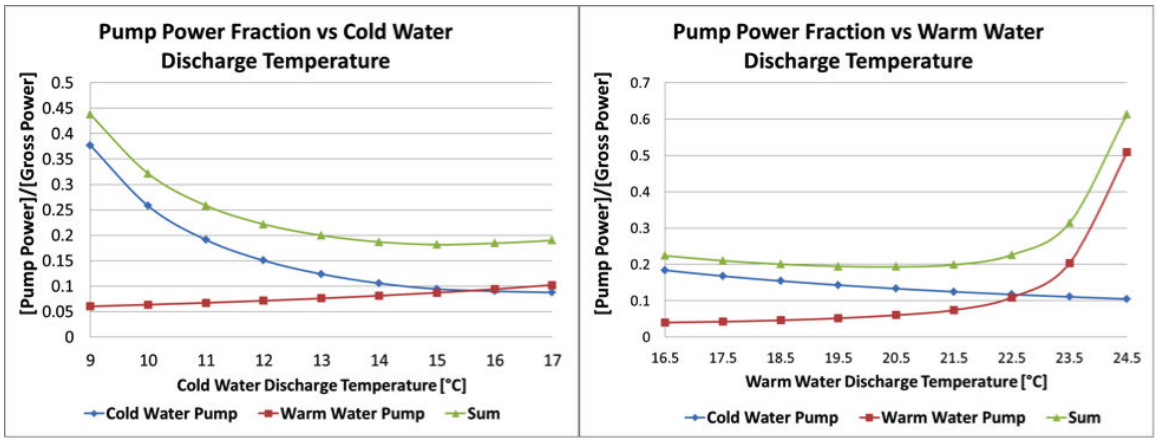

Figure 4.14: The combined pumping power is minimal when the cold water discharge is approximately $15°C$ and the hot water discharge is approximately $20.5°C$.

of the two. The additive nature of the effects makes optimizing the system with these two variables easier since all that is required is finding the maximum point for each individually, as opposed to two dependent variables, which might negate each other.

4.7 Analysis of Cold Water Pipe Diameter and Length

The cold water pipe is a uniquely large, yet simple component of the plant, and it has an indirect, but large, impact on power consumption by way of pumping power losses. Pumping losses in the cold water pipe come from two sources: hydrostatic pressure head from density imbalance, and viscous friction losses. The density imbalance leads to an effective pressure head because the higher density cold water inside the pipe is heavier than the water outside, thus it is not completely balanced by the less dense water outside. Therefore, the cold water requires pumping power to overcome the adverse hydrostatic pressure. This density difference is a consequence of the ocean thermal temperature gradient that is desired for plant operation in the first place, and is unavoidable.

The second source of pressure drop is viscous losses in the pipe, which is

attributable to both flow velocity and pipe length. This analysis looked first at the effects of the diameter, and then length, on plant performance. The diameter was varied from 2 to 8 meters, with the reference diameter being 4 meters, and pipe length was varied from zero to 20,000 meters. The length analysis covers such a wide range in order to see what the pumping power would be for both the most ideal case (i.e. cold and hot water both simultaneously available at the surface), as well as the length range for a shore-based plant.

Pipe diameter is an interesting design variable; a narrow pipe would be less expensive and easier to install, while a wide pipe would reduce water velocity at a given volumetric flow rate. The pipe diameter has a large effect on the cold water velocity because velocity has a non-linear relationship to diameter for a constant volumetric flow rate; as the diameter increases, the velocity scales as $\frac{1}{D^2}$. This scaling relationship to the pipe diameter is due to the fact that average flow velocity is equivalent to the volumetric flow rate divided by the cross sectional area. The non-linear effect is quite apparent when looking at the cold water pumping power in Figure 4.15. It is important to also note that the hot water piping parameters were held constant through this analysis, which is why hot water pumping power is level.

Figure 4.15 demonstrates the importance of avoiding under-sizing of the cold water pipe; however, it also shows that there are negligible returns for a larger diameter pipe. The trend at larger diameters is due to the design of the model; the heat exchangers are designed for certain water flow velocities, and the model will assume the flow is accelerated back to those values to pass through the heat exchangers. Therefore, while the pressure loss in the cold water pipe due to friction is an issue, it is relatively minor when compared with the heat exchanger losses, if the pipe is above a size of about 4 m. The reference case is based on a 4 m diameter cold water pipe

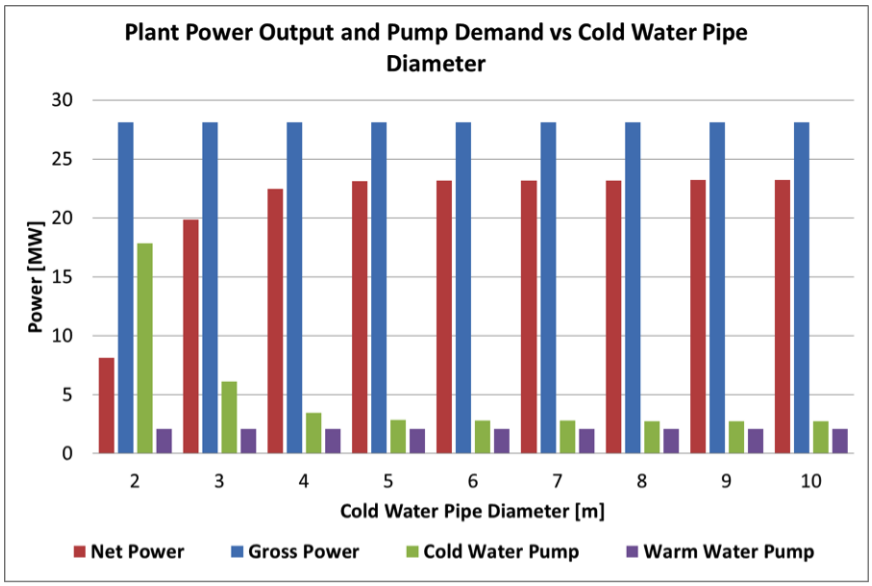

Figure 4.15: Cold water pumping power is a function of water velocity, which in turn is a function of pipe diameter.

because that is what the Sea Solar Power plant was designed with, and this analysis validates that decision.

As was mentioned, the model will change the cold water velocity to the reference design velocity of the heat exchanger if the water velocity is less than it. However, the model will use the calculated velocity if it is above the reference velocity, and scale heat exchanger pressure drop and heat transfer coefficient accordingly; these calculations are discussed in section 3.4. Figure 4.16 shows the effects of the increase in water velocity, due to a smaller diameter, on the condenser heat exchanger area.

These graphs show indirectly that water velocity can have a large impact on both the amount of heat exchanger area needed, as well as pressure drop. The sum of the heat exchanger area per kW values for the condenser and boiler in Figure 4.16 suggests that there might be a potential benefit to using a diameter of 3 meters, if minimizing heat exchanger area is a primary concern in the design. However, the cold

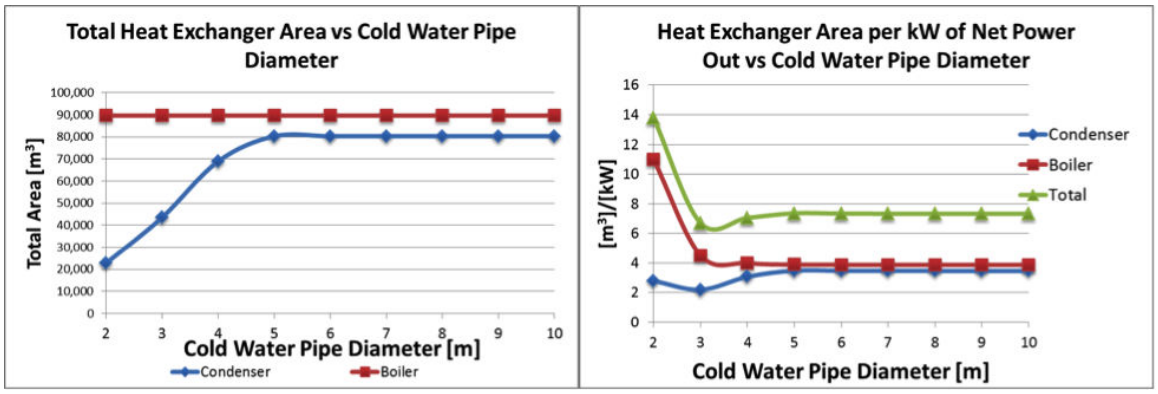

Figure 4.16: Cold water pumping power is a function of water velocity, which in turn is a function of pipe diameter.

water pumping power is increased while the gross power remains constant, as seen in Figure 4.15; therefore, it is reasonable to infer that the fraction of the cold water pump is increased, and in turn overall plant efficiency decreased. All of this analysis leads to the conclusion that cold water pipe diameter should be optimized based on the cold water flow rate demands of the plant. The diminishing effects of using a larger pipe diameter suggest that the pipe should be sized such that water velocity in the pipe is approximately equal to the desired flow rate in the heat exchangers.

Assessing pipe length to pipe diameter equally in terms of operational impact is not a fair comparison, since the pipe length will ultimately be dictated by site conditions, while the diameter is a more arbitrary decision. However, looking at cold water length still offers insight for the purposes of site planning, specifically by allowing for the comparison of on-shore and off-shore pipe lengths. Typically, an offshore plant is designed with a suspended pipe approximately 1000 meters long. An on-shore plant must build the pipe down the slope of the seafloor to sufficiently cool water. This analysis looks at two different length ranges, with one range for potential offshore plants and one range for onshore plants. To test the effects of pipe length on a typical offshore plant, a pipe length range of zero to 2000 m was chosen. For the

onshore, few places in the world have cold water resources directly next to shore, so this analysis uses a range of 5 to 20 km as an approximate pipe length range. Figure 4.17 is the typical gross, net, and pumping power graph for this analysis, except in plotted point form instead of bar chart form, and plotted to cover both ranges. The full test range was therefore zero to 20 km, with uneven step spacing, to capture trends at both short and very long length scales.

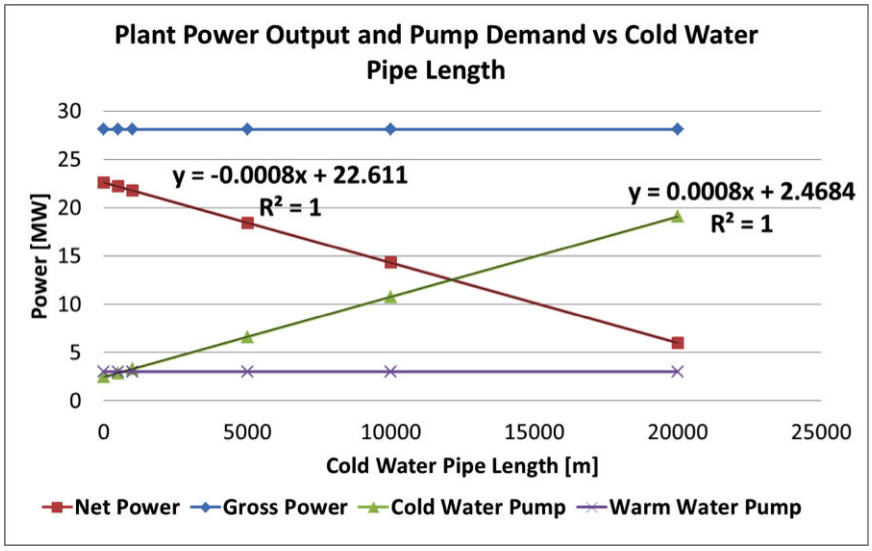

Figure 4.17: Cold water pumping power approaches a minimum but nonzero value at short pipe lengths, and increases linearly with length.

Again, Figure 4.17 captures two length scales on the x-axis, from 0 to 2000 meters, and from 5 to 20 km, but the slope of pump power change is the same for both scales. The linear slope is a function of the cold water pump power equation, found in section 3.4, which is a linear function of length. By fitting equations to the cold water pump, a net-power-loss-to-length value was obtained. This slope suggests that the power loss per meter of cold water pipe is 0.8 kW; or put another way, for every meter of cold water pipe length, the plant would need an additional 0.8 kW of pumping power. Again, this analysis is assuming all other design variables are held

constant. The fitted equations also demonstrate that the impact of cold water pipe length is a completely linear change in power.

The purpose of the 0 and 500m length calculations was to demonstrate that even if the cold water resource was closer, or even effectively at entrance of the plant, it would still require a non-trivial amount of energy to pump it through the cold water heat exchangers. At the other end of the spectrum, this graph shows that net power production would eventually go to zero at a value of approximately 28km, if all other design variables were held the same. This analysis demonstrates the reasoning for an off-shore plant that minimizes cold water pipe length. However, the analysis also suggests that performance only linearly decreases, and if a non-performance variable such as cost of building offshore increased at a non-linear rate, then there might be instances where building an on-shore or perhaps a coastal shelf stilted platform plant might be viable.

4.8 Analysis of Working Fluid Mass Flow Rate

Working fluid mass flow rate is one of the fundamental driving variables of this model, and as such it was a natural choice for analysis. The model uses the boiling and condensing temperatures, based on the specified water temperatures and TTD, then uses the specified mass flow rate to calculate the gross power generated, as well as the required heating and cooling source and sink provided by the hot and cold water. If the working fluid mass flow rate increases, the heating and cooling demands increase, and visa versa. Therefore, the required water flow rates are indirectly a function of working fluid mass flow rate; furthermore, pumping power demand is ultimately tied to working fluid mass flow rate as well. Secondary impacts of working fluid mass flow rate on the system result in non-linear relationships to net power output and

pumping power demands, as seen in Figure 4.18.

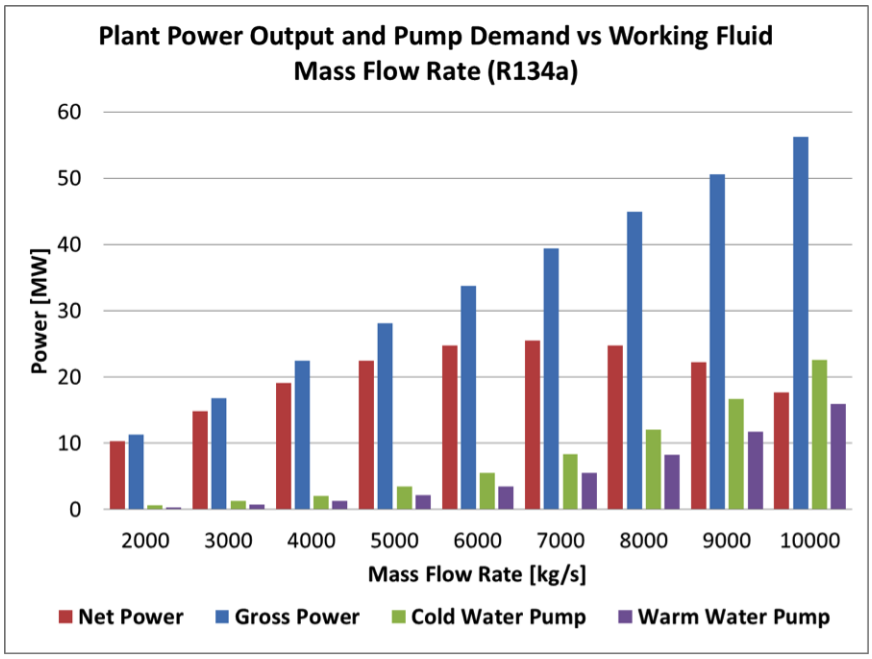

Figure 4.18: Cold water pumping power is a function of water velocity, which in turn is a function of pipe diameter.

Figure 4.18 suggests that mass flow rate is an obvious target for further optimization, since it exhibits a local maximum for net energy production that is higher than the reference value. The net energy production peaks, while the gross power keeps increasing linearly. The peak is due to the linear increase in gross power generation being outpaced by the non-linear increase in pump power demand due to higher water velocities (because of greater water flow rates). With the geometrical parameters constant, water velocity is linearly related to water volumetric flow rate, and pump power in turn is a function of water velocity raised to the 1.8, as discussed in Section 3.4. Based on these trends, it would appear that increasing the mass flow rate of working fluid would be optimal for performance.

However, a lower mass flow rate could be determined as optimal when evaluating by the water mass flow rate per net kW and heat exchanger area per net kW

metrics, which are both shown in Figure 4.19. The figure shows that the plant's water pumps require a lower fraction of the gross power to operate when the working fluid mass flow rate is low; the graph of cold and hot water flow rates per net kW, also demonstrates the same sort of trend.

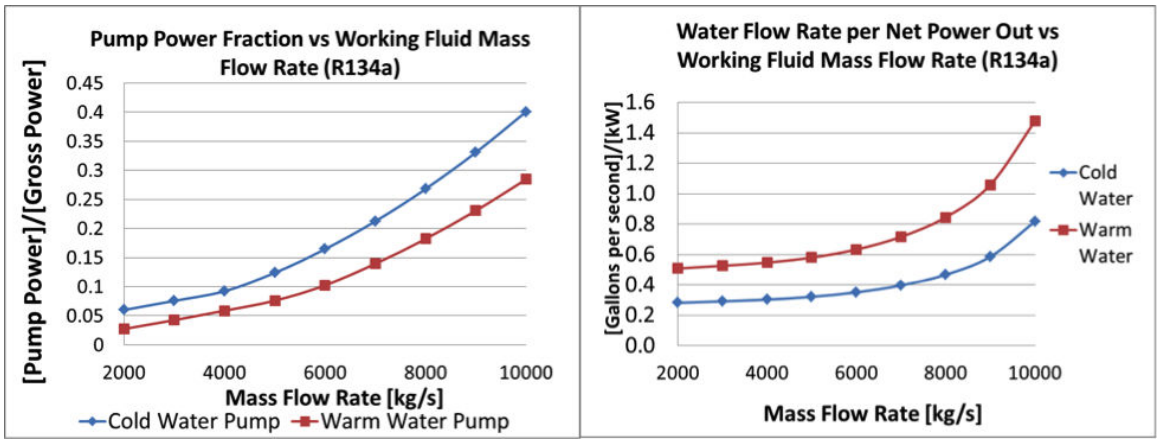

Figure 4.19: Pump power fraction and water flow rate per net kW suggest a lower working fluid mass flow rate for more efficient operation.

The pump power fraction is lower at low flow rates because less water is needed, because the overall heat duty of the plant is lower, which in turn means the water flow rate is slower, and hence pump power is reduced. Less gross power is generated, but even less is needed for pumping water. Based on analysis drawn from Figure 4.19, using a modular system, with multiple staged power systems in parallel, could provide an optimal solution. Such a setup would reduce water flow rates and produce the desired amount of power more efficiently. These designs are pursued to a certain degree, but face certain design and operational limitations not captured in the model. The analysis is based on the reference pipe diameters, and so systems in parallel, in order to maintain the low flow velocities, would require much larger hot and cold water piping systems. Also, smaller systems may operate less efficiently, due to heat loss/gain to or from the surroundings, or because smaller turbines, motors, and other machine

components tend to get less efficient with decreases in size. Costs are also usually non-linear for small equipment, meaning a plant builder might pay significantly more per kW of turbine capacity for a 1MW turbine than you would for a 7 MW turbine. However, parallel system modules would also add some beneficial redundancy to the system, allowing it to potentially operate at reduced power by shutting off one of the parallel modules completely, as might be needed for maintenance or if demand is low.

This analysis also demonstrates the potential for economically throttling back the power output by decreasing working fluid mass flow rate. Knowing that the plant operates more efficiently, albeit at a lower net power output, could be beneficial for the plant operator. If demand were low, it would be much better to operate the plant more efficiently at reduced load by lowering mass flow rate, and avoid the wear and tear on pumps and other equipment.

The model works somewhat backward from other plant design models, in that this model sets the temperatures, working fluid mass flow rate, and the other design parameters, and then calculates the plant performance from these [11, 25, 31, 43, 51]. Another method of analysis would be to specify a desired net power output, and optimize with the flexible mass flow rate and temperature variables to achieve the desired power output. This other method was not chosen because it does not lend itself as easily to performance comparison, due to the fixed net power output, although it could more accurately represent plant design. In the end, both models would perform the same calculations, just from different sides of the equal sign.

4.9 Conclusions from Thermal Fluids Systems Analysis

The analysis of a hypothetical 20 MW OTEC plant using the thermal fluids systems model looked at the effects that the plant parameters specified in Table 4.1

had on plant performance. The analysis was done by varying the values over the specified ranges, and looking at the impact on net electrical power output, pumping power fraction, heat exchanger area per net kW, and other performance metrics.

Staging was shown to be very beneficial over single stage plant design. However, performance returns diminish after 3-4 stages as the marginal increase in gross power output is negated by increased pumping power losses. The ideal number of stages was determined to likely be 2 to 4, depending on other factors such as the costs of extra equipment, piping, and valves, as well as the efficiencies of smaller plant components compared to larger ones.

The effects of the overall heat transfer coefficient, $\bar{U}$, and the heat exchanger pressure drop, Δp_{hx}, on performance were large, and underscored the need to have optimally designed heat exchangers. Improving $\bar{U}$ decreases the heat exchanger area required to handle the heat duty, which lowers the pumping power demand, and in turn improves the net electricity output. Conversely, a lower $\bar{U}$ means that much more heat exchanger area is needed, and as a result, pumping power losses are higher as well. There are diminishing returns at very high heat transfer coefficients because at that point the pumping power demand has been reduced such that the bulk of the losses come from the pipes and fittings, and not from the heat exchangers themselves.

This analysis assumed that Δp_{hx} was a fixed value over the range of $\bar{U}$, which is not entirely realistic of the real world, but Δp_{hx} was analyzed separately because the relationships between Δp_{hx} and $\bar{U}$ are heat exchanger dependent. Analysis of Δp_{hx} showed that net electricity output decreases linearly with increasing Δp_{hx}, with a slope of nearly 1.2 $\frac{MW}{psi}$. This slope was based on all other parameters being held at their reference values. Taken together, it is clear that a heat exchanger must be optimized both on pressure drop and heat transfer coefficient performance, and must

ultimately be optimized with the price of the heat exchanger when determining the optimal configuration.

Variation of the water inlet temperature yielded a linear relationship between water inlet temperature and power output. The analysis involved varying the hot and cold water temperatures individually. The corresponding exit temperature was also varied in order to maintain the same temperature change between inlet and exit, in order to focus primarily on the overall effect of the temperature differential between the hot and cold inlet temperatures with all else being equal. With all other variables held at their reference values, variation of both the cold and hot inlet temperatures produced very similar results. The minimum ocean water temperature differential needed to keep the plant running, based on the reference parameters, is approximately $15°C$. The other primary takeaway from this analysis was that power output linearly scales with temperature differential, with a slope of approximately 2.8 or 2.9 $\frac{MW}{°C}$, depending on whether it is the hot or cold inlet water temperature that is varying.

The TTD and discharge water temperature analysis were analyzed in order to assess the effects of varying the temperature difference between the water and the working fluid in the plant. Analysis of the TTD exposed how it leads to competing objectives of maximizing temperature differential and minimizing heat exchanger area (which in turn minimizes pumping power). A higher TTD increases heat transfer ability, reducing heat exchanger area, but at the cost of lowering the temperature differential between the boiler and condenser, which decreases power output. Conversely, a lower TTD increases the temperature differential, which increases power output, but at the cost of requiring more heat exchanger area and thus more pumping power. The optimal TTD depends on the performance metric is deemed most

important; looking only at net power output suggests a TTD of $.75°C$ is optimal for the reference plant, whereas the pump power fraction suggests a TTD of approximately $2.5°C$ would be better. This analysis highlights the importance of optimizing plant parameters for desired performance.

The discharge water temperature analysis consisted of holding the inlet water temperatures constant while varying only one exit temperature at a time. The purpose of this particular analysis was to asses the impact of the water temperature change on plant performance. It was similar to the TTD analysis in that the $\Delta T_{in,out}$ causes competition between the boiling and condensing temperature differential and the pumping power demands. In this analysis, the pumping demand impact was not from heat exchanger area, but rather from the impact on the required amount of water. While the power cycle output increases with a narrowing of the hot or cold water $\Delta T_i n, out$, there is a definite peak in the net power output for each discharge temperature. Therefore, when designing a plant, it is important to assess discharge temperature in the context of water temperature change in order to strike the optimal balance of flow rate and power output. The optimal values of both TTD and water discharge temperature (or water temperature change) are dependent on the rest of the plant; a plant with lower water pressure drop could operate with a smaller TTD, whereas a plant with a higher pressure drop would find it non-optimal.

Analysis of the cold water pipe diameter and length yielded expected results. Since the water velocity is inversely proportional to the diameter squared, as the diameter of the plant is increased, water velocity drastically increases to maintain the proper flow rate. Decreasing pipe diameter too much leads to massive pumping power requirements as the pressure drop also drastically increases. Conversely, since the heat exchangers are designed for a certain minimum flow rate, a very large diameter pipe

just reduces the cold water pipe losses to a negligible value, but the heat exchanger pressure drop still remains. Therefore the cold water pipe should be sized such that it is large enough to meet the flow rate at the prescribed flow velocity for the heat exchangers, and that oversizing the cold water pipe would only be beneficial if the plant were going to be designed to operate above its rated output on a regular basis.

The cold water pipe length analysis was simply to determine what effects the pipe length had on pump power demand and power output. The cold water temperature was assumed to be constant, and the length was varied over a wide range. The analysis showed that with all other plant parameters the same, the pipe length only affects the electrical power output by 0.0008 MW or 0.8kW per meter. This suggests that for a floating plant, it would be advantageous from a performance standpoint to deploy a 1500 meter long pipe rather than a 500 meter long pipe if it meant decreasing the inlet temperature by $1°C$, since the nominal power increase would still be 2MW (2.8MW - 0.8MW). This analysis did not account for temperature change of the water in the pipe as it traveled from the pipe inlet to the condenser, nor did it include any economic variables associated with pipe length, both of which would ultimately need to be considered when designing the cold water pipe.

Lastly, the working fluid mass flow rate was varied over the specified range in order to determine how it affects plant performance. Increasing $\dot{m}_{wf}$ leads to a higher thermal energy demand to boil and condense all of the working fluid, which means that water flow rates also increase. The increase in power produced competes with the increase in pumping power, similar to the variation of TTD and water discharge temperature. This behavior leads to an optimal mass flow rate of 6,000 to 7,000 $\frac{kg}{s}$ of working fluid based on net power output. However, the pump power fraction suggests that operating the plant at very low flow rates is optimal. At small $\dot{m}_{wf}$, even though

the plant produces much less power, the pumps consume proportionally less than the reference case, so operation is highly efficient. The trade-off is that the plant is still sized for producing much more power, and so the economics of such operation are likely non-optimal. While the working fluid analysis does not suggest it directly, the efficient half-power operation, and the ability to produce slightly more electricity at higher mass flow rates, suggests that an OTEC plant might be able to operate with more flexibility than only providing constant baseload power, if it is sized to meet the largest expected demands. A plant could potentially ramp up or down if needed while still operating in a favorable manner.

The analysis of an OTEC plant from a purely performance standpoint is inherently limited, as financial viability will ultimately decide which configuration is chosen. The next chapter looks at the economics of OTEC by performing a simplified levelized cost of electricity (LCOE) calculation in order to perform a simple economic analysis. The methodology presented in this chapter as well as the next chapter could be re-applied or adapted to another plant configuration if more performance and/or cost information is known. However, the economic analysis in the next chapter only uses the reference case for economic comparison in order to keep the variables and assumptions to a minimum.

Chapter 5

Economic Feasibility Analysis

5.1 Introduction

While knowing the general performance of an OTEC plant based on design and operating parameters is important, it does not ultimately govern whether or not such a plant would be a feasible source of power. The economic viability of a power plant is a key component in deciding whether or not to use one type of generation over another. While the concept has been proven technically, a full-scale OTEC plant has yet to be built because of the high capital cost and uncertainty of economic viability, among other things.

The economic modeling variables were limited to estimated cost ranges based on published cost information from several reports, and scaled to 2011 dollars via the consumer price index [11, 25, 31, 43, 51]. This analysis will take these cost estimations for various plants and their components, and use this information to estimate a range for the capital cost and Levelized Cost of Electricity (LCOE) for different plant designs and operating configurations. The cost values determined are not meant to be a quotable price for OTEC power, but rather provide a rough estimate of what would probably be the lower bound.

5.2 Economic Literature Review

The integration of economic variables into the performance model has uncertainty due to the relative lack of published cost data. Aside from a handful of

sub-MW demonstration projects, there has not been a commercial scale OTEC plant built. However, there have been numerous design and feasibility studies performed by companies with experience in cost estimation for such large projects. This economic modeling portion is primarily based on these design studies. Specifically, in 1979, the Department of Energy (DoE) issued a request for proposals for a 10MW OTEC power generation module that could be used as either a stand-alone plant, or as part of a larger assembly.

The 10MW feasibility studies provide the closest corollary, in terms of costs, for a 20MW plant. The costs for the platform, electrical cabling, cold water pipe, and other large expenses would be roughly the same between 10 and 20MW, as compared to the same costs for a 100MW plant. Therefore, since the economic modeling is meant to provide a order of magnitude approximation, it was assumed that the estimates for the 10MW plant modules would provide a sufficiently accurate cost range for this analysis. Additionally, the costs for the heat exchangers were scaled to a per-sqft basis, and the pumps, motors, and turbogenerators were all scaled to a per-kW basis. This variation is where the primary cost differences between 10 and 20MW plants comes into play.

Several abbreviated versions of these proposals can be found in the conference proceedings of the 6th Ocean Thermal Energy Conversion Conference [11, 25, 31, 43, 51]. Specifically, cost values from the following five reports were used:

- Bakstad, P. J., and Pearson, R. O."Design of a 10MWe(net) OTEC Power Module using Vertical, Falling-Film Heat Exchangers" [11]
- Denton, J.W., Bakstad, P., and McIlroy, K. "Design of a 0.2MWe (net), Plate-Type, OTEC Heat Exchanger Test Article and a 10MWe (net) Power Module" [25]

- George, James F. "System Design Considerations for a Floating OTEC Modular Experiment Platform" [31]
- Olmstead, M.G., Mann, M.J., and Yang, C.S. "Optimizing Plant Design for Minimum Cost per Kilowatt with Refrigerant-22 Working Fluid" [43]
- Scott, R.J. "Conceptual Designs and Costs of OTEC 10 & 40 MW Spar Platforms" [51]

These five reports were all for 10MWe power modules, to be operated either as stand-alone plants, or as part of a larger plant. The individual components and plant designs vary widely between proposals, particularly different types of heat exchangers and cold water pipe designs, so a summary of the relevant information contained in each report is summarized in Table 5.1. Components not included in the reports, or not explicitly itemized are also noted in Table 5.1.

The range of cost variables derived from these reports covers a broad spectrum of plant design possibilities. Also, since the focus of this thesis has been an approximately 20 MW plant, and the plant scale is roughly the same, these numbers provide a reasonably good starting point for analysis. The values from the report were not averaged or normalized to provide a baseline cost estimate, but rather they were used more qualitatively to estimate a reasonable range or order-of-magnitude cost estimate for each of the economic variables in the model. In order to assess the effects of different design configurations and operating parameters, the pumps, turbines, and generators were normalized to a \$/kW value; heat exchanger costs were similarly scaled to \$/sqft value. Cold water pipe, platform, power cable system were assumed to be constant. Table 5.2 contains a low-medium-high estimation of each of the primary economic variables based on the reports.

Table 5.1: Plant size, relevant economic information, and other notes on the feasibility studies.

Author	*Plant Size*	*Relevant Values*	*Other Notes*
Bakstad	10 MWe	Turbine/generators, Evaporator and condenser, power cycle, misc. costs	DID NOT explicitly state whether or not platform, mooring, cold water pipe,or electrical cabling costs were included. Did include HX areas, allowing for a $/sqft calculation
Denton	10MWe	Turbine/generators, Evaporator and condenser, power cycle, water pumps, misc. costs	DID NOT explicitly state whether or not platform, mooring, cold water pipe,or electrical cabling costs were included. Did include HX areas, allowing for a $/sqft calculation
George	10MWe	Platform, cold water pipe, power cycle (including evaporator and condenser), water systems costs.	Explicitly stated that it DOES NOT include electrical cabling costs. Concrete-based platform and CWP designs
Olmstead	10 MWe	Heat exchanger information, turb/gen information	Collaborated with Sea Solar Power; use similar heat exchanger design, R22 working fluid
Scott	10&40MWe	Platform, cold water pipe, electrical cabling, warm and cold water pumps, other misc. costs	Steel hull spar design. Does not itemize out cost of heat exchangers or turbine/generators. Does include cost estimates for electrical cabling

Table 5.2: Estimated range and average for OTEC plant cost variables based on literature review.

Capital Cost Variables	*Units*	*Low*	*Medium*	*High*
Heat exchangers	[$/sqft]	20	40	80
Turbo-generators	[$/kW]	700	1,000	2,000
Cold water pumps	[$/kW]	700	1,000	2,000
Warm water pumps	[$/kW]	700	1,000	2,000
Cold water pipe	[$]	10,000,000	30,000,000	50,000,000
Hull/Platform	[$]	30,000,000	90,000,000	150,000,000
Power cabling	[$]	20,000,000	30,000,000	50,000,000
Other costs	% of capital cost subtotal	20	20	20

The power value (kW) by which the [$/kW] cost variable is multiplied is specific to that variable. For example, the turbo-generator $/kW is multiplied by the gross power output from the power cycles turbines. The cold water pump $/kW is multiplied by the power demands of the cold water pump. The cost variables are NOT on a basis of $ per net kW generated. In order to help account for these values potentially not including installation costs or auxiliary equipment, an additional factor of 20% of the total calculated capital cost will be included. While it is not ideal to use such dated design and cost information, the fundamental design of the major equipment has not drastically changed, particularly pumps and electric motor/generators, which should at least provide for an order-of-magnitude estimate. Included in this reasoning is the assumption that increases in some costs would be negated by decreases in others. When these analyses were performed, the offshore oil industry, and by extension the large-scale off-shore construction industry, were not nearly as well established and mature as they are now. Again, the goal of this analysis was to provide an estimated range for the purposes of assessing potential viability, and the

general effects of different components on overall cost. As for operations and maintenance costs, the reports become even more vague; many do not include an estimation, aside from potential cleaning or replacement of heat exchangers. For a conservative O&M estimation, this analysis uses an annual O&M cost 5% of the capital cost of the plant. The assumption is that the first OTEC plant could have lifetime O&M costs roughly equivalent to replacing the entire plant, and that for an expected 20 year operating lifetime, that equates to an approximation of 1/20th or 5% per year. While a 5% O&M cost is not explicitly stated in any writings, it does seem to be a sufficiently conservative estimate. The labor cost estimation is similarly arbitrary, with this analysis making the assumption of $1 million per year for salaries and benefits, which would pay for 5-10 full time workers. Again, these assumptions are somewhat arbitrary, with some proposals assuming a nearly autonomous plant, and others assuming a full time staff of dozens; the main goal is to account for a labor cost in the million-dollar range when calculating the LCOE. A more recent paper, written by Dr. Luis Vega and presented as part of the 2010 Offshore Technology Conference, discusses the general economics of both open and closed-cycle OTEC plants in the context of previous OTEC proposals [63]. Vegas 2010 report is an update to a paper he wrote on OTEC economics in 1992. As part of the 2010 report, he also compiled and converted other cost estimations from other sources to 2009 dollars for plants ranging from 1.35 to 100 MW in size. The Vega report is discussed further in Section 5.4, and used as a means of benchmarking the results of the economic modeling.

5.3 Economic Modeling Methodology

The financing and economics of power production are complicated, with many external variables that affect the end cost of electricity. This analysis is only going to focus on performing a simplified calculation of the $LCOE$ based on estimated capital

costs and annual O&M costs. $LCOE$ is the annualized capital costs, plus yearly operational costs, divided by the amount of kWh of electricity produced by that plant in a year. The Capital Expenditure ($CAPEX$), Cost Recovery Factor (CRF), Operating Expenses ($OPEX$), and Capacity Factor (CF) are the primary variables that go into calculating the $LCOE$. Capital expenditures are the large up-front costs associated with building the plant itself; these costs include the materials, manufacturing and installation of the major plant components. For this analysis $CAPEX$ is explicitly a sum of the total heat exchanger costs ($C_{heatex.}$), sum of the warm and cold water pump costs as well as the cold water pipe costs (collectively $C_{watersys.}$), total turbo-generator costs ($C_{turbogen}$), platform cost ($C_{platform}$), and power cable cost (C_{power}). The heat exchanger, pump, and turbo-generator costs are functions of the heat exchanger area, pump power demands, and gross power output respectively shown in Equations 5.1 to 5.4. The cold water pipe, platform, and power cable costs are all assumed to be lumped constant values. The sum is then multiplied by a constant, K, to account for other auxiliary equipment, contingency money, and to help account for costs that might not have been included in the explicit values. For this analysis, K will assumed as 1.2, or an additional 20% of the explicit sum of the capital costs.

$$CAPEX[\$] = K\left[C_{heat\ ex.} + \sum C_{water\ sys.} + C_{turbogen} + C_{platform} + C_{power}\right] \quad (5.1)$$

$$C_{heat\ ex.}[\$] = A_{total}[ft^2] \times c_{hx\ \$\ per\ sqft.}\left[\frac{\$}{ft^2}\right] \quad (5.2)$$

$$\sum C_{water\ sys.} = C_{cw\ pipe} + \sum \dot{W}_{cw\&hw\ pumps} \times c_{pump\ \$\ per\ kW}\left[\frac{\$}{kW}\right] \quad (5.3)$$

$$C_{turbogen.}[\$] = \dot{W}_{gross}[kW] \times c_{turbogen\ \$\ per\ kW.}\left[\frac{\$}{kW}\right] \quad (5.4)$$

For the sake of simplicity, this model is assuming one value of $c_{hx\ \$\ per\ sqft.}$ for both the boiler and condenser. Similarly, the warm and cold water pumps are assumed to have the same $c_{pump\ \$\ per\ kW}$. The model itself is programmed to handle individual values for these inputs, should more specific or detailed cost information become available. For the sake of this analysis, $CAPEX$ is considered the total up-front cost of the plant, and would paid for by some sort of loan. The annual loan payments of $CAPEX$ are calculated by multiplying $CAPEX$ by the Cost Recovery Factor.

Cost Recovery Factor (CRF) is the fraction of the capital cost that must be paid each year for the life of the loan. CRF is a function of the interest rate of the loan (or the discount rate of capital), and the loan length. For this analysis, it is assumed that payments will be made annually at the end of the year. The calculation of this factor given in Equation 5.5, where i is the interest rate and n is the loan term in years.

$$CRF = \frac{i \times (1+i)^n}{(1+i)^n - 1} \tag{5.5}$$

Multiplying $CAPEX$ by the CRF yields the annual payment for capital expenditure loans. This annualized payment is the effective yearly cost of the upfront $CAPEX$ costs; the annualized cost is necessary for the $LCOE$ calculation, which essentially divides yearly costs by yearly electricity output.

The other portion of costs going into the $LCOE$ calculation are the operating expenditures, $OPEX$. For this simplified $LCOE$ calculation, the $OPEX$ is assumed to be a constant value. Assuming a fixed $OPEX$ is an idealization because expenses for repairs and maintenance would most likely vary from year to year. Since there are not any fuel costs associated with operation, and it is expected to be mostly baseload power, O&M costs are expected to be roughly constant from year-to-year once the

plant has been up and running for a few years. The $OPEX$ costs are calculated Equation (5.6), using the O&M and labor methods and cost values discussed in the previous section.

$$OPEX\left[\frac{\$}{yr}\right] = C_{labor}\left[\frac{\$}{yr}\right] + C_{O\&M}\left[\frac{\$}{yr}\right] \tag{5.6}$$

$$C_{labor} = 10[employees] \times 100,000\left[\frac{\$\ per\ employee}{yr}\right] = 1,000,000\left[\frac{\$}{yr}\right] \tag{5.7}$$

$$C_{O\&M} = 0.05 \times CAPEX\left[\frac{\$}{yr}\right] \tag{5.8}$$

The last components of the $LCOE$ calculation are $\dot{W}_{electricty}$, which is just the net electrical power output of the plant, and the capacity factor CF. CF is the fraction of the year that the plant is producing power at its rated power output. Multiplying $\dot{W}_{electricty}$ by the number of hours in a year, and by the fraction of the year the plant was generating, yields the total number of kilowatt hours (kWh) the plat produced. This product is the denominator in the $LCOE$ calculation, shown in equation 5.9. The $LCOE$ is a means of evaluating the total annual cost of a power plant per kWh it produces, or put another way, it is the minimum cost at which the electricity would have to be sold for the plant to break even for the year. This simplified $LCOE$ calculation does not include insurance costs, taxes, environmental costs, or any other fees.

$$OPEX\left[\frac{\$}{kWh}\right] = \left[\frac{CAPEX[\$] \times CRF\,[yr^{-}1] + OPEX\left[\frac{\$}{yr}\right]}{\dot{W}_{electricty}[kW] \times 8760\left[\frac{hr}{yr}\right] \times CF}\right] \tag{5.9}$$

$LCOE$ allows for comparison between both traditional power plants and other renewable energy technologies, as well as comparison with electricity prices in various markets.

As a reminder, this analysis is very simplified, and does not include many of the costs affecting power plants. Taxes, environmental regulatory costs, and many other externalities were not included. Therefore, the estimated $LCOE$ is skewed lower than what the actual $LCOE$ would be for the given $CAPEX$ and $OPEX$ inputs. The Range of $LCOE$ calculated with the inputs from the previous section are meant to provide a good order-of-magnitude estimation, as well as provide upper and lower bounds on the estimation. The calculation of these values is provided in the following section.

5.4 Calculation and Comparison of LCOE with Current Technologies and Markets

The ultimate goal for the economic analysis was to provide a first-cut estimation of the cost to generate electricity with a first-generation OTEC plant built for approximately 20MW output, so that a preliminary evaluation of economic feasibility could be made. The economic equations described in the previous section were integrated into the MATLAB model of the plant, and the $LCOE$ was then calculated for the range of $CAPEX$ variables described in Table 5.2 of Section 5.2. The plant design and operating variables used for the reference case in Section 4.2 were used as the input variables for the thermal fluid systems model for the economic analysis. To summarize, Table 5.3 contains the relevant outputs of the thermal-fluid systems model, as well as the economic model variables.

For this analysis, the warm and cold water pumps are assumed to have the same cost per kW of power demand, and the boiler and condenser are also assumed to have the same cost per square foot. This assumption is just a modeling simplification, since the actual costs would most likely differ somewhat, but the prices would most likely still be within the same magnitude, so it is not unreasonable. With the inputs

Table 5.3: Summary of relevant thermal-fluids model outputs and economic variables for economic analysis

Relevant Thermal-Fluid Model Outputs			
Gross Power [kW]	*Net Power [kW]*	*Pump Power [kW]*	*Total HX Area [ft^2]*
28,110	22,491	5,619	1,706,412

Economic Model Cost Variable Ranges				
CAPEX Variables	*Units*	*Low*	*Medium*	*High*
Heat exchangers	[$/sqft]	20	40	80
Turbo-generators	[$/kW]	700	1,000	2,000
Cold water pumps	[$/kW]	700	1,000	2,000
Warm water pumps	[$/kW]	700	1,000	2,000
Cold water pipe	[$]	10,000,000	30,000,000	50,000,000
Hull/Platform	[$]	30,000,000	90,000,000	150,000,000
Power cabling	[$]	20,000,000	30,000,000	50,000,000
Other costs	% of capital cost subtotal	20	20	20

from Table 5.3, the economic analysis model was run. Table 5.4 contains the range of $CAPEX$, $\$/kW$, and $LCOE$ estimated from the input design and economic variables. Again, these values are meant to be an first-cut approximation, meant to establish the probable range of $LCOE$ for a typical first generation $OTEC$ plant.

Table 5.4: Summary of calculated outputs from the economic model

		Calculated Cost Values		
Economic Output Variables	*Units*	*Low*	*Medium*	*High*
CAPEX	[$]	143,960,000	310,050,000	553,360,000
CAPEX per kW	$\left[\frac{\$}{kW}\right]$	6,400	13,785	24,603
LCOE	$\left[\frac{\$}{kWh}\right]$	0.13	0.32	0.65
OPEX	$\left[\frac{\$}{yr}\right]$	6,998,200	13,919,000	24,057,000

The calculation of the 'Low - Medium - High estimates are based on optimistic cost estimations, roughly average estimations, and conservatively high estimations respectively. Such a broad range is meant to provide a solid upper and lower bound on what the costs would be for a floating OTEC plant of roughly 20MW rated output. The 20MW output distinction is made because several of the costs are highly non-linear, and would benefit from economies of scale; therefore these $LCOE$ estimations are NOT meant for plants much larger or smaller than 20MW.

The output of the economic model shows that the $LCOE$ would most likely fall into the range of approximately \$0.13 to \$0.65 per kWh, with a best-guess estimate of approximately \$0.32 per kWh. While the range of $LCOE$ is nearly a factor of five between lowest and highest, the ranges between low and high for the economic input variables are also of that same magnitude. For comparison purposes, \$0.32 per kWh will be assumed to be the $LCOE$ for a hypothetical 20MW plant operating with the

design and temperature inputs described in Appendix B.

Dr. Vega's 2010 paper on the economics of OTEC was used as an initial benchmark for the models LCOE calculation. Based on his prior work, and the works of others, Vega compiled a list of OTEC plants with their estimated capital cost per kW in 2009 dollars, as reproduced in Table 5.5. These reports were scaled to 2009 dollars using the 20-year average for equipment price-index inflation [63].

Table 5.5: Compilation of cost estimations for a range of OTEC plants, as sourced from Dr. Luis Vegas Economics of Ocean Thermal Energy Conversion: an Update [63].

Plant Size, MW	*Capital Cost, $/kW*	*Land/Floating*	*Source*
1.35	41,562	L	*Vega, 1992*
5	22,812	L	*Jim Wenzel, 1995*
5.3	35,237	F	*Vega et al, 1994*
10	24,071	L	*Vega, 1992*
10	18,600	F	[*Vega, 2010*]
35	12,000	F	[*Vega, 2010*]
50	11,072	F	*Vega, 1992*
53.5	8,430	F	[*Vega, 2010*]
100	7,900	F	[*Vega, 2010*]

Additionally, Vega curve-fit these numbers in order to provide a rough estimate for cost per kW for intermediate plant sizes, which reproduced in Equation (5.10) [63]. CC is the installed capital cost per kW, and P is the nominal name-plate power output of the plant.

$$CC\left[\frac{\$}{kW}\right] = 53,160 \times (P[MW])^{-.418} \tag{5.10}$$

Using this equation with the nominal output from the thermal fluids model, approximately 22MW, the estimated cost per kW is approximately $14,000. The

curve fit estimation is in relatively good agreement with the economic models estimation of $13,785, which would round up to $14,000 based on significant figures. This comparison doesnt provide much insight, as the equation is merely a curve fit to other estimated values, but it does show that the economic model produces an estimation in line with other independent calculations.

Vega also performed an *LCOE* calculation based on the capital costs in Table 5.5. He assumed combined labor and repair costs of slightly over 5%, and loan terms of both 8% for 15 years and 4.2% for 20 years, the latter being representative of a government bond. The *LCOE* as calculated by Vega in 2009 dollars were reproduced in Table 5.6 [63].

Table 5.6: Levelized Cost of Electricity estimations based on previous feasibility studies, as calculated by Luis Vega in "Economics of OTEC: an Update" [63].

Plant Size, MW	*Capital Cost, $/kW*	*O&M, $M/yr*	*R&R, $M/yr*	*LCOE, $/kWh)*
1.35	41,562	2.0	1.0	0.94
5	22,812	2.0	3.5	0.50
10	18,600	3.4	7.7	0.44
53.5	8,430	3.4	20.1	0.19
100	7,900	3.4	36.5	0.18

The economic models estimation of $0.32/kWh seems to fall in line with the estimations as calculated by Vega. An *LCOE* of $0.31 per kWh was obtained by performing a similar curve fit to the *COE* values in Figure 5.6. Again, obtaining a similar value to Vega's estimation is not necessarily validation of the of the estimated cost itself, but it does provide a useful benchmark to show that the model estimates an *LCOE* in the same range reached through separate analysis.

While it was not the focus of the economic analysis, the economies of scale do come into play with OTEC power generation. Since larger OTEC plants would likely make use of modular designs, the design costs would be lower per installed kW. The cold water piper, while larger in diameter, would not cost orders of magnitudes more because much of the design, manufacturing, and deployment costs would not scale linearly; the cost for the cold water pipe for a 100MW might be double that of a 20MW plant, but it would be producing 5X more power. Similarly, the electrical cabling run from the plant to the shore would have to be higher capacity, and the transformers and other power conditioning equipment would also have to scale up, but the cost of installation for a 10 MW and a 100MW cable would likely be similar, which would in-turn lower the overall cost per-kW installed. On the opposite end of the spectrum, a significantly smaller plant, such as a 1-2 MW plant, would still have to pay similar prices for specialized design, manufacturing, and installation of the major plant components, but it wouldn't be producing nearly as much electricity as a larger plant, driving the installed costs up.

For either scenario (much larger than or much smaller than 20MW) the per-kW and per-sqft costs of the pumps, turbogenerators, and heat exchangers are likely to be similar. However, there are other costs that would be less dependent on size, to a point, which tend to produce a highly nonlinear $/kW installed curve as the costs shift from being installation dominated to material dominated. Since the LCOE for OTEC plants is primarily driven by the installed cost, the LCOE also trends the same way. Vega's curve fit of estimates from a survey of previous OTEC feasibility studies (Equation 5.10, Table 5.6) showed that building larger plants improves economies of scale [63]. A larger OTEC plant, on the scale of 50 to 100MW, would be able to take advantage of several economies of scale in terms of design, permitting, deployment, and other costs, and could potentially be much more cost-competitive on a $/kWh

bases [63].

The next comparison is with estimated $LCOE$ for various power generation technologies in the year 2016, as calculated by the EIA using the assumptions cited in paper [28]. Table 5.7 contains the $LCOE$ for most of the standard electricity generating technologies, as estimated by the EIA, for the year 2016 as part of the Annual Energy Outlook 2011 report [28]. The original data were adjusted to 2011 \$/kWh from 2009 \$/MWh used in the EIA report. Keep in mind the EIA $LCOE$ assumptions use a lower interest rate (7.2%) and a longer loan life (30 years) for their calculations than the LCOE calculations performed in this paper [28].

Table 5.7: Estimated LCOE values for various generation technologies for the year 2016, as calculated by the EIA in their Annual Energy Outlook 2011 report [28].

	Range of Total System LCOE $\left[\frac{\$}{kWh}\right]$		
Plant Type	*Min*	*Average*	*Max*
Conv. Coal	0.090	0.100	0.116
Adv. Coal	0.106	0.115	0.128
Adv. Coal with CCS	0.133	0.143	0.162
N.G. Conv. Combined Cycle	0.063	0.069	0.078
N.G. Adv. Combined Cycle	0.060	0.066	0.074
N.G. Conv. Combustion Turbine	0.085	0.094	0.109
N.G. Adv. Combustion Turbine	0.104	0.131	0.151
Adv. Nuclear	0.091	0.131	0.124
Wind	0.086	0.102	0.121
Offshore Wind	0.196	0.255	0.367
Solar PV	0.167	0.221	0.340
Solar Thermal	0.201	0.327	0.674
Geothermal	0.096	0.107	0.121
Biomass	0.104	0.118	0.140
Hydro	0.061	0.091	0.127

The EIA report was looking at 2016 because of the lead time it would take to build some of the hypothetical projects they included in their analysis, namely large-

scale offshore wind and large-scale PV and concentrated solar. The 2016 estimation is useful because an OTEC plant would also take 4 to 5 years to build and deploy due to the designing, building, and deployment lead times that would be required of a plant starting today. The EIA estimations are for building a new plant using the noted technology, and the capacity factors and regional correction factors noted in the baseline reference case of the 2011 report [28]. It is important to remember that these numbers are for the United States, and not for remote small island communities. Regardless, they provide a sense of scale for the estimated OTEC LCOE.

Based on the EIA estimations, the OTEC $LCOE$ would not be a practical alternative compared to all of the standard baseload and firm power technologies, such as coal and natural gas. However, according to these numbers OTEC could be cost-competitive with solar thermal generation, and potentially with offshore wind and solar PV as well. The EIA $LCOE$ do not account for the added costs of firming power required for the intermittent renewables, and so the total $LCOE$ for the grid might be higher. It is interesting to note that OTEC is not even considered in the EIA analysis, which is most likely due to the lack of commercial-scale pilot plant, and site-specific nature of the technology.

The last assessment for the economic viability based on the model-estimated $LCOE$ looked at retail electric rates in various island communities. The retail electric rate inherently covers the $LCOE$, plus any taxes or tariffs not factored into the $LCOE$ calculation, as well as any profits or guaranteed returns that might be made above the marginal costs. Therefore, the retail rate sets the upper limit for economically viable $LCOE$s in that market. If a plant cannot generate electricity at a marginal cost lower than the retail rate, then it will not be financially viable without some sort of additional financial support, such as a renewable energy production credit. The

electric rates and notes about the generation sources for several Islands are provided in Table 5.8.

Table 5.8: Retail electric prices for Hawaii, Puerto Rico, Fiji, and the Cayman Islands

Island(s)	***Average Retail Price***	*Notes*
Hawaii	$0.2512/kWh avg. in 2010, was $0.292/kWh in 2008	Nearly 80% of power is from Petroleum fired power plants, so price of electricity tracks price of oil. [29]
Puerto Rico	Approximately $0.22/kWh in 2010	69% oil, 15% coal, 15% natural gas. 5.8GW of capacity, 3.7GW peak demand [65].
Fiji	$0.34/kWh for residents, $0.42/kWh for commercial in 2010	Approximately 138MW of peak load. Traditionally all diesel fired, but has built 10MW wind farm and 40MW hydro power projects recently to reduce fuel costs. [7]
Cayman Islands	Approx. $0.35/kWh for residents in 2011	146MW of diesel generators at a single facility. Generators range from 1.45MW to 12.25MW. Price is $0.10/kWh + base cost + Fuel surcharge and taxes ($0.25/kWh) [20]

The retail electric rates listed in Table 5.8 give a better sense to the potential economic viability of OTEC for some island communities, particularly the smaller and more remote locations. An $LCOE$ of nominally $0.20 to $0.25/kWh does fall within the range of $0.13 to $0.65/kWh as predicted by the model, though it is still well below the $0.32/kWh of the best-guess estimate. This analysis does not mean that OTEC could not be viable in Hawaii or Puerto Rico, but rather that a 20MW-class OTEC plant would not likely be financially viable, based on the assumptions of

this analysis. Additionally, as Vega's survey of reports suggests, building larger plants improves economies of scale, and based on this line of reasoning, a larger OTEC plant, on the scale of 50 to 100MW, would be able to take advantage of several economies of scale, and could potentially be much more cost-competitive on a $/kWh bases for the islands of Hawaii and Puerto Rico.

While the larger islands might not make economic sense for a 20MW OTEC plant built purely for commercial power generation, the high costs of electricity on Fiji and Cayman Islands offers a much better opportunity. Both smaller islands have electricity rates in the $0.35 to $0.40/kWh, which is slightly higher than the models $0.32/kWh estimate. While the $0.32/kWh is a best-guess estimate of a simplified $LCOE$, the fact that the estimated value is less than the retail electric rate by several cents is evidence that an OTEC plant could potentially be financially viable for these small communities.

5.5 Conclusion

The purpose of the economic modeling was to establish a range and a best-guess estimate for the Levelized cost of electricity, rather than estimate a price. The calculated range was $0.13 to $0.65/kWh, covering the best and worst-case scenarios, and the best-guess estimation of $0.32/kWh was based on the approximate average of values obtained from previous feasibility studies of similarly sized plants. This was in good agreement with another more recent feasibility study by Luis Vega, which compiled costs estimates for various plants to estimate LCOE values.

Comparing OTEC with the estimated $LCOE$ for various common generation technologies in 2016, as estimated by the EIA, showed that a 20MW OTEC would most likely not be a cost-competitive option for the US, except for possibly in com-

parison with solar thermal or offshore wind. A non-competitive LCOE was expected, since conventional technologies and even wind, have become mature technologies, while OTEC has not. The cost estimates for OTEC are so high because any plant built would be the first of its kind at that scale, and the manufacturing and installation would be a highly customized and engineered process.

Lastly, the economic models estimation was compared with retail electric rates on the islands of Hawaii, Puerto Rico, Cayman Islands, and Fiji. The larger islands of Hawaii and Puerto Rico, have the larger populations and much higher power demand, and thus have a large enough demand to support larger, more economically efficient power plants. The smaller Island communities, Fiji and Cayman, are limited nearly entirely to small-scale diesel generation. Their power costs are not only tied to the high cost of the fuel itself, but also to the additional expenses of having it shipped to the island. All of the Island communities have a large dependence on diesel or petroleum for electricity generation, which exposes them not only to high prices, but also high price volatility. These factors make OTEC a particularly interesting potential source of electricity, since it could potentially readily displace a significant portion of the diesel generation that is currently used for baseload power.

Chapter 6

Conclusions and Final Thoughts

The purpose of this analysis was to assess the feasibility and viability of OTEC power generation from both a fundamental engineering standpoint, as well as an economic standpoint.

In order to provide a reference frame for the analysis, a 20 MW closed cycle OTEC plant was modeled based on fundamental thermodynamic, heat transfer, and fluid mechanics relationships. The thermal fluids systems model was developed in order to integrate and analyze the effects different design and operating parameters have on plant performance. The purpose of this model was to estimate OTEC plant performance from first principles, and to make the model flexible and broad enough to function for a wide variety of design and operational specifications.

While these findings are not necessarily groundbreaking and new, they do prove from a first-principles perspective that the design and operational parameters impact plant performance in different ways. The analysis showed that staging is very beneficial for plant performance over a single stage, but faces diminishing returns beyond 3-4 stages. The importance of having a good ocean temperature differential was an obvious finding, but the analysis still provide useful by providing a sense of the operational limits. For this particular model, the minimum operational temperature, the point at which the plant would not even be able to produce enough power to run the water pumps, was approximately $15°C$. More interesting and nonlinear impacts were seen when analyzing TTD, water inlet/exit temperature change, and working

fluid mass flow rate. The non-endpoint maxima suggests that these variables be carefully optimized when designing a plant in order to produce the optimal power output. The analysis also showed the importance of heat exchanger performance for efficient plant operation, but also that gains from highly efficient heat exchangers could be negated by poor design and non-optimized temperature variables.

The economic feasibility analysis assigned costs to major plant parameters and outputs in order to calculate a simplified LCOE range based on low, average, and high costs. While the estimated LCOE range was quite large, from \$0.13/kWh to \$0.65/kWh, the average of \$0.32/kWh was found to be in line with similarly estimated LCOEs for OTEC plants. The estimated LCOE range shows the potential for OTEC, but also the uncertainty that has kept investors away from funding such large capital investments. When the average LCOE is compared to mainland US generation LCOE, it appears to be non-competitive for the United States. However, when compared with the retail prices for electricity on small islands that depend entirely on diesel generation, the economics suggest that OTEC could be viable, and that a more detailed analysis should be performed.

The economies of scale for OTEC power generation are what prompted most original OTEC plant designs to be of the 100MW+ size. While it was not the focus of the economic analysis, the economies of scale do come into play with OTEC power generation, as the cost to design, build, and deploy a system would get cheaper per installed kW with increasing system size. Larger OTEC plants could potentially be cost competitive for the larger Islands of Hawaii and Puerto Rico, where a 20MW plant might not.

However, from a performance perspective, scaling up size would likely lead to only minimal performance gains beyond a certain size. Small plants, on the order of 1-

5MW would likely be less efficient than a 10-20MW plant because of the smaller design leading to comparatively more losses in the system. On the larger end of the spectrum, most of the designs for large 100MW plants utilize modules of smaller 10-20MW power systems operating in parallel, so there would likely be minimal increase in performance going from 20MW to 100MW. Additionally, large 50 to 100MW+ plants are unlikely to be pursued until the real-world operational lifetime and reliability of an OTEC plant is known.

OTEC for power generation is an old idea that could benefit from new technology. When first tested in the 1970s, manufacturing methods and offshore operation were not what they are today. The combination of modern materials, sophisticated modeling and simulation software, and automated manufacturing could all benefit OTEC plant design and construction. A properly designed OTEC plant, deployed and operated in favorable thermal conditions could be financially viable and beneficial for many island communities, and it would provide invaluable experience and knowledge to improve designs and scale the technology, which would improve costs in the long term. The potential for OTEC is real, but it still must be proven in the real world, over the span of years and decades, in order to prove long-term operational viability, from both an engineering and economic standpoint.

Appendices

Appendix A

Glossary of Abbreviations, Symbols, Subscripts, and Terms

A.1 Abbreviations

OTEC: Ocean Thermal Energy Conversion

R&D: research and development

km: kilometers

TW: terawatts

MW: megawatts

kW: kilowatts

kWe: Kilowatts of electrical power

m: meters

CC: closed cycle

OC: open cycle

HC: hybrid cycle

NELHA: National Renewable Energy Laboratory of Hawaii Authority

gal: gallons (US)

ft: foot

sqft: square foot

SSP: Sea Solar Power

kPa: kilopascals

HX: heat exchanger

psi: pounds per square inch (pressure)

°**C**: celsius

°**F**: fahrenheit

kg: kilogram

BTU: british thermal unit

CAPEX: captal expenditures

OPEX: operational expenditures

CRF: capital recovery factor

O&M: operations and maintenance

A.2 Equation Symbols

A.2.1 Power Cycle Model

$\dot{m} \equiv [\frac{kg}{s}]$: Mass flow rate

$\dot{m}_{wf}$: Working fluid mass flow rate

$\dot{m}_{wf,stage}$: Working fluid mass flow rate in a single stage

$\dot{m}_{wf,total}$: Total working fluid mass flow rate in the entire plant (sum of all stages)

$\dot{m}_{cw}$: Cold water mass flow rate

$\dot{m}_{hw}$: Hot water mass flow rate

$\dot{Q} \equiv [\frac{kJ-thermal}{s}]$: Thermal power (i.e. Heat energy flow rate)

$\dot{Q}_{in}$: Heat energy flow rate into the power cycle, from the hot water into the boiler.

$\dot{Q}_{out}$: Heat energy flow rate into the power cycle, from the cold water into the condenser.

$\dot{W} \equiv [\frac{kJ-electricity}{s}]$: Electrical power (i.e. electric work rate). All $\dot{W}$-related equations incorporate motor/generator efficiency to account for mechanical to electrical conversion.

$\dot{W}_{netcycle}$: Net power output from the power cycle

$\dot{W}_{turbogen}$: Power generated from the turbine

$\sum losses$: Power lost to system inefficiencies

$\dot{W}_{wf\ pump}$: Working fluid pump power demand

$\eta_T \equiv [\frac{\dot{W}_{turbine,\ actual}}{\dot{W}_{turbine,\ ideal}}]$: Ratio of the actual power produced by the turbine, to the ideal (isentropic) power potential between inlet and exit.

$\eta_P \equiv [\frac{\dot{W}_{pump,\ ideal}}{\dot{W}_{pump,\ actual}}]$: Ratio of the ideal (isentropic) power demand for the pump, to the actual power demand to pressurize the fluid from the inlet to the exit state.

$\eta_M \equiv [\frac{\dot{W}_{mechanical\ power\ out}}{\dot{W}_{electrical\ power\ in}}]$: Ratio of mechanical power produced by an electric motor, to the electrical power supplied to the motor (always less than 1).

$\eta_G \equiv [\frac{\dot{W}_{electrical\ power\ out}}{\dot{W}_{mechanical\ power\ in}}]$: Ratio of mechanical power produced by an electric motor, to the electrical power supplied to the motor (always less than 1).

$h \equiv [\frac{kJ-thermal}{kg}]$: Specific enthalpy; a measure of the heat and pressure energy in a substance.

$v_1 \equiv [\frac{m^3}{kg}]$: Specific volume, used in the incompressible flow assumption for the compression process of the power cycle.

$s \equiv [\frac{kJ}{kgK}]$: Specific entropy

$x \equiv [\frac{kg_{vapor}}{kg_{vapor+liquid}}]$: Saturated mixture quality, which is the mass fraction of vapor phase to the overall mixture. $x = 0$ means fully saturated liquid, $x = 1$ means fully saturated vapor.

$\Delta T_{cw,overall}$: The overall change in cold water temperature from plant inlet to plant exit

$\Delta T_{cw,stage}$: The change in cold water temperature from stage inlet to stage exit

$\Delta T_{hw,overall}$: The overall change in hot water temperature from plant inlet to plant exit

$\Delta T_{hw,stage}$: The change in hot water temperature from stage inlet to stage exit

n_{stages}: The number of cascaded power cycles in the plant

T_{cond}: The temperature in the condenser of a power cycle. Equivalent to the temperature at states 1 and 4

T_{boiler}: The temperature in the boiler of a power cycle. Equivalent to the temperature at state 3

TTD_{boiler}: The terminal temperature difference in the boiler of a power cycle. Also known as the temperature approach or pinch point temperature difference

TTD_{cond}: The terminal temperature difference in the condenser of a power cycle

A.2.2 Heat Exchanger Model

$LMTD$: The Log mean Temperature Difference

$\bar{U}$: The overall heat transfer coefficient for the heat exchangers

C_{hw}: The specific heat for the hot water, i.e. the amount of heat required to heat one kg one degree C

C_{cw}: The specific heat for the cold water

$A_{heat\ exchanger}$: The effective heat exchanger area

R: The thermal resistance in the heat transfer thermal circuit

R''_{foul}: The thermal resistance per unit area due to fouling of the heat exchanger surface

η_0: The surface efficiency of the heat exchanger (for non-flat surfaces and fins)

$\bar{h}$: The convection coefficient for heat transfer

$r_{o,i}$: The outer/inner radii of a pipe wall

k: Thermal conductivity

L: Length

D_h: Hydraulic diameter of a pipe or duct (used for estimating non-circular ducts as circular)

Re_{D_h}: Reynolds Number for a duct with a hydraulic diameter of D_h

Nu_{D_h}: Nusselt Number for a duct with a hydraulic diameter of D_h

Pr: Prandtl Number

$\bar{v}_{water}$: Average water velocity in heat exchanger passages

A_{cs}: Cross-sectional area of duct

P: Perimeter of the duct

A.2.3 Pressure Drop and Pump Demand Model

$\dot{W}_{cw/hw\ pump}$: Cold or hot water pump power demand

$\Delta()$: To take the difference between the inlet and exit properties inside

p: Water pressure

Δp: Water pressure drop through the system

g: Gravity

z: h]Height

ρ_{cw}: Density of cold ocean water

$\rho_{ocean,avg}$: Average density of the ocean water column from the surface to the depth of the inlet

$\sum h_{losses} \equiv [\frac{kW}{kg/s}]$: The pressure head losses in a fluid system due to viscous drag on the pipe walls and fittings

$h_{l,hx}$: The pressure head losses in a fluid system due to viscous drag in the heat exchangers

$h_{l,piping}$: The pressure head losses in a fluid system due to viscous drag in the piping

$h_{l,inlet}$: The pressure head losses in a fluid system due to viscous drag at the inlet

$\sum h_{l,fittings}$: The pressure head losses in a fluid system due to viscous drag in the elbows, valves, reducers, and any other fittings

D: Pipe diameter

L: Pipe length

f: Friction factor

K: Pressure drop coefficient

A.2.4 Economic Model

$C_{heat\ ex}$: Total embodied cost of the heat exchangers (materials, labor, installation, etc.)

$\sum C_{water\ sys.}$: Total embodied cost of both water systems

$C_{turbogen}$: Total embodied cost of the turbogenerator assemblies

$C_{platform}$: Total embodied cost of the plant platform or hull structure

C_{power}: Total embodied cost of the electrical power transmission equipment (power cable, transformers, etc.)

K: Adjustment factor to account for miscellaneous costs

A_{total}: Total heat exchanger area (sum of all boiler and condenser areas)

$c_{hx\ \$\ per\ sqft}$: Embodied cost per square foot for heat exchangers

$C_{cw\ pipe}$: Total embodied cost of the cold water pipe

$C_{pump\ \$\ per\ kW}$: Embodied cost per kW of pump demand capacity

$C_{turbogen\ \$\ per\ kW}$: Embodied cost per kW of turbogenerator power capacity

CRF: Capital Recover Factor; the annualized capital cost based in an interest rate i and loan period n

i: Interest rate

n: Loan term in years

C_{labor}: Total embodied cost of human personnel

$C_{O\&M}$: Total embodied cost of operations and maintenance

CF: Capacity Factor; the fraction of time that the plant is running at rated power over the course of the year

A.3 Subscripts

$\boldsymbol{wf}$: working fluid, the fluid used for the power cycle, in this case R134a. Mass flow rates labeled with either wf or R134a are referring to the same thing.

cw: cold water, designation for properties and variables of the water cooling the condenser.

hw: hot water, designation for properties and variables of the surface water providing the boiler heat load.

in: At the inlet of the stage (if followed by i) or plant

in: At the exit of the stage (if followed by i) or plant

i: Denotes that the value is for a specific single stage only

stage: Denotes that the value is for any single stage

1,2,3,4: numbers refer to the stages in the power cycle. Anything with a numeric subscript is assumed to be a property of variable of the working fluid.

s: A variable that was solved for by assuming constant entropy.

sl: Saturated Liquid, i.e. $x = 0$.

sv: Saturated Vapor, $x = 1$.

lv: The difference in between the liquid and vapor values for a variable at a given saturation point.

ref: The reference value, used in the scaling models for heat transfer and pressure drop calculations.

Appendix B

Reference Case Model Inputs and Outputs

Table B.1: Baseline Reference Model Inputs

Power Cycle Parameters	***Symbol***	***Baseline Reference Value***
Number of stages	n	4
Working fluid	R134a	
Overall working fluid mass flow rate	$\dot{m}_{wf}$	5,000 $\frac{kg}{s}$
Stage working fluid mass flow rate	$\frac{\dot{m}_{wf}}{n}$	1,250 $\frac{kg}{s}$
Working fluid feed pump efficiency	η_P	.85
Pump motor efficiency	η_M	.95
Turbine efficiency	η_T	.94
Generator efficiency	η_G	.98

Table B.2: Baseline Reference Model Inputs: Ocean Water Parameters

Ocean Water Parameters	***Symbol***	***Baseline Reference Value***
Cold water density	ρ_{cw}	1027.68 $\frac{kg}{m^3}$
Cold water specific heat	$C_{p,cw}$	3.995 $\frac{kJ}{kg}$
Cold water viscosity	μ_{cw}	0.000108 $\frac{Ns}{m^2}$
Cold water inlet temperature	$T_{cw,in}$	4.5°C
Cold water discharge temperature	$T_{cw,out}$	13.0°C
Hot water density	ρ_{hw}	1023.34 $\frac{kg}{m^3}$
Hot water specific heat	$C_{p,hw}$	3.987 $\frac{kJ}{kg}$
Hot water viscosity	μ_{hw}	0.000108 $\frac{Ns}{m^2}$
Hot water inlet temperature	$T_{hw,in}$	26.5°C
Hot water discharge temperature	$T_{hw,out}$	21.6°C
Terminal Temperature Difference	TTD	2.0°C

Table B.3: Baseline Reference Model Inputs: Boiler and Condenser Parameters

Heat Exchanger Parameters	***Symbol***	***Baseline Reference Value***
Boiler heat transfer coeff	$\bar{U}_{boiler}$	5 $\frac{kW}{m^2}$
Boiler pressure drop coeff.	Δp_{boiler}	3 psi
Ref. boiler area	A_{hwref}	64,032 m^2
Ref. boiler water velocity	$v_{hw,ref}$	2.134$\frac{m}{s}$
Condenser heat transfer coeff.	$\bar{U}_{cond}$	5 $\frac{kW}{m^2}$
Condenser pressure drop coeff.	Δp_{cond}	4 psi
Ref. condenser area	A_{cwref}	39,703 m^2
Ref. condenser water velocity	$v_{cw,ref}$	1.8 $\frac{m}{s}$

Table B.4: Baseline Reference Model Inputs: Cold Water System Parameters

Cold Water System Parameters	***Symbol***	***Baseline Reference Value***
Cold water pump efficiency	η_P	.85
Cold water pump motor efficiency	η_M	.95
Cold water pipe diameter	$D_{cw\ pipe}$	4 meters
Cold water pipe length	L	1219 meters
Cold water pipe roughness	e	1.5×10^{-6} meters
Loss coeff., cold water pipe inlet	$h_{inlet,cw}$	0.78

Table B.5: Baseline Reference Model Inputs: Hot Water System Parameters

Hot Water System Parameters	***Symbol***	***Baseline Reference Value***
Hot water pump efficiency	η_P	.85
Hot water pump motor efficiency	η_M	.95
Number of inlets	N_{inlets}	2
Hot water pipe diameter	$D_{hw\ pipe}$	4 meters
Hot water pipe length	L	100 meters
Hot water pipe roughness	e	0.046×10^{-3} meters
Loss coeff., Hot water inlet	$h_{inlet,hw}$ 0.5	

Appendix C

MATLAB Code

C.1 Thermal-Fluids Systems Model Code, Thesis_baseline.m

This MATLAB '.m' file is the program used to generate the baseline model outputs. Its overall structure and functions are the same as those used for the analyses performed in Chapter 4. Therefore it is given here as the representative MATLAB code, instead of including all iterations. This version also contains the economic modeling as well.

Thesis_baseline_economics.m:

```
%%%%%          OTEC Thermal-Fluid Systems and Economic Model          %%%%%
%%%%%          MADE BY CHARLES UPSHAW, UNIVERSITY OF TEXAS            %%%%%
clear all
format short G


%%%%% SET UP ALL COMMON INPUT VARIABLES %%%%%
densitycw = 1027.68; %[kg/m^3] approx. sea water w/ 35 ppt salt @ ~5 degC
cpcw = 3.995; %KJ/Kg of water
visccw =.000108; %N*s/m^2
densityhw = 1023.34; %[kg/m^3] approx. sea water w/ 35 ppt salt @ ~25 degC
cphw = 3.987; %KJ/Kg of water
vischw =.000108; %viscosity of water [N*s/m^2]
for step = 1:3; %Step variable, used for some mult-iteration calculations


%%%SET UP FOR-LOOPS FOR STEPPING THROUGH VARIABLE RANGES %%%
n = 4; %number of stages(for loop on p instead of n for other analyses)
p = 1; %Iteration variable used for range analyses (1 for stage analysis)

%Input OTEC Plant Variables
fluid       = 'R134a'; % Sets model working fluid to R134a
mdotf       = 5000; %[kg/s] total working fluid mass flow rate in plant
mdotfs      = mdotf/n; %wf flow rate per stage
TTDb        = 2.0;    %C Boiler TTD
TTDc        = 2.0;    %C Condenser TTD
Tcwin       = 4.5;    %C Cold water inlet temp (~40.1 F)
Tcwout      = 13.0;   %C Cold water exit temp (~55.4 F)
Thwin       = 26.5;   %C Hot water inlet temp (~79.7 F)
Thwout      = 21.6;   %C Hot water exit temp (~70.9 F)
Zboilers    = 0;      %height of condenser above boilers
pumpeff     = .85; %working fluid feed pump efficiency
```

```
turbeff     = .94;
effegen     = .98;
effemotor   = .95;

%Input HX variables
Ucwref      = 4; % condenser overall HX coefficient [kW/m^2]
Vcwref      = 1.8;%reference cw velocity of ~6 ft/s
Uhwhref     = 4; % boiler (but pre-boiling) overall HX coefficient [kW/m^2]
Vhwref      = 2.1336;%reference hw velocity of ~6 ft/s
Uhwbref     = 4; % boiler (at boiling) overall HX coefficient [kW/m^2]
Acwref      = 39793; %reference area for condenser. Calc with ref HX values
Ahwref      = 64032; %reference area for boiler. Calc with ref HX values.

%Input Cold and Hot water pump variables
%Cold water system values
Dpipecw         = 4;%cold water pipe Diameter[m]
Apipecw         = pi*(Dpipecw^2/4);
Lpipecw         = 1219;%cold water pipe length [m]
effpumpcw       = .85;       %cold water pump efficiency
roughnesscw     = .0015e-3;  %roughness of PVC pipe in meters
densityavgsea   = 1/2*(densityhw+densitycw);%taking a rough estimation of
%the density of the water outside the cold water pipe. Has a direct effect
%on pump power required.
deltPcref       = 4*6894.75729; %psi to pascals conversion of HX pressure
%drop coefficient for ref. size HX at ref velocity
Kcinlet         = .78;    %K for re-entrant style inlet
Kfctot          = 200+20*n;    %Fittings losses in cold water piping system
%hot water system values
Dpipehw         = 4;%Assume inlet piping is similar to cold water pipe
Apipehw         = pi*(Dpipehw^2/4);
numofinletshw   = 2; %assuming two inlets based on drawing
Lpipehw         = 100;% Estimate of entrance length for hw system
effpumphw       = .85;
roughnesshw     = .046e-3;% bookvalue for wrougt steel (close enough to wrought Al)
deltPbref       = 3*6894.75729;%boiler pressure drop coefficient
Kbinlet         = .5;%hot water inlet loss coefficient
Kfbtot          = 200+20*n;%hot water fittings losses


%Calculate the boiling and condensing temperatures for each plant stage
PCS = pcstaging(Tcwin,Tcwout,TTDc,Thwin,Thwout,TTDb,n);
 Tcwins  = PCS(1,:);
 Tcwouts = PCS(2,:);
 Thwins  = PCS(3,:);
 Thwouts = PCS(4,:);
 Tboil   = PCS(5,:);
 Tcond   = PCS(6,:);


%Powercycle calculation for each stage. Indivual outputs then combined for
%totals out
for i = 1:n
PC(i,:) = powercycle(fluid,mdotfs,Tcond(i),Tboil(i),pumpeff,turbeff,effegen,effemotor
    ,Zboilers);
    pcWdotout(i) = PC(i,1);
    pcWdotfp(i)  = PC(i,2);
    Qdotinheatstage(i)  = PC(i,3);
    Qdotinboilstage(i)  = PC(i,4);
    Qdotoutstage(i)  = PC(i,5);
    dTstage(i) = Tboil(i)-Tcond(i);
end
%Sum stage ouputs for overall power cycle outputs
    Wdotout(n,1) = sum(pcWdotout);
```

```
    Wdotfp(n,1)  = sum(pcWdotfp);


%Calculate required water mass flow rates, corrected heat exchanger heat
%transfer and pressure drop values, heat exchanger area
HX = heatexchangers(Tcwins,Tcwouts,Thwins,Thwouts,Tboil,Tcond,n,Qdotinheatstage,
    Qdotinboilstage,Qdotoutstage,Ucwref,Vcwref,Uhwhref,Uhwbref,Vhwref,deltPcref,
    deltPbref,cpcw,cphw,densitycw,densityhw,Apipecw,Apipehw,numofinletshw,Acwref,
    Ahwref);
    mdotcw(n,1) = HX(1);
    mdothw(n,1) = HX(2);
    Vcwavg(n,1) = HX(3);
    Vhwavg(n,1) = HX(4);
    Qcw(n,1)    = HX(5);
    Qhw(n,1)    = HX(6);
    deltPcond(n,1)  = HX(7);
    deltPboil(n,1)  = HX(8);
    Acwtot(n,1)  = HX(9);
    Ahwtot(n,1)  = HX(10);
    Ucw(n,1)     = HX(11);
    Uhwh(n,1)     =HX(12);
    Uhwb(n,1)     =HX(13);

%Calculate pumping power for cold and warm water pumps
%Run coldwaterpump.m
CWP = coldwaterpump(n,mdotcw(n),densitycw,visccw,Dpipecw,Lpipecw,effpumpcw,effemotor,
    roughnesscw,densityavgsea,deltPcond(n,1),Kcinlet,Kfctot);
    Wdotcwp(n,1)        = CWP;
%wRun warmwaterpump.m
HWP = warmwaterpump(n,mdothw(n),densityhw,vischw,numofinletshw,Dpipehw,Lpipehw,
    effpumphw,effemotor,roughnesshw,deltPboil(n,1),Kbinlet,Kfbtot);
    Wdothwp(n,1)         = HWP(1);


%%%%%%%%%%%%%%%%%%%%%%%%%%%%%%%%%%%%%%%%%%%%%%%%%%%%%%%%%%%%%%%%%%%%%%%%%%%%
%%%%%%      TFS Model Output Calculations        %%%%%
Wdotnetout(n,1) = Wdotout(n,1) - Wdotfp(n,1);
fppumpfrac(n,1) = Wdotfp(n,1)/Wdotnetout(n,1);
Wdotnet(n,1)    = Wdotnetout(n,1) - Wdotcwp(n,1) - Wdothwp(n,1);
cwpfrac(n,1)    = Wdotcwp(n,1)/Wdotnetout(n,1);
hwpfrac(n,1)    = Wdothwp(n,1)/Wdotnetout(n,1);
mdotcwperkw(n,1)= mdotcw(n,1)/Wdotnet(n,1);
mdothwperkw(n,1)= mdothw(n,1)/Wdotnet(n,1);
Qcwperkw(n,1)   = Qcw(n,1)/Wdotnet(n,1);
Qhwperkw(n,1)   = Qhw(n,1)/Wdotnet(n,1);
Ahwtotperkw(n,1)= Ahwtot(n,1)/Wdotnet(n,1);
Acwtotperkw(n,1)= Acwtot(n,1)/Wdotnet(n,1);
%%%%%%%%%%%%%%%%%%%%%%%%%%%%%%%%%%%%%%%%%%%%%%%%%%%%%%%%%%%%%%%%%%%%%%%%%%%%

%%_________________Economics portion of the model_____________________%%



%CAPEX Variables
grosspower       = Wdotout(n,1);        % Gross power produced by the power cycle (
    before water pump demand is subracted off)
ratedpower       = Wdotnet(n,1);        % the net electric power out of the plant (
    after water pump demands included)
hwhxarea         = Ahwtot(n,1)*10.7639; % Hot water heat exchanger area, in ft^2
cwhxarea         = Acwtot(n,1)*10.7639; % Cold water heat exchanger area, in ft^2
cwpumppower      = Wdotcwp(n,1);        % Cold water pump power requirement in kW (
    pump and pump motor)
```

```
hwpumppower      = Wdothwp(n,1);        % Warm water pump power requirement in kW
turbgencostperkw = [700,     1000,     2000];          % Cost per turbine based on a
    $ perkW cost per turbine/generator setup
hxcostpersqft    = [20,      40,      80];                % Cost covers:raw material
    cost, all machining and manufacturing cost
cwpumpcostperkw  = [1000,       2000,   3000];              % Cost of the cold
    water pump per kW of power required
hwpumpcostperkw  = [1000,       2000,   3000];              % Cost of the warm
    water pump per kW of power required (pump and pump motor)
cwpipecosts      = [1e7,        30000000,       50000000];
platformcosts    = [30000000,   90000000,       150000000,]; % Total cost for the
    materials, conststruction, and deployment of the platform itself (includes water
    system piping and power cycle piping)
powerlinecost    = [20000000,   30000000,       50000000];   % Cost of the power
    electronics and power line from the plant to the shore/customer
othercostsfrac   = [0.2,0.2,0.2];
capfactor        = [0.9,0.8,0.7];               % plant operating capacity factor
%OPEX variables
workers          = [10,      10,     10];                % Number of full-time
    employees operating the plant
workercosts      = [100000,     100000,     100000];             % Salary/benefits/
    taxes for workers
OandMfrac        = [0.05,   0.05,   0.05];                % Fraction of the plant
    CAPEX that is required for routine operation and mainanance
%inflation   <<probably need to include this

% Capital Recovery Factor variabless
intrate          = [0.1,    0.1,    0.1];
loanperiod       =  [20,    20,     20];


costs = economics_thesis(grosspower,cwpumppower,hwpumppower,ratedpower,
    turbgencostperkw(step),hwhxarea,cwhxarea,hxcostpersqft(step),cwpumpcostperkw(step
    ),hwpumpcostperkw(step),cwpipecosts(step),platformcosts(step),powerlinecost(step)
    ,capfactor(step),intrate(step),loanperiod(step),workers(step),workercosts(step),
    OandMfrac(step),othercostsfrac(step));

CAPEX(n,1)              = costs(1);
capexperkw(n,1)         = costs(2);
LCOE(n,1)               = costs(3);
OPEX(n,1)               = costs(4);
turbgencosts(n,1)       = costs(5);
hxcosts(n,1)            = costs(6);
cwpumpcosts(n,1)        = costs(7);
hwpumpcosts(n,1)        = costs(8);

N(n,1) = n;
P(n,1) = p;

OUTPUT(step,1:17) = [P(n,1),Wdotnetout(n,1),Wdotcwp(n,1),Wdothwp(n,1),Wdotnet(n,1),
    Qcw(n,1),Qhw(n,1),Acwtot(n,1),Ahwtot(n,1),cwpfrac(n,1),hwpfrac(n,1),Acwtotperkw(n
    ,1),Ahwtotperkw(n,1),mdotcwperkw(n,1),mdothwperkw(n,1),Qcwperkw(n,1),Qhwperkw(n
    ,1)];

ECONOMICS(step,1:9) = [P(n,1),CAPEX(n,1),capexperkw(n,1),LCOE(n,1),OPEX(n,1),hxcosts(
    n,1),turbgencosts(n,1),cwpumpcosts(n,1),hwpumpcosts(n,1)];
end
% OUTPUT;
%     OUTPUTtitles = ['P,','Wdotnetout,','Wdotcwp,','Wdothwp,','Wdotnet,','vdotcw,','
    vdothw,','Acwtot,','Ahwtot,','cwpfrac,','hwpfrac,','Acwperkw,','Ahwtotperkw,','
    mdotcwperkw,','mdothwperkw,','vdotcwperkw,','vdothwperkw,'];
%     dlmwrite('/Users/charlesupshaw/Dropbox/Thesis Stuff/Thesis/20MW system/
    Thesis_ANALYSIS_stages.txt',OUTPUTtitles,'delimiter','')
```

```
%     dlmwrite('/Users/charlesupshaw/Dropbox/Thesis Stuff/Thesis/20MW system/
    Thesis_ANALYSIS_stages.txt',OUTPUT,'-append','delimiter',',','precision',6)
% %     %PC file location: E:\20MW system\20mwbaseline.txt
%     %Mac file location:
% ECONOMICS;
%     ECONOMICStitles = ['P,','CAPEX,','capexperkw,','LCOE,','hxcostsfrac,','
    cwpipecostfrac,','cwpumpcostfrac,','hwpumpcostfrac,','cwsystemcostfrac,','
    hwsystemcostfrac,','turbcostsfrac,','gencostsfrac,','stagecostfrac,','
    fluidcostfrac,','platformcostfrac,','powerlinecostfrac,','wscostsfrac,','
    pscostsfrac,','OPEX,'];
%     dlmwrite('/Volumes/UPSHAW_1/20MW system/ANALYSIS_Uhx.txt',ECONOMICStitles,'-
    append','roffset',3,'delimiter','')
%     dlmwrite('/Volumes/UPSHAW_1/20MW system/ANALYSIS_Uhx.txt',ECONOMICS,'-append','
    delimiter',',','precision',6)
 OUTPUT
 ECONOMICS
```

C.2 Thermal-Fluids and Economic Model: subsystem functions, and other files

C.2.1 Temperature Calculations for Staging: pcstaging.m

```
function F  = pcstaging(Tcwin,Tcwout,Tcoffset,Thwin,Thwout,Tboffset,Stages)

n        = Stages;
DeltaTcw = (Tcwout - Tcwin)/n;
DeltaThw = (Thwin  - Thwout)/n;


for i = 1:n
Tcwins(i)    = Tcwout - i*DeltaTcw;
Tcwouts(i)   = Tcwout - (i-1)*DeltaTcw;
Thwins(i)    = Thwin -(i-1)*DeltaThw;
Thwouts(i)   = Thwin - i*DeltaThw;

Tboil(i)    = Thwouts(i) - Tboffset;
Tcond(i)    = Tcwouts(i) + Tcoffset;

end


F = [Tcwins;Tcwouts;Thwins;Thwouts;Tboil;Tcond];
```

C.2.2 Power Cycle Subsystem: powercycle.m

powercycle.m:s

```
%%%%Rankine Power Cycle Model%%%%

%  Input Variables and System Parameters
function X = powercycle(fluid,mdotf,Tcondenser,Tboiler,pumpeff,turbeff,effegen,
    effemotor,Zboilers)

%Start cycle after the condensor.
    %Working fluid leaves the condensor as a sat liquid,
    %where Tsat = Tcondensor (X = 0, P = Psat@Tcond)
```

```
%Step 1-2: Pressurize saturated liquid to the saturation pressure of the
%boiler. Assume incompressable fluid

X1 = 0;
T1 = Tcondenser;
T2 = Tboiler;

pumpoutput = feedpump(T1,X1,T2,pumpeff,mdotf,fluid,effemotor,Zboilers);
    Wdotpump = pumpoutput(1);
    ElecPfp  = Wdotpump;
    T2       = pumpoutput(2);
    P2       = pumpoutput(3);
    X2       = 0;


%Step 2-3: Heat and boil working fluid
    %assume zero pressure drop in working fluid
    %assume adiabatic (no lost heat)
boileroutput = boiler(T2,P2,Tboiler,X2,mdotf,fluid);
    T3     = boileroutput(1);
    P3     = boileroutput(2);
    X3     = boileroutput(3);
    Qdotinheat = boileroutput(4);
    Qdotinboil = boileroutput(5);


%Step 3-4: Expand working fluid through Turbine
    %assume isentropic
    %assume adiabatic
    %assume expansion all the way to T4,P4 (into saturation region)
turbineoutput = turbine(T3,X3,Tcondenser,turbeff,mdotf,fluid);
    T4 = turbineoutput(1);
    P4 = turbineoutput(2);
    X4 = turbineoutput(3);
    Wdotout = turbineoutput(4);
    ElecPout   = Wdotout*effegen;


%Step 4-1: Condense working fluid to fully saturated liquid state (X = 0)
    %assume zero pressure drop accross condensors
    %assume adiabatic (all cold water heating for working fluid heat loss)
    %assume no subcooling taking place, Tout = Tsat
condoutput = condenser(T4,P4,Tcondenser,X4,mdotf,fluid);
    Xout    = condoutput(3);
    Qdotout = condoutput(4);

X = [ElecPout,ElecPfp,Qdotinheat,Qdotinboil,Qdotout];
```

C.2.2.1 powercycle.m sub-functions

feedpump.m:

```
%1-2 Working Fluid Pump
    %Assume:Incompressable Fluid, Adiabatic

function p = feedpump(Tin,Xin,Tboiler,pumpeff,mdotf,fluid,effemotor,Zboilers)

propsin  = propcalc(Tin,0,Xin,fluid);
Pin      = propsin(1);
vin      = propsin(4);
```

```
hin      = propsin(2);
propsout = propcalc(Tboiler,0,0,fluid);
Pout     = propsout(1);

%solve for hout using pump efficiency and incompressable fluid assumption
Pgrav     = gravfeedpump(Tin,Pin,Xin,fluid,Zboilers);

Pin       = Pin + Pgrav;

if Pin >= Pout
    Pin = Pout;
end

houta    = hin+vin*(Pout-Pin);

Tout     = Tin;


%Solve for work rate required by the pump

Wdota = 1/(pumpeff)*mdotf*(houta-hin);
fppumppower = Wdota*1/effemotor;

p = [fppumppower,Tout,Pout];
end
function gp = gravfeedpump(Tin,Pin,Xin,fluid,Zboilers)
%get density of liquid column
props = propcalc(Tin,Pin,Xin,fluid);
density = props(6);
%assume constant crossectional area and fluid velocity for pressure calc:

gp = 9.81*density*Zboilers/1e3; %divide by 1000 to get in kPa
end
```

boiler.m:

```
            %Hot side heat exchanger
%Assume zero pressure drop
%Assume zero heat loss (all heat goes from water to working fluid)
%Assume no superheating of the workingfluid : exit conditions of T3 = Tboiler, P =
    Psat@T3, X = 1
function hx = boiler(Tin,Pin,Tboiler,Xin,mdotf,fluid)

%Calculate Qdotin
    Tout = Tboiler;
    Pout = Pin;
    Xsatliq = 0;
    Xout = 1;


    % Assume that the Uin ~ Usaturated liquid at Tin (ie, P>Psat@Tin doesn't effect
        the internal energy)
    propsin  = propcalc(Tin,Pin,Xin,fluid);
    uin      = propsin(5);


    %Need to heat working fluid to boiling temperature before phase change (saturated
         liquid, X = 0)
    propssl    = propcalc(Tout,Pout,Xsatliq,fluid);
    usatliq    = propssl(5);
    hsatliq    = propssl(2);
```

```
    propsout   = propcalc(Tout,Pout,Xout,fluid);
    hout       = propsout(2);
    Qdotinheat = mdotf*(usatliq-uin);
    Qdotinboil = mdotf*(hout-hsatliq);
    Qdotin     = Qdotinheat + Qdotinboil;

hx = [Tout,Pout,Xout,Qdotinheat,Qdotinboil];
end
```

turbine.m:

```
%Fuction uses the input variables to calculate the change in enthalpy

function Turb = turbine(Tin,Xin,Tout,turbeff,mdotf,fluid)

% Use property call function to find the enthalpy and entropy at the inlet
% state

propsin = propcalc(Tin,0,Xin,fluid);
    hin = propsin(2);
    sin = propsin(3);


%calculate X
sl = scalc(Tout,0,0,fluid);
sv = scalc(Tout,0,1,fluid);

Xouts = (sin-sl)/(sv-sl);

%Calculate hout, and the Power out
propsout = propcalc(Tout,0,Xouts,fluid);
Pout  = propsout(1);
houts = propsout(2);

Wdotouts = mdotf*(hin-houts);


houta = hin - turbeff*(hin-houts);

houtsl = hcalc(Tout,Pout,0,fluid);
houtsv = hcalc(Tout,Pout,1,fluid);

Xouta  = (houta-houtsl)/(houtsv-houtsl);

Wdotouta = mdotf*(hin-houta);
Qlosses  = Wdotouts - Wdotouta;

Turb = [Tout,Pout, Xouta, Wdotouta, Qlosses];
end
```

condenser.m:

```
            %Cold side heat exchanger
%Assume zero pressure drop
%Assume zero heat loss (all heat goes from working fluid to cold water)
%Assume no subcooling of working fluid: Tout = Tboiler = Tsat, Pout = Psat
function hx = condenser(Tin,Pin,Tcondenser,Xin,mdotf,fluid)

%Calculate Qdotout
    Tout = Tcondenser;
    Pout = Pin;
```

```
    Xsatliq = 0;
    Xout    = Xsatliq;
    %Calculate Inlet values
    propsin  = propcalc(Tin,Pin,Xin,fluid);
    hin      = propsin(2);

    %Need to cool working fluid to fullly saturated liquid state (ie. to X=0)
    propssl  = propcalc(Tout,Pout,Xsatliq,fluid);
    hsatliq  = propssl(2);

%Calculate Qdotout
    Qdotout   = mdotf*(hin-hsatliq);



hx = [Tout,Pout,Xout,Qdotout];
```

propcalc.m:

```
%%%%%   EXAMPLE PROPCALC.M FILE
%%%%%   TABLE IS OMITTED
%%%%%   CONTACT CHARLES UPSHAW FOR FULL .M FILE

function f = propcalc(T_cel,P_kPa,X,fluid)

P = P_kPa;


%Property matrix column catagories:
%[T_celsius,Psat,density_liq,density_vap,specvolume_liq,specvolume_vap,intenergy_liq,
    ingenergy_vap,enthalpy_liq,enthalpy_vap,entropy_liq,entropy_vap]

%Available working fluids: R134a, Ammonia, Propylene, R1234yf, R1234ze, R22, Propane

if strcmpi(fluid, 'r134a') %fluid == 'R134a'|'r134a'
% disp('R134a');
propmatrix =   [0.00000000, 292.80318, 1294.7770, 14.428201, 0.00077233376,
    0.069308708, 199.77386, 378.30965, 200.00000, 398.60347, 1.0000000, 1.7270857
                0.025000000, 293.06849, 1294.6944, 14.440808, 0.00077238303,
                    0.069248203, 199.80723, 378.32359, 200.03359, 398.61805,
                    1.0001222, 1.7270718
                0.050000000, 293.33399, 1294.6118, 14.453423, 0.00077243231,
                    0.069187761, 199.84060, 378.33752, 200.06718, 398.63264,
                    1.0002444, 1.7270580
                0.075000000, 293.59967, 1294.5292, 14.466047, 0.00077248160,
                    0.069127383, 199.87397, 378.35145, 200.10077, 398.64723,
                    1.0003666, 1.7270441
                0.10000000, 293.86554, 1294.4466, 14.478680, 0.00077253091,
                    0.069067068, 199.90734, 378.36538, 200.13436, 398.66181,
                    1.0004888, 1.7270302

%%%%%%%%%%%%%%%%%%%%%%%%%%%%%%%%%%%%%%%%%%%%%%%%%%%%%%%%%%%%%%%%%%%%%%%%%%%%%%%
%%%%    REST OF TABLE OMITTED FOR BREVITY, CONTACT FOR REAL .m FILE   %%%%%


                29.900000, 767.98550, 1187.8535, 37.425067, 0.00084185465,
                    0.026720059, 240.93132, 394.24929, 241.57785, 414.76991,
                    1.1430296, 1.7145262
                29.925000, 768.53775, 1187.7556, 37.452599, 0.00084192403,
                    0.026700417, 240.96693, 394.26179, 241.61398, 414.78206,
                    1.1431472, 1.7145176
```

```
                29.950000, 769.09031, 1187.6577, 37.480148, 0.00084199344,
                    0.026680791, 241.00255, 394.27428, 241.65012, 414.79422,
                    1.1432649, 1.7145091
                29.975000, 769.64315, 1187.5598, 37.507714, 0.00084206286,
                    0.026661182, 241.03817, 394.28678, 241.68626, 414.80637,
                    1.1433826, 1.7145005
                30.000000, 770.19630, 1187.4619, 37.535298, 0.00084213231,
                    0.026641589, 241.07380, 394.29927, 241.72240, 414.81852,
                    1.1435003, 1.7144920];


i = 1;

while   propmatrix(i,1)< T_cel
    i = i+1;
end

%i is the row number whose Temp is immediately greater than T_cel
%Find the fractional amount between T_cel and the values immediately above
%and below in the table. linearly interpolate
T_lo = propmatrix((i-1),1);
T_hi = propmatrix(i,1);
K = (T_cel-T_lo)/(T_hi-T_lo);

Psat    = propmatrix((i-1),2) + K*(propmatrix((i),2)-propmatrix((i-1),2));

if P == 0
% disp('sat mix')

elseif (P-Psat) > .001

%  disp('Liquid');
    X = 0;

elseif (P-Psat) < -.001

%  disp('Superheated gas');
    X =1;
end


hl     = propmatrix((i-1),9) + K*(propmatrix((i),9)-propmatrix((i-1),9));
hv     = propmatrix((i-1),10) + K*(propmatrix((i),10)-propmatrix((i-1),10));
sl     = propmatrix((i-1),11) + K*(propmatrix((i),11)-propmatrix((i-1),11));
sv     = propmatrix((i-1),12) + K*(propmatrix((i),12)-propmatrix((i-1),12));
vl     = propmatrix((i-1),5) + K*(propmatrix((i),5)-propmatrix((i-1),5));
vv     = propmatrix((i-1),6) + K*(propmatrix((i),6)-propmatrix((i-1),6));
ul     = propmatrix((i-1),7) + K*(propmatrix((i),7)-propmatrix((i-1),7));
uv     = propmatrix((i-1),8) + K*(propmatrix((i),8)-propmatrix((i-1),8));
dl     = propmatrix((i-1),3) + K*(propmatrix((i),3)-propmatrix((i-1),3));
dv     = propmatrix((i-1),4) + K*(propmatrix((i),4)-propmatrix((i-1),4));
%Output variables, calculate based on Saturation

h    = hl + X*(hv-hl);
s    = sl + X*(sv-sl);
vmix = vl + X*(vv-vl);
u    = ul + X*(uv-ul);
dmix = dl + X*(dl-dv);

f = [Psat,h,s,vmix,u,dmix];
end
```

hcalc.m:

```
function h = hcalc(Tin,Pin,Xin,fluid)
Props = propcalc(Tin,Pin,Xin,fluid);
h = Props(2);
```

scalc.m:

```
function s = scalc(T,P,X,fluid)
V = propcalc(T,P,X,fluid);
s = V(3);
```

C.2.3 Heat Exchanger Subsystem: heatexchangers.m

heatexchangers.m:

```
function HX =heatexchangers(Tcwins,Tcwouts,Thwins,Thwouts,Tboil,Tcond,n,
    Qdotinheatstage,Qdotinboilstage,Qdotoutstage,Ucwref,Vcwref,Uhwhref,Uhwbref,Vhwref
    ,deltPcref,deltPbref,cpcw,cphw,densitycw,densityhw,Apipecw,Apipehw,numofinletshw,
    Acwref,Ahwref)

%Find the maximum Qdot in/out of the system, use this to find the maximum
%flow rate of water needed
Qout = max(Qdotoutstage);
Qin  = max(Qdotinheatstage+Qdotinboilstage);

%Calculate the water mass flow rate needed for the stage with the largest
%heat in/out demand
mdotcw = Qout/(cpcw*(Tcwouts(1)-Tcwins(1)));
mdothw = Qin/(cphw*(Thwins(1)-Thwouts(1)));


%Calculate average water velocities(Vavg) from volume flow rates (Qcw,Qhw)
Qcw    = mdotcw/densitycw;
Qhw    = mdothw/densityhw;
Vcwavg = Qcw/Apipecw;
Vhwavg = Qhw/(Apipehw*numofinletshw);


%Check to see if flow velocities are lower than the reference flow
%velocities.  If the calc flow velocity is lower than the reference,
%assume the reference value (as in the flow is necked down into the HX
%to get to Vref, otherwise it's not)
if Vcwavg < Vcwref
    Vcwavg = Vcwref;
else
    Vcwavg = Vcwavg;
end
if Vhwavg < Vhwref
    Vhwavg = Vhwref;
else
    Vhwavg = Vhwavg;
end

%scale the reference overall heat transfer coefficient as Vavg^.8/Vref^.8
Ucw = Ucwref*(Vcwavg/Vcwref)^.8;
Uhwh = Uhwhref*(Vhwavg/Vhwref)^.8;
Uhwb = Uhwbref*(Vhwavg/Vhwref)^.8;
```

```
%calculate the boiling temperature, LMTD for the heating of the working
%fluid

for i = 1:n
Thwb(i) = Thwouts(i) + (Qdotinheatstage(i)/(mdothw*cphw));
%Alternate calculation assumes water is heated from the incoming warm
%water, not the exiting warm water
%Thwba(i) = Thwins(i) - (Qdotinheatstage(i)/(mdothw*cphw));

LMTDc(i) = (Tcwins(i)-Tcwouts(i))/log((Tcond(i)-Tcwouts(i))/(Tcond(i)-Tcwins(i)));
LMTDh(i) = ((Thwb(i)-Tboil(i))-(Thwouts(i)-Tcond(i)))/log((Thwb(i)-Tboil(i))/(Thwouts
    (i)-Tcond(i)));
LMTDb(i) = (Thwins(i)-Thwb(i))/log((Thwins(i)-Tboil(i))/(Thwb(i)-Tboil(i)));
%LMTDha(i) = ((Thwins(i)-Tcond(i))-(Thwba(i)-Tboil(i)))/log((Thwins(i)-Tcond(i))/(
    Thwba(i)-Tboil(i)));
%LMTDba(i) = (Thwba(i)-Thwouts(i))/log((Thwba(i)-Tboil(i))/(Thwouts(i)-Tboil(i)));

%Calculate required heat exchanger area with corrected heat transfer values
%and the LMTDs
Acond(i)   = Qdotoutstage(i)/(Ucw*LMTDc(i));
Aheat(i)   = Qdotinheatstage(i)/(Uhwh*LMTDh(i));
Aboil(i)   = Qdotinboilstage(i)/(Uhwb*LMTDb(i));
%Aheata(i)   = Qdotinheatstage(i)/(Uhwh*LMTDha(i));
%Aboila(i)   = Qdotinboilstage(i)/(Uhwb*LMTDba(i));
end

%sum areas
Acwtot   = sum(Acond);
Ahtot   = sum(Aheat);
Abtot   = sum(Aboil);
Ahwtot  = Ahtot+Abtot;


if n == 1
Acwref = Acwtot;
Ahwref = Ahwtot;
end
%Scale pressure head as a function of Vavg^1.8/Vref^1.8, reference area.
deltPcond = deltPcref*(Vcwavg/Vcwref)^1.8*Acwtot/Acwref;
deltPboil = deltPbref*(Vhwavg/Vhwref)^1.8*Ahwtot/Ahwref;
HX = [mdotcw,mdothw,Vcwavg,Vhwavg,Qcw,Qhw,deltPcond,deltPboil,Acwtot,Ahwtot,Ucw,Uhwh,
    Uhwb];
```

C.2.4 Hot and Cold Water Pump Subsystem: coldwaterpump.m, warmwaterpump.m

coldwaterpump.m:

```
%Calculation of the power requirement of the cold water pump
%add K values and other loss coefficients directly into the code for now
function F = coldwaterpump(n,mdotcw,densitycw,visccw,Dpipecw,Lpipecw,effpumpcw,
    effemotor,roughnesscw,densityavgsea,deltPcond,Kinlet,Kftot)
%Assume constant values for the density of the cold water and viscosity:
density = densitycw; %kg/m^3
visc    = visccw; %N*s/m^2
D = Dpipecw;
L = Lpipecw;
A = (pi*D^2/4);
```

```
mdot = mdotcw;
rr = roughnesscw/D;
%calculate the volumetric flow rate
Q = mdot/density;
%calculate the average fluid velocity
V_avg = Q/A;
%calculate the Reynold's number of the flow
Re = Re_calc(D,visc,Q,density);
%Calculate the friction factor for the pipe: First guess
    f0 = .25*(log10((rr)/3.7+(5.74/Re^.9)))^-2;
%Now Iterate
i = 1;
f = f0;
  Fleft = (1/(f^.5));
  Fright = -2*log10(((rr)/3.7)+(2.51/(Re*f^.5)));
  fdiff =Fleft-Fright;
while i < 50 &&  (abs(fdiff)>.000001)
  Fleft = (1/f^.5);
  Fright = -2*log10(((rr)/3.7)+(2.51/(Re*f^.5)));
  fdiff =Fleft-Fright;
    if  fdiff>0
      f = (1+fdiff/(Fleft+Fright))*f;
      i=i+1;
    else
      f = (1-abs(fdiff)/(Fleft+Fright))*f;
      i=i+1;
   end
end
hl_inlet = Kinlet*V_avg^2/(2);
h_fittings = f*Kftot*V_avg^2/(2);
hl_pipedrag = f*L/D*V_avg^2/(2);
hl_tot = hl_pipedrag + hl_inlet + h_fittings;
%Assume a hydrostatic pressure head loss because of the heigher density fluid inside
    the tube
    %total deltZ =  (1-pipedensityavgsea/densitypipe)*L; %meters
    densitypipe = density;
    deltZ =  (1-densityavgsea/densitypipe)*L;%Assumed pressure head differential from
         density difference;

pumppower = (1/effemotor)*(1/effpumpcw)*mdot*(deltPcond/densitycw + hl_tot+9.807*
    deltZ)/1e3; %divide by 1e3 to get into KW
F = [pumppower];
```

warmwaterpump.m:

```
%Calculation of the power requirement of the cold water pump
%add K values and other loss coefficients directly into the code for now
function F = warmwaterpump(n,mdothw,densityhw,vischw,numofinletshw,Dpipehw,Lpipehw,
    effpumphw,effemotor,roughnesshw,deltPboil,Kbinlet,Kfbtot)
%Assume constant values for the density of the cold water and viscosity:
density = densityhw; %kg/m^3
visc    = vischw; %N*s/m^2
D = Dpipehw;
L = Lpipehw;
A = (pi*D^2/4)*numofinletshw;
mdot = mdothw;
%Assumed Hot Water Pipe characteristics
 e = roughnesshw;
    rr = e/D;
%calculate the volumetric flow rate
Q = mdot/density;
%calculate the average fluid velocity
```

```
V_avg = Q/A;
%calculate the Reynold's number of the flow
Re = Re_calc(D,visc,Q,density);
%Calculate the friction factor for the pipe: First guess
    f0 = .25*(log10((rr)/3.7+(5.74/Re^.9)))^-2;
%Now Iterate
i = 1;
f = f0;
  Fleft = (1/(f^.5));
  Fright = -2*log10(((rr)/3.7)+(2.51/(Re*f^.5)));
  fdiff =Fleft-Fright;
while i < 50 &&  (abs(fdiff)>.000001)
  Fleft = (1/f^.5);
  Fright = -2*log10(((rr)/3.7)+(2.51/(Re*f^.5)));
  fdiff =Fleft-Fright;
    if  fdiff>0
      f = (1+fdiff/(Fleft+Fright))*f;
      i=i+1;
    else
      f = (1-abs(fdiff)/(Fleft+Fright))*f;
      i=i+1;
   end
end
hl_inlet = Kbinlet*V_avg^2/(2);
hl_fittings = f*Kfbtot*V_avg^2/(2);
hl_pipedrag = f*L/D*V_avg^2/(2);
hl_tot = hl_pipedrag + hl_inlet + hl_fittings;
%Calc pump power from head losses and mdot.  Divide by 1000 to get into kW
pumppower = (1/effemotor)*(1/effpumphw)*mdot*(deltPboil/densityhw+hl_tot)/1000;

F = [pumppower];
```

Re_calc.m:

```
%Reynolds Number calculator
function Re = Re_calc(D,viscosity,V_avg,density)

%Basic Reynolds number calculation: Re = (density*vel_avg*D)/viscosity;
%For calc with flow rate: Re = (4*density*Q)/(pi*viscosity*D);

Re = (density*V_avg*D)/viscosity;
```

C.2.5 Economic Modeling Subsystem: economics_thesis.m

economics_thesis.m:

```
%   OTEC ECONOMICS MODEL   %
function E = economics_thesis(grosspower,cwpumppower,hwpumppower,ratedpower,
    turbgencostperkw,hwhxarea,cwhxarea,hxcostpersqft,cwpumpcostperkw,hwpumpcostperkw,
    cwpipecosts,platformcosts,powerlinecost,capfactor,intrate,loanperiod,workers,
    workercosts,OandMfrac,othercostsfrac)

%Calculate the Capital Recovery Factor
i = intrate;
lp = loanperiod;

CRF = i*(1+i)^lp/((1+i)^lp-1);
```

```
%Calculate the three subsystem costs

    turbgencosts = turbgencostperkw*grosspower;

    hxcosts   = cwhxarea*hxcostpersqft + hwhxarea*hxcostpersqft;

    cwpumpcosts = cwpumppower*cwpumpcostperkw;
    hwpumpcosts = hwpumppower*hwpumpcostperkw;
    wscosts   = cwpipecosts + cwpumpcosts + hwpumpcosts;

%Unadjusted CAPEX costs
plantcosts = (hxcosts + wscosts + turbgencosts + platformcosts + powerlinecost);

%Adjusted CAPEX to account for deployment costs and other things that may
%have been left out of other estimates
CAPEX = (1+othercostsfrac)*plantcosts;


%OPEX Variables
humancosts       = workers*workercosts;
OandMcosts       = OandMfrac*(hxcosts + wscosts + turbgencosts + platformcosts +
    powerlinecost);


%Calculate Capex, Opex, and LCOE


capexperkw = CAPEX/ratedpower;

OPEX  = (humancosts + OandMcosts );

LCOE  = (CAPEX*CRF + OPEX)/(8760*ratedpower*capfactor);

E = [CAPEX,capexperkw,LCOE,OPEX,turbgencosts,hxcosts,cwpumpcosts,hwpumpcosts];
```

Bibliography

[1] Energy Information Agency. Texas Renewable Energy Profile 2010. http://205.254.135.7/renewable/state/texas/, March 2012.

[2] J. Anderson. Sea Solar Power Website. www.seasolarpower.com.

[3] J. H. Anderson. A Compact Heat Exchanger Concept for Ocean Thermal Power Plants. In *Proceedings of the 5th Ocean Energy Conference*, volume 3, pages 321–344, 1978. Sea Solar Power Inc.

[4] J. H. Anderson. Ocean Thermal Power–The Coming Energy Revolution. *Solar and Wind Technology*, 2, 1985.

[5] J. H. Anderson, D. H. Dellinger, and R. S. Lyman. The SSP Compact Heat Exchanger Test Results. In *Proceedings of the 7th Ocean Energy Conference*, volume 1, 1980. Sea Solar Power Inc.

[6] Jim H. Anderson. Ocean Thermal Energy Conversion (OTEC): Choosing a Working Fluid. In *ASME Power 2009 Conference Proceedings*, pages 645–653, 2009.

[7] Fiji Electric Authority. Fiji Electric Authority Website: New Tariff - November 2010. http://www.fea.com.fj/pages.cfm/customer-care/new-tariff--september-2009.html, 2009.

[8] W. H. Avery and C. Wu. *Renewable Energy From the Ocean – A Guide to OTEC*. Oxford University Press, 1994.

[9] S. Bailey and L. Vega. OTEC Mooring and Anchoring Systems: Technology Development Plan. In *Proceedings of the 8th Ocean Energy Conference*, volume 1, 1981. Giannotti and Associates Inc.

[10] P. J. Bakstad, J. W. Denton, R. H. Douglass, W. J. Tallon, and R. R. Rothfus. Vertical Tube Falling Film Heat Exchangers in an OTEC Power System. In *Proceedings of the 5th Ocean Energy Conference*, volume 2, 1978. TRW Defense and Space Systems Group, and Carnegie-Mellon University.

[11] Paal J. Bakstad and Russell O. Pearson. Design of a 10 MWe(net) OTEC Power Module using Vertical Falling-Film Heat Exchangers. In *Proceedings of the 6th Ocean Energy Conference*, volume 1, 1979. TRW Systems and Energy.

[12] R. A. Barr and P. Murphy. Methods for Reducing Structural Loads on OTEC Plant Cold Water Pipes. In *Proceedings of the 5th Ocean Energy Conference*, volume 2, 1978. Hydronautics, Inc.

[13] E. J. Barsness, R. T. Miller, and S. Cunninghis. Conceptual Design of an OTEC Power System Using Modular Heat Exchangers. In *Proceedings of the 5th Ocean Energy Conference*, volume 2, 1978. Westinghouse Electric Corp., Gibbs and Hill Inc.

[14] T. Berndt and J. W. Connell. Plate Heat Exchangers for OTEC. In *Proceedings of the 5th Ocean Energy Conference*, volume 3, 1978. Alfa-Laval Inc.

[15] Blelkeman. BEC and OTE Corp. Signs MoU for two OTEC plants in

the Bahamas. http://www.otecnews.org/2011/09/640/, September 2011.

[16] Blelkeman. OTEC International LLC Chosen for Hawaii OTEC Demonstration. http://www.otecnews.org/2011/11/otec-international-llc-chosen-for-hawaii-otec-demonstration/, November 2011.

[17] Georges Claude. Power from the Tropical Seas. *Mechanical Engineering*, 52:1039–1044, 1931.

[18] B. Coffay and D. A. Horazak. Selection of OTEC Working Fluids Based on Power System Costs. In *Proceedings of the 7th Ocean Energy Conference*, volume 1, pages 7.2–1 to 7.2–14, 1980.

[19] S. K. Combs and R. W. Murphy. Experimental Studies of OTEC Heat Transfer Condensation of Ammonia on Vertical Fluted Tubes. In *Proceedings of the 5th Ocean Energy Conference*, volume 3, 1978. Oak Ridge National Laboratory.

[20] Caribbean Utilities Company. The Facts Regarding CUC's Electricity Rates. http://cuc-cayman.com/PDF/off\%20the\%20wire/fiscal\%202011/facts\%20regarding\%20rates\%20131011.pdf, October 2011.

[21] Dennis J. Cooper. Ocean Thermal Energy Conversion (OTEC). www.govenergy.com/2010/Files/Presentations/Renewables/Renewables_Session9_Cooper.pdf, August 2010.

[22] A. M. Czikk, H. D. Fricke, E. N. Ganic, and B. I. Sharma. Fluid Dynamic and Heat Transfer Studies of OTEC Heat Exchangers. In *Proceedings of the 5th Ocean Energy Conference*, volume 3, 1978. Linde Division, Union Carbide Corp.

[23] Jacques-Arsène d'Arsonval. Utilisation des Forces Naturelles Avenir del'èlectricitè. *Revue Scientifique*, 17:370–372, 1881.

[24] H. Davidson and T. E. Little. OTEC Platform Station Keeping Analysis. In *Proceedings of the 5th Ocean Energy Conference*, volume 2, 1978. Westinghouse Electric Corp.

[25] J. W. Denton, P. J. Bakstad, and K. McIlroy. Design of a 0.2 MWe(net) Plate-Type, OTEC Heat Exchanger Test Article and a 10 MWe(net) Power Module. In *Proceedings of the 6th Ocean Energy Conference*, volume 1, 1979. TRW Inc., Defense and Space Systems Group and Union Carbide, Linde Division.

[26] N. Domingo and J. W. Michel. Ammonia Condensation Experiments at Oak Ridge National Laboratory. In *Proceedings of the 8th Ocean Energy Conference*, volume 1, 1981. Oak Ridge National Laboratory.

[27] The Economist. Power from the Sea: Second Time Around... http://www.economist.com/node/21542381, January 2012.

[28] EIA. Levelized Cost of New Generation Resources in the Annual Energy Outlook 2011. Annual Report, Energy Information Agency, 2010. Presents LCOEs for technologies brought on line in 2016.

[29] EIA. State Electricity Profiles 2010. Annual Report, Energy Information Agency, 2010. Hawaii information.

[30] R. W. Fox and A. T. McDonald. *Introduction to Fluid Mechanics*. Wiley and Sons, 4th edition, 1998.

[31] James F. George. System Design Considerations for a Floating OTEC Modular Experiment Platform. In *Proceedings of the 6th Ocean Energy Conference*, volume 1, 1979. Johns Hopkins University Applied Physics Laboratory.

[32] Arthur Griffin and Louis Mortaloni. Baseline Designs for Three OTEC Cold Water Pipes. In *Proceedings of the 7th Ocean Energy Conference*, volume 1, 1980. TRW Inc.

[33] G. T. Heydt. An Assessment of Ocean Thermal Energy Conversion as an Advanced Electric Generation Methodology. *Proceedings of the IEEE*, 81:409–418, 1993.

[34] F. P. Incropera and D. P. DeWitt. *Fundamentals of Heat and Mass Transfer 4th Ed.* Wiley and Sons, 4th edition, 1996.

[35] G. H. Jirka, J. M. Jones, and F. E. Sargent. Intermediate Field Plumes from OTEC Plants: Predictions for Typical Site Conditions. In *Proceedings of the 8th Ocean Energy Conference*, volume 1, 1981. Cornell University.

[36] Naveen Kumar. Chasing a Green Engineering Dream. http://www.ecofriend.com/entry/chasing-a-green-engineering-dream/, October 2007.

[37] D. Lew, M. Milligan, G. Jordan, L. Freeman, N. Miller, and R. Clark, K /and Piwko. How do Wind and Solar Power Affect Grid Operations: The Western Wind and Solar Integration Study. In *Proc. of the 8th International Workshop on Large Scale Integration of Wind Power and on Transmission Networks for Offshore Wind Farms*, 2009.

[38] Lockheed-Martin. U.S. Department of Energy Selects Lockheed Martin to Advance Ocean Thermal Energy Conversion Utility Power Plans. http://www.lockheedmartin.com/us/news/press-releases/2010/march/USDepartmentEnergySelects.html, 2010.

[39] Terence McGuinness, Arthur Griffin, and Duane Hove. Preliminary Designs of Cold-Water Pipes for Barge and Spar-Type OTEC Plants. In *Proceedings of the 6th Ocean Energy Conference*, volume 1, 1979. NOAA, TRW Inc., and Science Applications Inc.

[40] Gèrard C. Nihous. An Order-of-Magnitude Estimate of Ocean Thermal Energy Conversion Resources. *Journal of Energy Resources Technology*, 127:328–333, December 2005.

[41] Gèrard C. Nihous. An Estimate of Atlantic Ocean Thermal Energy Conversion (OTEC) Resources. *Journal of Ocean Engineering*, 34:2210–2221, July 2007.

[42] Gèrard C. Nihous. Mapping Available Ocean Thermal Energy Conversion Resources around the Main Hawaiian Islands with State-of-the-Art Tools. *Journal of Renewable and Sustainable Energy*, 2, July 2010.

[43] M. G. Olmstead, M. J. Mann, and C. S. Yang. Optimizing Plant Design for Minimum Cost per kiloWatt with Refrigerant R-22 Working Fluid. In *Proceedings of the 6th Ocean Energy Conference*, volume 1, 1979. General Electric Company.

[44] W. L. Owens. Correlation of Thin Film Evaporation Heat Transfer Coefficients for Horizontal Tubes. In *Proceedings of the 5th Ocean Energy Conference*, volume 3, 1978. Lockheed Missiles and Space Company.

[45] C. Panchal, D. Hillis, L. Seren, D. Yung, J. Lorenz, J. Thomas, and N. Sather. Heat Exchanger Tests at Argonne National Laboratory. In *Proceedings of the 8th Ocean Energy Conference*, volume 1, 1981. Argonne National Laboratory.

[46] M. Ravindran and R. Abraham. The Indian 1 MW Demonstration OTEC Plant and the Development Activities. In *Proceedings of OCEANS '02 MTS/IEEE*, volume 3, pages 1622–1628, 2002.

[47] Jonathan Ross and William Wood. OTEC Mooring System Development: Recent Accomplishments. In *Proceedings of the 8th Ocean Energy Conference*, volume 1, 1981. NOAA, Giannotti and Associates Inc.

[48] R. R. Rothfus and G. H. Lavi. Vertical Falling Film Heat Transfer: A Literature Survey. In *Proceedings of the 5th Ocean Energy Conference*, volume 3, 1978. Carnegie Mellon University.

[49] N. Sather, L. G. Lewis, J. J. Lorenz, and D. Yung. Performance Tests

of 1MWt OTEC Heat Exchangers. In *Proceedings of the 5th Ocean Energy Conference*, volume 3, 1978. Argonne National Laboratory.

[50] P. S. Schmidt, O. A. Ezekoye, J. R. Howell, and D. K. Baker. *Thermodynamics: An Integrated Learning System.* Wiley and Sons, 2006.

[51] R. J. Scott. Conceptual Designs and Costs of OTEC 10/40 MW Spar Platform. In *Proceedings of the 6th Ocean Energy Conference*, volume 1, 1979. Gibbs & Cox, Inc.

[52] R. J. Scott and W. W. Rogalski. Considerations in Selection of OTEC Platform Size and Configuration. In *Proceedings of the 5th Ocean Energy Conference*, volume 2, 1978. Gibbs & Cox, Inc.

[53] R. K. Shah and D. P. Sekulic. *Fundamentals of Heat Exchanger Design.* Wiley and Sons, 2003.

[54] W. C. L. Shih and D. T. Hove. OTEC Cold Water Pipe Design Loads. In *Proceedings of the 5th Ocean Energy Conference*, volume 2, 1978. Science Applications, Inc.

[55] F. Sinama, F. Lucas, and F. Garde. Modeling of Ocean Thermal Energy Conversion (OTEC) Plant in Reunion Island. In *ASME 2010 Conference on Energy Sustainability Proceedings*, volume 1, pages 929–936, 2010.

[56] J. E. Snyder. 1 MWe Heat Exchangers for OTEC Status Report February 1978. In *Proceedings of the 5th Ocean Energy Conference*, volume 3, 1978. TRW Systems and Energy.

[57] S. Mack Sullivan and Mary Quinby-Hunt. A Preliminary Environmental Assessment of the OTEC Pilot Plant Program. In *Proceedings of the 8th Ocean Energy Conference*, volume 1, 1981. Interstate Electronics Corp., Lawrence Berkley Laboratory.

[58] H. Takazawa, A. Murata, and T. Kajikawa. Sensitivity Analysis of Ocean-Based Closed Cycle OTEC Power System. *Electrical Engineering in Japan*, 107, 1987.

[59] M. B. Tate and L. L. Perini. Dynamic Loads Induced by Severe Storms in Elastic Cold Water Pipes Attached to OTEC Ships by Fixed and Hinged Connections. In *Proceedings of the 5th Ocean Energy Conference*, volume 2, 1978. Johns Hopkins Univ. Applied Physics Laboratory.

[60] Anthony Thomas, James Lorenz, David Hillis, David Yung, and Norman Sather. Performance Tests of 1 MWt Shell-and-Tube and Compact Heat Exchangers for OTEC. In *Proceedings of the 6th Ocean Energy Conference*, volume 2, 1979. Argonne National Laboratory.

[61] L. C. Trimble and C. M. Robidart. A Power System Module Configuration using Aluminum Heat Exchangers. In *Proceedings of the 5th Ocean Energy Conference*, volume 2, 1978. Lockheed Missiles and Space Company.

[62] Luis Vega. Ocean Thermal Energy Conversion Primer. *Marine Technology Society Journal*, 36:25–35, 2002.

[63] Luis A. Vega. Economics of Ocean Thermal Energy Conversion

(OTEC): An Update. In *Proceedings of OTC the 2010 Offshore Technology Conference*, 2010.

[64] R. L. Waid. OTEC Platform Design Optimization. In *Proceedings of the 5th Ocean Energy Conference*, volume 2, 1978. Lockheed Missiles and Space Company.

[65] Judith Waite and Jeffrey Panger. Puerto Rico Electric Power Authority; Retail Electric. Bond Rating Analysis Report, Standard & Poor's, 2010. Retail price, generation capacity information.

[66] C. Wu and T. J. Burke. Intelligent Computer Aided Optimization on Specific Power of an OTEC Rankine Power Plant. *Journal of Applied Thermal Engineering*, 5:295–300, 1997.

[67] R. H. Yeh, T. Z. Su, and M. S. Yang. Maximum Output of an OTEC Power Plant. *Ocean Engineering*, 32:685–700, 2005.

[68] C. Zener. Solar Sea Power. *Bulletin of the Atomic Scientists*, 35, 1976.